Published for SISSA by Springer

Received: November 1, 2022
Accepted: December 19, 2022
Published: January 24, 2023

Stability of the cascading gauge theory de Sitter DFPs

Alex Buchel

Department of Physics and Astronomy, University of Western Ontario, London, Ontario N6A 5B7, Canada

Perimeter Institute for Theoretical Physics, Waterloo, Ontario N2J 2W9, Canada

E-mail: abuchel@perimeterinstitute.ca

Abstract: We study stability of the Dynamical Fixed Points (DFPs) of the cascading gauge theory at strong coupling in de Sitter space-time. We compute the spectra of the perturbative fluctuations and identify stable/unstable DFPs, characterized by the ratio of the strong coupling scale Λ of the gauge theory and the Hubble constant H of the background space-time. We discover a new phenomenon in the spectrum of gravitational fluctuations of a non-conformal holographic model: distinct branches of the fluctuations for $H \gg \Lambda$ coalesce for sufficiently low $\frac{H}{\Lambda}$, leading to the removal of some excited modes from the spectrum. We establish that, at least in a dual supergravity approximation, the cascading gauge theory does not have a stable DFP for some $H \sim \Lambda$. Initial states of the theory for $H \gg \Lambda$ evolve to a stable DFP with unbroken chiral symmetry; while for $H \ll \Lambda$ the states evolve to a de Sitter vacuum with spontaneously broken chiral symmetry.

Keywords: AdS-CFT Correspondence, Gauge-Gravity Correspondence, Non-Equilibrium Field Theory

ArXiv ePrint: 2210.17380

https://doi.org/10.1007/JHEP01(2023)130

JHEP01(2023)130

Contents

JHEP01(2023)130

1 Introduction and summary

The cascading gauge theory[1] [2] is $\mathcal{N}=1$ supersymmetric four-dimensional $\mathrm{SU}(N+M)\times\mathrm{SU}(N)$ gauge theory. It is non-conformal, and has a strong coupling scale Λ. The high-energy physics of the theory is exotic:[2] it undergoes perpetual sequence of Seiberg [4] dualities, $N\to N+M$, effectively rendering the rank parameter N energy dependent [5],

$$N=N(E)\ \propto\ M^2\ \ln\frac{E}{\Lambda}\,,\qquad \text{as}\qquad \frac{E}{\Lambda}\to\infty\,. \tag{1.1}$$

In the renormalization group flow to the infrared (IR), the rank parameter N decreases as $N\to N-M$, with each realization of the Seiberg duality. In Minkowski space-time, $R^{3,1}$, the moduli space of vacua of the theory was thoroughly analyzed in [6] — when N is an integer multiple of M, the cascading gauge theory ends up in the IR as the $\mathcal{N}=1$ $\mathrm{SU}(M)$ Yang-Mills theory. It confines with a spontaneous breaking of the $\mathrm{U}(1)_R$ chiral symmetry,

$$\mathrm{U}(1)_R\ \to\ \mathbb{Z}_2\,. \tag{1.2}$$

When $M\gg 1$, the cascading gauge theory has a String Theory holographic dual [7, 8] realized by a consistent truncation of Type IIB supergravity on warped deformed conifold with fluxes [9]. Owing to the fact that the cascading gauge theory in the IR shares the staples of QCD at strong coupling, namely confinement and the chiral symmetry breaking, the precise holographic dual allows to explore properties of strongly coupled non-conformal gauge theories which are difficult (and often impossible) to access otherwise: the thermal phase diagram [9–11]; the hydrodynamic transport [12, 13], the gauge theory dynamics in curved space [1, 14, 15] and in cosmological setting [16, 17]. The late-time properties of the cascading gauge theory in de Sitter space-time is the subject of this paper.

Before we present the results of the analysis, we would like to clearly distinguish the concept of a **de Sitter vacuum** [18] of a QFT and a **de Sitter DFP** of a QFT [19]. It is useful to start with a conformal field theory (CFT). Typically,[3] an arbitrary initial state of an interactive CFT in $R^{3,1}$ thermalizes. In a dual holographic picture this dynamics is encoded in the gravitational collapse and the black brane formation [22]. Following the second law of thermodynamics, as a CFT state equilibrates, its non-equilibrium entropy density $s(t)$ monotonically increases, $\dot{s}(t)\geq 0$, and reaches at late times the *finite* thermal entropy density $s_{\rm thermal}$, determined by the late-time thermal equilibrium temperature T,

$$\lim_{t\to\infty} s(t)=s_{\rm thermal}<\infty\,. \tag{1.3}$$

The existence of the above limit, equivalently the equilibration of a generic state, implies that the entropy production rate vanishes at late times, i.e.,

$$\lim_{t\to\infty}\frac{\dot{s}(t)}{s(t)}=0\,. \tag{1.4}$$

[1] See [1] for a recent review.

[2] Remarkably, the cascading gauge theory remains (holographically) renormalizable as a four-dimensional quantum field theory (QFT) [3] when formulated on an arbitrary background space-time manifold $\mathcal{M}_4$.

[3] Some of the counterexamples are the integrable systems, Fermi-Pasta-Ulam-Tsingou problem [20], and the gravitational collapse in AdS [21].

JHEP01(2023)130

Consider now the dynamics of this CFT in Friedmann-Lemaitre-Robertson-Walker (FLRW) Universe. Since the background geometry

$$ds^2_{FLRW} = -d\tau^2 + a(\tau)^2\, d\boldsymbol{x}^2 = a^2\, \left(-dt^2 + d\boldsymbol{x}^2\right) = a^2\, ds^2_{\text{Minkowski}}\,, \tag{1.5}$$

where $a(\tau)$ is a cosmological scale factor and $dt \equiv \frac{d\tau}{a(\tau)}$ is the conformal time, is Weyl equivalent to Minkowski space-time, there is a precise translation of the CFT dynamics in $R^{3,1}$ and FLRW. For example, the expectation values of the theory stress-energy tensor are related as

$$\langle T_{\mu\nu}(\tau,\boldsymbol{x})\rangle\Big|_{FLRW} = \frac{1}{a^4}\cdot\langle T_{\mu\nu}(t,\boldsymbol{x})\rangle\Big|_{\text{Minkowski}} + \frac{c}{8\pi^2}\left(R^{\rho\sigma}R_{\rho\mu\sigma\nu} - \frac{1}{12}R^2\cdot g_{\mu\nu}\right), \tag{1.6}$$

where c is the central charge of the CFT, $g_{\mu\nu}$ and $R_{\rho\mu\sigma\nu}$ are the metric (1.5) and the corresponding Riemann tensor. When a CFT has a holographic dual, the Weyl equivalence (1.5) is nothing but a diffeomorphism transformation of the gravitational dual [23]. Furthermore, when the non-equilibrium entropy is associated with the apparent horizon (AH) of the gravitational dual, its Minkowski space-time production rate is identical, Weyl invariant, to the corresponding FLRW comoving entropy production rate with respect to the conformal time [23]. This implies that the equilibration of a CFT state in Minkowski space-time is mapped to the evolution of the corresponding state in FLRW, where the comoving entropy approaches a constant at late-time. This late-time state is a **FLRW vacuum** of the CFT, characterized by the asymptotically vanishing comoving entropy production rate.

While it difficult to map dynamics of a massive QFT in Minkowski and FLRW Universe from the path integral viewpoint, the problem is tractable if the theory has a holographic dual. From the dual gravitational perspective, a gravitational bulk diffeomorphism relating the two boundary backgrounds (1.5) acts on a relevant coupling constant λ_Δ of a dimension $\Delta < 4$ operator $\mathcal{O}_\Delta$ as [23]

$$\lambda_\Delta \to \hat{\lambda}_\Delta(t) = a(\tau(t))^{4-\Delta}\, \lambda_\Delta\,, \tag{1.7}$$

i.e., a massive QFT dynamics with a coupling constant λ_Δ in FLRW is equivalent to the quenched dynamics of the same theory in Minkowski space-time, where the coupling $\hat{\lambda}_\Delta$ evolves according to (1.7). When $a(\tau \to +\infty) \to$ const, the QFT coupling constant is quenched as $\hat{\lambda}_\Delta(0) \equiv \lambda_\Delta \ \to \hat{\lambda}_\Delta(+\infty)$. Holographic quenches of just this type were extensively studied in [24–26]:

- the theory eventually thermalizes at late times;
- the thermalization process is irreversible — the entropy density production rate is always positive.

The last statement implies that the comoving entropy production rate of the QFT in FLRW is positive as well. When the FLRW scale factor $a(\tau)$ diverges as $\tau \to +\infty$, the mapped quenched coupling $\hat{\lambda}_\Delta$ diverges at late time as well (1.7) — it is not clear whether or not the

JHEP01(2023)130

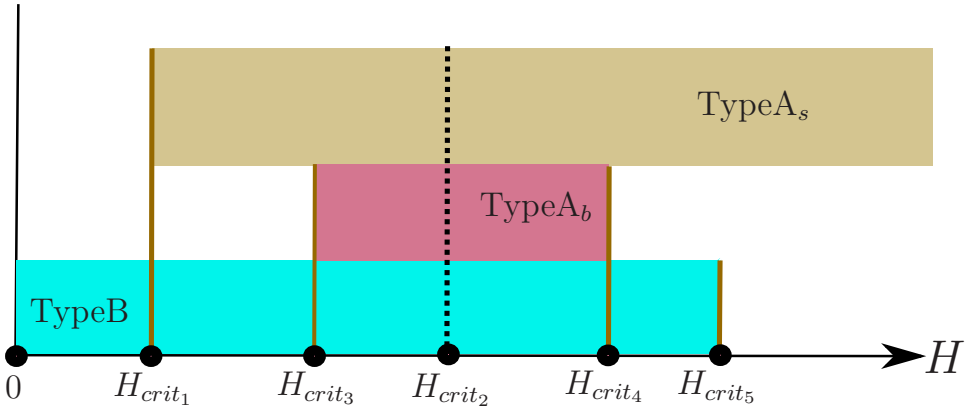

Figure 1. de Sitter vacua (TypeB) and de Sitter DFPs (TypeA$_s$ and TypeA$_b$) of the cascading gauge theory with a fixed strong coupling scale Λ. The vertical brown lines indicate the existence range for different phases: TypeA$_s$ exists for $H \in (H_{\rm crit_1}, +\infty)$; TypeA$_b$ exists for $H \in (H_{\rm crit_3}, H_{\rm crit_4})$; TypeB exists for $H \in (0, H_{\rm crit_5})$. In the range $H \in (H_{\rm crit_3}, H_{\rm crit_2})$, indicated by a vertical dashed line, TypeA$_b$ DFP is the preferred phase.

theory thermalizes; irrespectively, it can be rigorously shown[4] that the comoving entropy production rate is always positive: if $s(\tau)$ is the physical entropy density, the entropy current is given by [19]

$$\mathcal{S}^\mu = s(\tau)\ u^\mu\,, \qquad u^\mu \equiv (1,0,0,0)\,, \tag{1.8}$$

leading to the entropy density production rate $\mathcal{R}$,

$$\mathcal{R}(\tau) \equiv \nabla\cdot S = \frac{1}{a(\tau)^3}\ \frac{d}{d\tau}\left(a(\tau)^3 s(\tau)\right) = \frac{1}{a(\tau)^3}\ \frac{d}{d\tau} s_{\rm comoving}(\tau)\ \geq\ 0\,. \tag{1.9}$$

If $\mathcal{R}(\tau)$ vanishes at late times, we say the state of the QFT evolves to a FLRW vacuum; if the rate approaches a constant, we say that the state of the QFT evolves[5] to a **Dynamical Fixed Point** [19]. In case the FLRW Universe is de Sitter, i.e.,

$$a(\tau) = e^{H\tau}\,, \tag{1.10}$$

where H is the Hubble constant, the existence of the late-time limit for the entropy density production rate implies that there is a late-time limit for a physical entropy density,

$$\lim_{\tau\to\infty}\left(\nabla\cdot\mathcal{S}\right) = 3H\ \lim_{\tau\to\infty} s(\tau) = 3H\ s_{\rm ent}\,, \tag{1.11}$$

with the latter being called the *vacuum entanglement entropy* [30].

de Sitter vacua and DFPs of the cascading gauge theory were analyzed in details in [17]; we identified the following late-time spatially homogeneous and isotropic phases of the theory:

[4] This was done explicitly in case-by-case holographic models [17, 23, 25, 27–29]; we believe though that the general proof is possible.

[5] More precisely, both for a vacuum and a DFP we additionally require that one-point correlation functions of the stress-energy tensor and gauge-invariant local operators are homogeneous and time-independent.

JHEP01(2023)130

- TypeA$_s$ — the de Sitter DFP with unbroken chiral symmetry,

$$s_{\rm ent}(\Lambda, H)\Big|_{\rm TypeA_s} \neq 0\,; \tag{1.12}$$

- TypeA$_b$ — the de Sitter DFP with spontaneously broken chiral symmetry,

$$s_{\rm ent}(\Lambda, H)\Big|_{\rm TypeA_b} \neq 0\,; \tag{1.13}$$

- TypeB — the de Sitter vacuum with spontaneously broken chiral symmetry,[6]

$$s_{\rm ent}(\Lambda, H)\Big|_{\rm TypeB} = 0\,. \tag{1.14}$$

These results are summarized in figure 1:

- all phases can be reliably constructed in the supergravity approximation within a fixed range of the ratio $\frac{H}{\Lambda}$, specifically,

$$\begin{aligned}
&\text{TypeA}_s: && H \in (H_{\rm crit_1}, +\infty)\,, && H_{\rm crit_1} \approx 0.7\Lambda\,, && \\
&\text{TypeA}_b: && H \in (H_{\rm crit_3}, H_{\rm crit_4})\,, && H_{\rm crit_3} = 0.92(1)\Lambda\,; && H_{\rm crit_4} \approx 0.93\Lambda\,, \\
&\text{TypeB}: && H \in (0, H_{\rm crit_5})\,, && H_{\rm crit_5} \approx 0.97\Lambda\,, &&
\end{aligned} \tag{1.15}$$

  where we used $\approx$ to indicate that the corresponding value of $H_{\rm crit}$ is estimated from the breakdown of the supergravity approximation, see [17]. The critical value $H_{\rm crit_3}$ can be computed with an arbitrary precision within the supergravity approximation, hence we used the $=$ sign.

- Given the ratio $\frac{H}{\Lambda}$, the preferred phase is the one with the larger vacuum entanglement entropy $s_{\rm ent}$ — the latter quantity determines the entropy production rate (1.11) at late times, and the dual gravitational evolution always proceeds towards the late-time attractor with the largest apparent horizon comoving area density.[7] Thus, whenever a de Sitter DFP exists, i.e., for

$$H > H_{\rm crit_1}\,, \tag{1.16}$$

  no state of the cascading gauge theory would evolve to a vacuum (TypeB).

- It was established in [17] that

$$\begin{aligned}
&s_{\rm ent}\Big|_{\rm TypeA_b} > s_{\rm ent}\Big|_{\rm TypeA_s} && \text{for} \quad H \in (H_{\rm crit_3}, H_{\rm crit_2})\,, \\
&s_{\rm ent}\Big|_{\rm TypeA_s} > s_{\rm ent}\Big|_{\rm TypeA_b} && \text{for} \quad H > H_{\rm crit_2}\,,
\end{aligned} \tag{1.17}$$

[6] This vacuum is smoothly connected to a supersymmetric Klebanov-Strassler Minkowski vacuum [2] in the limit $\frac{H}{\Lambda} \to 0$.

[7] This is nothing but the restatement of the phase selection principle in approach to thermal equilibrium in microcanonical ensemble for de Sitter dynamics with multiple dynamical fixed points. The latter statement was explicitly verified in the holographic setting in [19].

JHEP01(2023)130

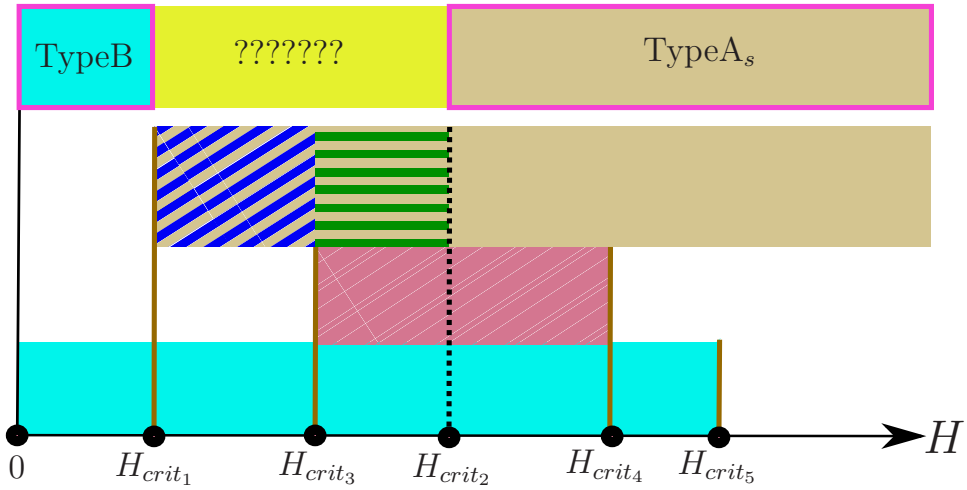

Figure 2. Diagonal blue shaded regions indicate: perturbative instability of TypeA$_s$ cascading gauge theory DFP for $H < H_{\rm crit_3}$, and perturbative instability of TypeA$_b$ cascading gauge theory DFP, whenever it exists. Horizontal green shading for $H_{\rm crit_2} < H < H_{\rm crit_3}$ indicates TypeA$_s$ cascading gauge theory DFP which is while perturbatively stable, is unstable to sufficiently large amplitude chiral symmetry breaking fluctuations. The cascading gauge theory states in de Sitter with $H < H_{\rm crit_1}$ evolve to de Sitter vacuum, TypeB-labeled bordered rectangle. The cascading gauge theory states in de Sitter with $H > H_{\rm crit_2}$ evolve to TypeA$_s$ DFP. The late-time dynamics of the cascading gauge theory states for $H_{\rm crit_1} < H < H_{\rm crit_2}$, the yellow rectangle, is unknown.

where

$$H_{\rm crit_2} = 0.92(5)\Lambda\,, \tag{1.18}$$

computable with arbitrary precision within the supergravity approximation. Thus, TypeA$_b$ DFP is the preferred attractor over TypeA$_s$ DFP whenever the former exists and for $H < H_{\rm crit_2}$. For $H > H_{\rm crit_2}$ the de Sitter dynamical fixed point with unbroken chiral symmetry, i.e., TypeA$_s$, is the preferred attractor.

In this paper we analyze perturbative stability of TypeA$_s$ and TypeA$_b$ DFPs of the cascading gauge theory. Our main results are summarized in figure 2. We find:

- Precisely at $H = H_{\rm crit_3}$ there is a zero mode of TypeA$_s$ phase, associated with the spontaneous breaking of the chiral symmetry [17]. In the limit $H \to H_{\rm crit_3} + 0$ the chiral symmetry breaking order parameters of TypeA$_b$ phase, i.e., the expectation values of the pair of dimension $\Delta = 3$ operators $\mathcal{O}_3^{\alpha=1,2}$ and the dimension $\Delta = 7$ operator $\mathcal{O}_7$ of the cascading gauge theory, vanish as $\propto (H - H_{\rm crit_3})^{1/2}$, typical for a spontaneous symmetry breaking with a mean-field exponent $\frac{1}{2}$ [17]. This zero mode is purely dissipative away from $H_{\rm crit_3}$, and behaves differently in the two distinct DFPs. Specifically,
  - in the TypeA$_s$ DFP this mode, we index it with $_{\chi\rm SB}$, has[8]

$$\mathfrak{Im}[\ \mathfrak{w}_{\chi\rm SB}\ ]\Big|_{\rm TypeA_s} \quad \begin{cases} < 0\,, & H > H_{\rm crit_3}\,, \quad \Longrightarrow \text{ stable} \\ > 0\,, & H < H_{\rm crit_3}\,, \quad \Longrightarrow \text{ unstable} \end{cases}\,, \tag{1.19}$$

[8] We use reduced frequencies in the paper, $\mathfrak{w} \equiv \frac{\omega}{H}$.

JHEP01(2023)130

and includes fluctuations of $\mathcal{O}_3^{\alpha=1,2}$ and $\mathcal{O}_7$ operators of the cascading gauge theory;

- in the TypeA$_b$ DFP, this mode exists only for $H > H_{\text{crit}_3}$ (there is no TypeA$_b$ DFP for $H < H_{\text{crit}_3}$) and is unstable,

$$\mathfrak{Im}[\ \mathfrak{w}_{\chi\text{SB}}\ ]\Big|_{\text{TypeA}_b} > 0\,, \qquad H > H_{\text{crit}_3}\,. \tag{1.20}$$

In the symmetry broken TypeA$_b$ DFP this mode is much more complicated: it couples fluctuations of $\mathcal{O}_3^{\alpha=1,2}$, $\mathcal{O}_4^{\beta=1,2}$, $\mathcal{O}_6$, $\mathcal{O}_7$, and $\mathcal{O}_8$ operators of the cascading theory.

- Because of (1.19), TypeA$_s$ DFP is perturbatively unstable for $H < H_{\text{crit}_3}$, represented by the diagonal blue shading.
- While TypeA$_s$ DFP is perturbatively stable to chiral symmetry breaking fluctuations for $H \in (H_{\text{crit}_3}, H_{\text{crit}_2})$ (represented by the horizontal green shading), it can not be non-perturbatively stable: sufficiently large-amplitude chiral symmetry breaking fluctuations must force dynamics[9] towards the preferred TypeA$_b$ DFP attractor, see (1.17).
- TypeA$_b$ is always perturbatively unstable, represented by the diagonal blue shading.

Given the fluctuation spectra stability analysis, we establish that:

- all states of the cascading gauge theory in de Sitter with the Hubble constant $H > H_{\text{crit}_2}$ evolve to TypeA$_s$ DFP (bordered rectangle);
- all states of the cascading gauge theory in de Sitter with the Hubble constant $H < H_{\text{crit}_1}$ evolve to TypeB late-time attractor — the de Sitter vacuum (bordered rectangle).
- We do not know the late-time dynamics of the cascading gauge theory in de Sitter for $H \in (H_{\text{crit}_1}, H_{\text{crit}_2})$ (yellow rectangle) — in this range both TypeA$_s$ and TypeA$_b$ DFPs are unstable, and the late-time attractor can not be a de Sitter vacuum (TypeB), which has vanishing entropy density production rate, see (1.14). We expect that in this case the cascading gauge theory states evolve, spontaneously breaking chiral symmetry, to a naked singularity, similar to the evolution of the symmetry broken states in the toy model discussed in [19]

The rest of the paper is organized as follows. In section 2 we review the de Sitter vacua and dynamical fixed points of the cascading gauge theory [17]. In section 3 we explain why perturbative stability analysis of the de Sitter dynamical fixed points are difficult. We explain why the general "master framework" developed in [29] is not suitable for the cascading gauge theory, and what straightforward modification is required. We highlight the difficulty of imposing the boundary conditions for the gravitational fluctuations, and

[9] Identical phenomenon was observed in dynamical simulations in the model covered in [19].

JHEP01(2023)130

explain how to overcome it. In section 4 we study perturbative stability of TypeA$_s$ DFP. We separate fluctuations into sets preserving the chiral symmetry of this DFP, and the fluctuations that spontaneously break the chiral symmetry. We study both sets in the near-conformal regime, i.e., when $\ln \frac{H}{\Lambda} \gg 1$ and partial analytic treatment is possible, and follow the fluctuation spectra to $H \sim \Lambda$. We identify the unstable mode in the chiral symmetry breaking sector in TypeA$_s$ DFP when $H < H_{\text{crit}_3}$. The latter mode is marginal at $H = H_{\text{crit}_3}$, where the two DFP TypeA$_s$ and TypeA$_b$ are indistinguishable. We establish that there is no instability in the chiral symmetry preserving sector of fluctuations in TypeA$_s$ DFP, at least for $H > H_{\text{crit}_3}$. In section 5 we study perturbative stability of TypeA$_b$ DFP. We show that the marginal chiral symmetry breaking mode at $H = H_{\text{crit}_3}$ becomes unstable in TypeA$_b$ DFP, perturbatively in $(H - H_{\text{crit}_3}) > 0$. We demonstrate that this mode remains unstable at least as H approaches H_{crit_2}. Our numerics indicates that the mode remains unstable even after $H > H_{\text{crit}_2}$, but this is physically irrelevant since in this regime TypeA$_b$ DFP is not preferred relative to TypeA$_s$ DFP, see (1.17). Finally, we conclude with open questions and speculations in section 6. Whenever appropriate, we delegate the technical details to appendices and focus on the physics instead.

Any stability analysis of a gravitational model are necessarily technical. This is particularly the case for the theory analyzed here[10] — many equations are too long to be presented even in appendices; we collected them as a Maple worksheet available at [31].

2 de Sitter vacua and DFPs of the cascading theory

In this section we summarize the results of [17].

Consider SU(2) × SU(2) × $\mathbb{Z}_2$ invariant states of the cascading gauge theory on a 4-dimensional manifold $\mathcal{M}_4 \equiv \partial\mathcal{M}_5$. In the planar limit and at large 't Hooft coupling, one can consistently truncate the theory to a finite number of operators [9]: a stress-energy tensor T_{ij}, a pair of dimension-3 operators $\mathcal{O}_3^{\alpha=\{1,2\}}$ (dual to gaugino condensates for each of the gauge group factors), a pair of dimension-4 operators $\mathcal{O}_4^{\beta=\{1,2\}}$, and dimension-6,7,8 operators $\mathcal{O}_6, \mathcal{O}_7, \mathcal{O}_8$. Effective gravitational action on a 5-dimensional manifold $\mathcal{M}_5$ describing holographic dual of such states was derived in [9]:

$$
\begin{aligned}
&S_5\left[g_{\mu\nu} \leftrightarrow T_{ij}, \{\Omega_i, h_i, \Phi\} \leftrightarrow \{\mathcal{O}_3^\alpha, \mathcal{O}_4^\beta, \mathcal{O}_6, \mathcal{O}_7, \mathcal{O}_8\}\right] = \\
&\frac{108}{16\pi G_5}\int_{\mathcal{M}_5} \text{vol}_{\mathcal{M}_5}\ \Omega_1\Omega_2^2\Omega_3^2 \times \\
&\times\left\{R_{10} - \frac{1}{2}(\nabla\Phi)^2 - \frac{1}{2}e^{-\Phi}\left(\frac{(h_1-h_3)^2}{2\Omega_1^2\Omega_2^2\Omega_3^2} + \frac{1}{\Omega_3^4}(\nabla h_1)^2 + \frac{1}{\Omega_2^4}(\nabla h_3)^2\right)\right. \\
&-\frac{1}{2}e^{\Phi}\left(\frac{2}{\Omega_2^2\Omega_3^2}(\nabla h_2)^2 + \frac{1}{\Omega_1^2\Omega_2^4}\left(h_2 - \frac{P}{9}\right)^2 + \frac{1}{\Omega_1^2\Omega_3^4}h_2^2\right) \\
&\left.-\frac{1}{2\Omega_1^2\Omega_2^4\Omega_3^4}\left(4\Omega_0 + h_2(h_3 - h_1) + \frac{1}{9}Ph_1\right)^2\right\},
\end{aligned}
\tag{2.1}
$$

[10] For a technically less demanding introduction to the subject of DFPs and their stability the reader is encouraged to start with [27]; see also the citations to that work.

JHEP01(2023)130

where Ω_0 is a constant,[11] and R_{10} is given by

$$\begin{aligned} R_{10} = R_5 + \left(\frac{1}{2\Omega_1^2} + \frac{2}{\Omega_2^2} + \frac{2}{\Omega_3^2} - \frac{\Omega_2^2}{4\Omega_1^2\Omega_3^2} - \frac{\Omega_3^2}{4\Omega_1^2\Omega_2^2} - \frac{\Omega_1^2}{\Omega_2^2\Omega_3^2}\right) - 2\Box \ln\left(\Omega_1\Omega_2^2\Omega_3^2\right) \\ - \left\{(\nabla \ln \Omega_1)^2 + 2\,(\nabla \ln \Omega_2)^2 + 2\,(\nabla \ln \Omega_3)^2 + \left(\nabla \ln\left(\Omega_1\Omega_2^2\Omega_3^2\right)\right)^2\right\}, \end{aligned} \tag{2.2}$$

and R_5 is the five-dimensional Ricci scalar of the metric on $\mathcal{M}_5$,

$$ds_5^2 = g_{\mu\nu}(y) dy^\mu dy^\nu \,. \tag{2.3}$$

P is the other constant, and is related to the rank-difference of the cascading gauge theory group factors M as

$$M \equiv \frac{2P}{9\alpha'} \in \mathbb{Z}\,, \tag{2.4}$$

where $\alpha' = \ell_s^2$ is the string scale. Finally, G_5 is the five dimensional effective gravitational constant

$$G_5 = \frac{27}{16\pi^3}\, G_{10}\,, \tag{2.5}$$

where $16\pi G_{10} = (2\pi)^7 g_s^2 (\alpha')^4$ is the 10-dimensional gravitational constant of type IIB supergravity, and g_s is the asymptotic string coupling constant, which we set to 1.

de Sitter vacua and DFPs of the cascading gauge theory are holographically dual to the solutions of the effective action (2.1), when the boundary metric is de Sitter with the Hubble constant H,

$$ds^2\Big|_{\mathcal{M}_4 = \partial\mathcal{M}_5} = -d\tau^2 + e^{2H\tau} d\boldsymbol{x}^2\,, \tag{2.6}$$

and all the 7 gauge invariant scalar operators of the theory $\{\mathcal{O}_3^{\alpha=1,2}, \mathcal{O}_4^{\beta=1,2}, \mathcal{O}_6, \mathcal{O}_7, \mathcal{O}_8\}$ develop a spatially constant, $\boldsymbol{x}$, and time-independent, τ, expectation values. There are two equivalent ways to represent these cascading gauge theory states in the dual gravitational bulk:

- Using the Fefferman-Graham (FG) coordinate frame,

$$\begin{aligned} ds_5^2 &= \frac{1}{h^{1/2}\rho^2}\left(-d\tau^2 + e^{2H\tau} d\boldsymbol{x}^2\right) + \frac{h^{1/2}}{\rho^2}\,(d\rho)^2\,, \qquad h = h(\rho)\,, \\ \Omega_{i=1,2,3} &= \Omega_{i=1,2,3}(\rho)\,, \qquad h_{i=1,2,3} = h_{i=1,2,3}(\rho)\,, \qquad \Phi = \Phi(\rho)\,, \end{aligned} \tag{2.7}$$

with the radial coordinate ρ, the $\partial\mathcal{M}_5$ boundary is located at $\rho \to +0$,

$$\rho \in (0, +\infty)\,. \tag{2.8}$$

Close to the boundary the metric warp factor h takes the form,

$$h = \frac{1}{8} b + \frac{1}{4} K_0 - \frac{1}{2} b \ln \rho + \mathcal{O}(\rho \ln \rho)\,, \tag{2.9}$$

[11] In the conformal limit of the cascading gauge theory, $\Omega_0 = \frac{L^4}{108}$, where L is the asymptotic AdS_5 radius.

JHEP01(2023)130

where $b \equiv P^2$ and K_0 is related to strong coupling scale Λ of the cascading gauge theory as

$$\Lambda^2 = \frac{1}{b}\, e^{-\frac{K_0}{b}}\,. \tag{2.10}$$

DFPs, TypeA, are such nonsingular gravitational solutions that

$$\text{TypeA}: \qquad \lim_{\rho\to\infty} \frac{1}{h^{1/2}\rho^2} = 0\,, \tag{2.11}$$

with all the scalars being finite in this limit. There are two distinct types of the cascading gauge theory DFPs: TypeA$_s$ and TypeA$_b$. The former preserve the U(1)$_R$ (in the large-N supergravity approximation) chiral symmetry, while the latter spontaneously breaks it to $\mathbb{Z}_2$,

$$\begin{aligned} &\text{TypeA}_s: \qquad \Omega_2 \equiv \Omega_3 \qquad \text{and} \qquad h_1 \equiv h_3 \qquad \text{and} \qquad h_2 \equiv \frac{P}{18}\,, \\ &\text{TypeA}_b: \qquad \Omega_2 \not\equiv \Omega_3 \qquad \text{and} \qquad h_1 \not\equiv h_3 \qquad \text{and} \qquad \frac{d}{d\rho}h_2 \not\equiv 0\,. \end{aligned} \tag{2.12}$$

de Sitter vacua, TypeB, are nonsingular gravitational solutions within the ansatz (2.7), such that

$$\text{TypeB}: \qquad \lim_{\rho\to\infty} \Omega_3 = 0\,, \tag{2.13}$$

with all the other scalars, as well as the $g_{\tau\tau} \equiv -\frac{1}{h^{1/2}\rho^2}$ metric component, being finite in this limit.

- Using the Eddington-Finkelstein (EF) coordinate frame,

$$\begin{aligned} ds_5^2 &= 2dt\ (dr - a\ dt) + \sigma^2 e^{2Ht}\ d\boldsymbol{x}^2\,, \qquad a = a(r)\,, \qquad \sigma = \sigma(r)\,, \\ \Omega_{i=1,2,3} &= \Omega_{i=1,2,3}(r)\,, \qquad h_{i=1,2,3} = h_{i=1,2,3}(r)\,, \qquad \Phi = \Phi(r)\,, \end{aligned} \tag{2.14}$$

with the radial coordinate r, the $\partial\mathcal{M}_5$ boundary is located now at $r \to +\infty$,

$$r \in [r_{AH}, +\infty)\,, \tag{2.15}$$

and r_{AH} is the location of the apparent horizon in the uplifted 10-dimensional type IIB supergravity background, see [17] for detailed discussion,

$$\left[\, 3H \cdot \left(\sigma^3\Omega_1\Omega_2^2\Omega_3^2\right) + a \cdot \frac{d}{dr}\left(\sigma^3\Omega_1\Omega_2^2\Omega_3^2\right)\right] \Big|_{r=r_{AH}} = 0\,. \tag{2.16}$$

It can be shown that the radial derivative in (2.16), provided $\sigma^3\Omega_1\Omega_2^2\Omega_3^2$ does not vanish — which is the case for both TypeA$_s$ and TypeA$_b$ DFPs, is always positive, thus

$$\text{TypeA}: \qquad a\Big|_{r=r_{AH}} < 0\,, \tag{2.17}$$

which further implies that there must be a point $r = r_0 > r_{AH}$, such that

$$a\Big|_{r=r_0} = 0\,. \tag{2.18}$$

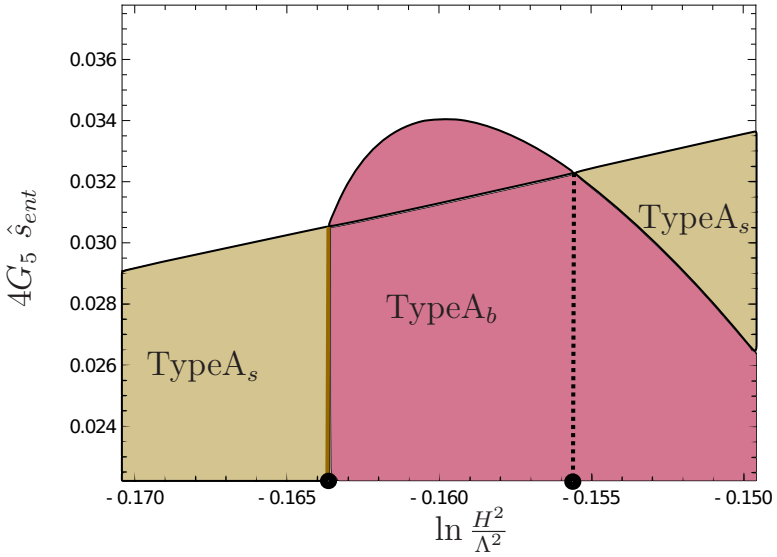

Figure 3. From [17]. Vacuum entanglement entropy densities of the chirally symmetric DFP (TypeA$_s$), and the DFP with spontaneously broken chiral symmetry (TypeA$_b$), as a function of $\ln \frac{H^2}{\Lambda^2}$.

In the EF frame description of the cascading gauge theory de Sitter vacua, i.e., TypeB, the apparent horizon is located where Ω_3 vanishes; this occurs at positive a,

$$\text{TypeB}: \qquad a\Big|_{r=r_{AH}} > 0\,. \tag{2.19}$$

EF frame description of the DFPs (or de Sitter vacua) links them directly with the late-time attractors for the evolution of the homogeneous and isotropic states[12] of the boundary gauge theory [23]: specifically, a holographic dual to such an evolution is a gravitational dynamics of (2.1) with the ansatz

$$\begin{aligned} ds_5^2 &= 2dt\ (dr - A\ dt) + \Sigma^2\ d\boldsymbol{x}^2\,, \qquad A = A(t,r)\,, \qquad \Sigma = \Sigma(t,r)\,, \\ \Omega_{1,2,3} &= \Omega_{1,2,3}(t,r)\,, \qquad h_{1,2,3} = h_{1,2,3}(t,r)\,, \qquad \Phi = \Phi(t,r)\,, \end{aligned} \tag{2.20}$$

leading to[13]

$$\lim_{t\to\infty}\left\{A(t,r)\,,\ \frac{\Sigma(t,r)}{e^{Ht}}\,,\ \Omega_i(t,r)\,,\ h_i(t,r)\,,\ \Phi(t,r)\right\} = \{a(r)\,,\ \sigma(r)\,,\ \Omega_i(r)\,,\ h_i(r)\,,\ \Phi(r)\} \tag{2.21}$$

of (2.14).

Note that besides distinct radial coordinates, ρ (FG) and r (EF), we used different bulk times τ (FG) and t (EF) in the two frames (2.7) and (2.14). There is a simple coordinate

[12]The restriction to spatially homogeneous and isotropic states, rather than *any* states, is likely not necessary for the evolution in de Sitter background, where momentum scale k inhomogeneities are red-shifted as $ke^{-H\tau}$.

[13]See [19, 27] for examples of implementation of such dynamics.

JHEP01(2023)130

transformation mapping the *full* DFP FG frame geometry, i.e., (2.7) with (2.11), to the $r \in [r_0, +\infty)$ *patch* of the corresponding EF frame geometry [17],

$$\begin{aligned} r - r_0 &= \frac{1}{\rho}\,, & t &= \tau - \int_0^\rho dz\, \sqrt{h(z)}\,, \\ a &= \frac{1}{2h^{1/2}\rho^2}\,, & \sigma &= \frac{1}{\rho h^{1/4}}\, \exp\left[H \int_0^\rho dz \sqrt{h(z)}\right]. \end{aligned} \tag{2.22}$$

The $r \in [r_{AH}, r_0)$ patch of the DFP EF frame geometry is invisible in the FG frame. Arguably, EF frame description of a dynamical fixed point is more important, as its vacuum entanglement entropy density, relatedly the late-time limit of the entropy density production rate of this DFP (1.11), is identified with the comoving gravitational entropy density of the apparent horizon in the corresponding holographic dual, see eq. (3.9) of [17],

$$s_{\rm ent} = H^3 b^2\ \hat{s}_{\rm ent} = \frac{1}{4G_5}\ 108\sigma^3\Omega_1\Omega_2^2\Omega_3^2\Big|_{r=r_{AH}}\,. \tag{2.23}$$

Figure 3 reproduces the main result of the [17]: it compares the vacuum entanglement entropy densities of the chiral symmetry preserving DFP, TypeA$_s$, and the DFP with spontaneously broken chiral symmetry, TypeA$_b$. TypeA$_b$ exists only for $H > H_{\rm crit_3}$, represented by a vertical solid brown line, and is the preferred late-time attractor for $H < H_{\rm crit_2}$, represented by a dashed black line, see (1.15). Outside the range $H \in (H_{\rm crit_3}, H_{\rm crit_2})$, and whenever it exists, i.e., for $H > H_{\rm crit_1}$, TypeA$_s$ DFP is the preferred attractor of the late-time dynamics.

Under the bulk diffeomorphism (2.22), the full EF frame background geometry corresponding to the cascading gauge theory de Sitter vacua (TypeB) is mapped to its full corresponding FG frame background geometry. Here, the vacuum entanglement entropy density vanishes [17],

$$s_{\rm ent} = H^3 b^2\ \hat{s}_{\rm ent}\Big|_{r=r_{AH}}^{\rm TypeB} = 0\,, \tag{2.24}$$

i.e., at late-times, the entropy density production rate vanishes. Since the vacuum entanglement entropy density of a dynamical fixed point is always nonzero, whenever a DFP exists, it is the preferred late-time dynamical attractor, compare to a de Sitter vacuum at the same Hubble constant. There are no DFPs of the cascading gauge theory for $H < H_{\rm crit_1}$, see (1.15).

3 Stability analysis framework of the cascading gauge theory de Sitter DFPs

Once a de Sitter DFP of a QFT is identified, it is important to analyze its stability to claim that it is indeed a late-time attractor. A DFP is *always* the preferred late-time state compare to a de Sitter vacuum of a QFT, however, a DFP can be unstable [19], in which case the late-time dynamics is unknown.[14]

[14] It is definitely not the de Sitter vacuum though!

JHEP01(2023)130

In a holographic setting, it is most natural to analyze stability of a DFP in the Eddington-Finkelstein coordinate frame of the gravitational dual [27]. Suppose a holographic QFT in d spatial dimensions has a de Sitter dynamical fixed point,

$$ds^2_{d+2} = 2dt\ \ (dr - a\ dt) + \sigma^2 e^{2Ht}\ d\boldsymbol{x}^2\,, \tag{3.1}$$

supported by the bulk scalars $\phi_j = \phi_j(r)$. We study, homogeneous and isotropic along the spatial boundary directions, linearized fluctuations $\{F_a,\, F_\sigma,\, F_j\}$ about the background (3.1),

$$a(r) \to a(r) + F_a(r)e^{-i\omega t}\,, \qquad \sigma(r) \to \sigma(r) + F_\sigma(r)e^{-i\omega t}\,, \qquad \phi_j(r) \to \phi_j(r) + F_j(r)e^{-i\omega t}\,. \tag{3.2}$$

Imposing a normalizability of the fluctuations at the asymptotic boundary, and regularity of the spatial profiles of $\{F_a,\, F_\sigma,\, F_j\}$ in the background (3.1) as $r \in [r_{AH}, \infty)$, we can compute the spectrum of fluctuations, i.e., the set of frequencies $\{\omega\}$. Since apparent horizon is dissipative, the frequencies will be complex. Any fluctuation mode with

$$\mathfrak{Im}[\omega] > 0 \tag{3.3}$$

signals an instability of the DFP, represented by (3.1).

Unfortunately, the above prescription can not be applied to the stability analysis of the cascading gauge theory DFPs, reviewed in section 2. The stumbling block is the relation between the EF and the FG frame time coordinates (2.22), which, given the asymptotic expansion for h (2.9), makes the EF frame $r \to \infty \iff \rho \to 0$ boundary asymptotics intractable.[15] The prescription to circumvent this difficulty was introduced in [32]. The cascading gauge theory DFPs are constructed in the FG coordinate frame [17]. To compute the vacuum entanglement entropy, the region of the FG geometry in the vicinity of $r = r_0 \iff \rho = \infty$, see (2.22), is mapped into EF coordinate frame, and further extended in this frame for $r \in [r_{AH}, r_0]$. Additional complexities of the EF frame appear when one studies linearized fluctuations, as in (3.2): here, one needs to solve equations not only for the bulk scalar fluctuations F_j, but for the fluctuations of the metric components as well, $\{F_a, F_\sigma\}$.

In [29] we explained how to compute the spectrum of fluctuations about a DFP directed in the FG coordinate frame, for any holographic model with an arbitrary "$d+2$ dimensional Einstein gravity plus arbitrary bulk scalars". The computational framework presented there is highly efficient: one needs to solve only the fluctuation equations for the bulk scalars, while the fluctuations of the metric components are determined algebraically from the latter. Unfortunately, this master equation framework can not be directly applied to the cascading gauge theory gravitational dual. Here, the issue is that the holographic models of [29] must have the standard Einstein-Hilbert term in the gravitational action, while in the cascading gauge theory gravitational dual the Einstein-Hilbert term is warped (2.1):

$$S_{d+2} \propto \underbrace{\int_{\mathcal{M}_{d+1}} d^{d+2}\xi\sqrt{-g}\Big[R + \cdots\Big]}_{\text{master equations}} \quad \text{vs.} \quad S_5 \propto \underbrace{\int_{\mathcal{M}_5} \text{vol}_{\mathcal{M}_5}\ \Omega_1\Omega_2^2\Omega_3^2\Big[R_5 + \cdots\Big]}_{\text{cascading gauge theory}}\,. \tag{3.4}$$

[15] The presence of high dimension operators of the cascading gauge theory, such as $\mathcal{O}_6$, $\mathcal{O}_7$ and $\mathcal{O}_8$, requires exquisite control of the asymptotic boundary data.

JHEP01(2023)130

Of course, we can always Weyl rescale the metric to remove the Einstein-Hilbert term warp factor, but this would require a new complicated differential relation between the FG frame radial coordinates, involving fractional powers of h. This causes the same problems as we faced in the EF coordinate frame: the boundary $\rho \to 0$ asymptotics become intractable; additionally, the change of variables dramatically complicates the master equations for the fluctuations.

Above difficulty is resolved noting that the effective five-dimensional gravitational action (2.1) is a Kaluza-Klein reduction of Type IIB supergravity on warped deformed conifold with fluxes. Thus, we should be apply the apply the master equations formalism of [29], more precisely its obvious variation, in ten dimensions without any problem. This is what we do in appendix[16] A.1.

We finish this section highlighting the subtlety developing the near-boundary $\rho \to 0$ asymptotic expansions of the equations representing the fluctuations. The equation of motion for a probe massive bulk scalar field dual to an operator of conformal dimension Δ, on AdS_5 background geometry takes the form,

$$\phi = \rho^{\Delta}\Big(A_0 + \sum_{k=1}^{\infty} A_k \rho^k\Big) + \rho^{4-\Delta}\Big(B_0 + \sum_{k=1}^{\infty} B_k \rho^k\Big)\,. \tag{3.5}$$

When $\Delta \in \mathbb{Z}$ or $\Delta \in \mathbb{Z}_{n+\frac{1}{2}}$ logarithmic terms appear in this asymptotic expansion, i.e., the series in brackets generalize as

$$\sum_{k=1}^{\infty} A_k \rho^k \to \sum_{k=1}^{\infty} \rho^k \sum_{m=0}^{M(k)} A_{k;m} \ln^m \rho\,. \tag{3.6}$$

It is important that the number of $\ln\rho$ terms at each fixed order in k is bounded by $M(k)$. In fact, the metric ansatz (2.7) for the cascading gauge theory, along with the ansatz for the scalars $\Omega_{1,2,3} \propto h^{1/4} f_{a,b,c}^{1/2}$ was proposed in [3] precisely so that the asymptotic expansions of the metric warp factor h, as well as the scalars $f_{a,b,c}$, have finite number of log-terms at each given order of ρ^k. This is evident in the asymptotic expansions of the background geometry dual to the cascading gauge theory DFPs, reviewed in appendix A.2. Finite number of log-terms in the asymptotic expansion is a fairly trivial complication. Rather, we find that the master formalism for the fluctuations, see appendix A.1, leads to an infinite number of log-terms in their asymptotic expansions at each finite order of ρ^k. In other words, the generalization (3.6) is yet further generalized:

$$\sum_{k=1}^{\infty} \rho^k \sum_{m=1}^{M(k)} A_{k;m} \ln^m \rho \;\to\; \sum_{k=1}^{\infty} \rho^k \cdot \mathcal{A}_k(\ln\rho)\,, \tag{3.7}$$

where $\mathcal{A}_k(z)$ are now nontrivial functions of $z \equiv \ln\rho$, and in developing the asymptotic expansions, at each order ρ^k, we must solve a coupled system (if there is more than one bulk scalar) of differential equations for $\mathcal{A}_k(z)$. This would be a hopeless task in general.

[16] While the discussion there is attempted to be self-contained, the reader does need familiarity with the formalism of [29].

JHEP01(2023)130

Lucking for the problem at hand, carefully analyzing the structure of log-term differential equations we find that their solution is given by (schematically)

$$\mathcal{A}_k(z) = \frac{1}{(b-4bz+2K_0)^{n(k)}} \sum_{m=0}^{M(k)} A_{k;m}\, z^m\,, \tag{3.8}$$

where $n(k)$ and $M(k)$ are some integers $\sim k$. The denominator factor in (3.8) is simply the order $\mathcal{O}(\rho^0)$ terms of asymptotic expansion of the h factor, see (2.9).

4 Stability analysis of TypeA$_s$ DFP

TypeA$_s$ dynamical fixed point of the cascading gauge theory preserves the chiral symmetry. There are two decoupled sets of fluctuations about this DFP: the fluctuations breaking the chiral symmetry (see section 4.1 with technical details in appendix B), and the fluctuations preserving the chiral symmetry (see section 4.2 with technical details in appendix C).

TypeA$_s$ DFPs were constructed in various computations schemes (see appendix C.1 of [17]): either parameterized by b with $K_0 = 1$, see (2.10),

$$\ln\frac{H^2}{\Lambda^2} = \frac{1}{b} + \ln b\,, \qquad b \in (0,1]\,, \tag{4.1}$$

or with $b = 1$ and

$$\ln\frac{H^2}{\Lambda^2} = K_0\,. \tag{4.2}$$

An excellent agreement was reported in the overlap of the two computational schemes, i.e., for $K_0 > 1$. The parameterization (4.1) is useful to analyze $b \to 0$, correspondingly $H \gg \Lambda$, near-conformal limit, where perturbative in b treatment is possible. The parameterization (4.2) is needed to access TypeA$_s$ DFP in $H < \Lambda$ region, not accessible with (4.1). We use the same strategy in computing the spectra of fluctuations: first we perform the computations in the near-conformal limit, and further extend the results for $H < \Lambda$.

4.1 Chiral symmetry breaking sector

Chiral symmetry breaking fluctuations about TypeA$_s$ DFP activate the cascading gauge theory operators of conformal dimensions $\Delta = \{3, 7\}$. Thus, in the near conformal limit, i.e., for $H \gg \Lambda$, we expect [29] discrete branches indexed with $n \in \mathbb{Z}_{\geq 3}$ and

$$\mathfrak{Re}[\mathfrak{w}^{(n)}_{\chi\text{SB}}] = 0\,, \qquad \mathfrak{Im}[\mathfrak{w}^{(n)}_{\chi\text{SB}}] \equiv -\Gamma^{(n)}_{\chi\text{SB}} \neq 0\,. \tag{4.3}$$

We use the subscript $_{\chi\text{SB}}$ to indicate that the fluctuations spontaneously break chiral symmetry of TypeA$_s$ DFP. We find that the branches with $3 \leq n \leq 6$ are doubly degenerate in the limit $b \to 0$, while those with $n \geq 7$ are triple degenerate in the conformal limit. In figure 4 dots represent the attenuation $\Gamma^{(n)}_{\chi\text{SB}}$ as a function of $\ln^{-1}\frac{H^2}{\Lambda^2}$ for the lowest $n = 3$ mode (the left panel) and the $n = 4$ mode (the right panel). The dashed curves indicate $\mathcal{O}(\sqrt{b})$ analytic leading order corrections, see appendix B.1.1, and the solid lines include next-to-leading $\mathcal{O}(b)$ order corrections:

$$\begin{aligned}\Gamma^{(3)}_{\chi\text{SB}} &= 3 \pm \sqrt{2b} - 1.57(5)\cdot b \pm \mathcal{O}(b^{3/2})\,,\\ \Gamma^{(4)}_{\chi\text{SB}} &= 4 \pm \sqrt{2b} + 1.93(4)\cdot b \pm \mathcal{O}(b^{3/2})\,,\end{aligned} \tag{4.4}$$

where b is related to $\frac{H}{\Lambda}$ as in (4.1).

JHEP01(2023)130

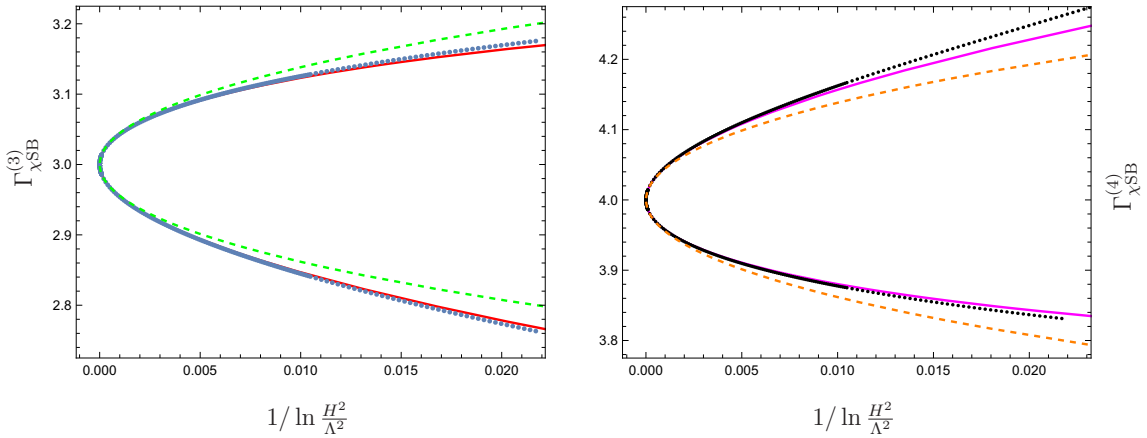

Figure 4. Attenuation $\Gamma^{(n)}_{\chi SB} \equiv -\mathfrak{Im}[\mathfrak{w}^{(n)}_{\chi SB}]$ of the chiral symmetry breaking fluctuations about cascading gauge theory TypeA$_s$ DFP for $H \gg \Lambda$. Dashed and solid curves are correspondingly the leading and the first subleading order corrections to the conformal spectra, see (4.4).

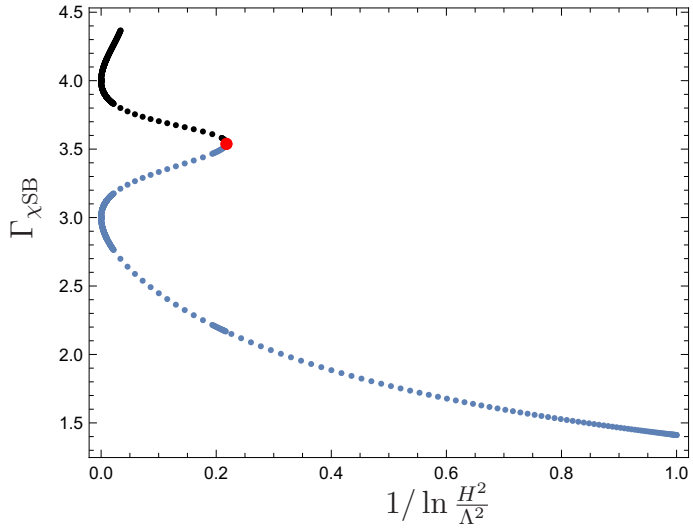

Figure 5. Sub-branches of the distinct in the conformal limit branches of the fluctuations coalesce as $\frac{H}{\Lambda}$ is lowered. The red dot, see (4.5), highlights this phenomenon for $n = 4$ and $n = 3$ sub-branches.

As b increases, we discover that the distinct branches of the fluctuations coalesce, see figure 5. Specifically we find that the lower sub-branch of the $n = 4$ branch and the upper sub-branch of the $n = 3$ branch combine at

$$\ln^{-1}\frac{H^2}{\Lambda^2} = 0.217(8)\,, \tag{4.5}$$

represented by the red dot, and are removed from the spectrum. This phenomenon is quite generic, and is observed for higher n branches as well. It can not be universal though: the lower sub-branch of the $n = 3$ branch is the lowest mode in the spectrum, thus, it does not have a partner to combine with.

It becomes numerically challenging to study higher n spectral branches at finite $\frac{H}{\Lambda}$. In particular, we could not stabilize numerics at $n = 7$ branch where the first triple degeneracy

JHEP01(2023)130

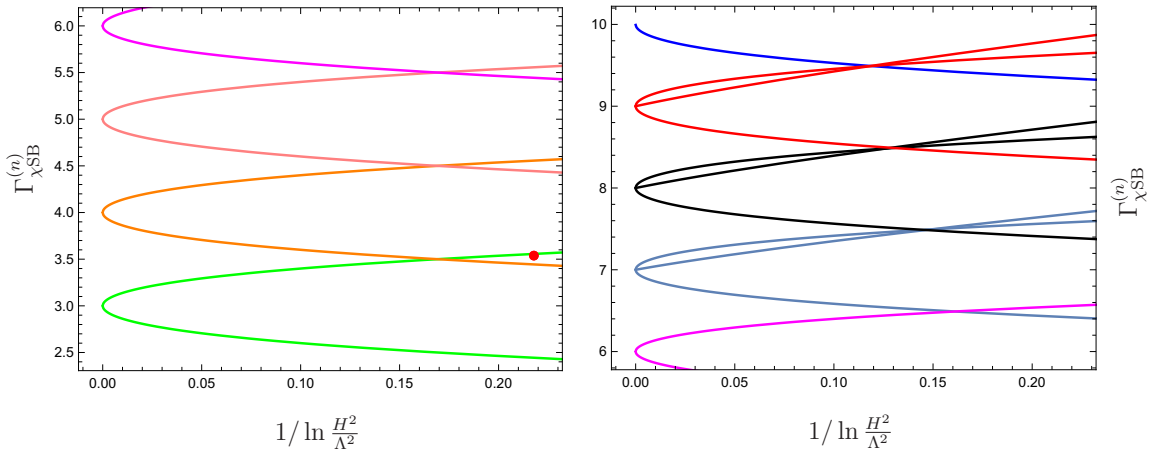

Figure 6. Leading order correction to the conformal spectra for the chiral symmetry breaking fluctuations at higher n. Note that the (perturbative) coalescence of various sub-branches is quite generic. The red dot (the left panel) is a replot of the red dot from figure 5.

occurs. There is no obstruction to study these branches perturbatively in the small b, the near conformal limit, e.g., see appendices B.1.2 and B.1.3. In figure 6 we present leading order correction to the conformal spectra for $3 \leq n \leq 6$ (the left panel) and for $6 \leq n \leq 10$ (the right panel). Note that the non-analytic sub-branches, see appendix B.1, (perturbatively) combine — as the red dot (the left panel), replotted from figure 5, indicates the perturbative prediction for the coalescence is quite reasonable.[17] It appears (the right panel) that for $n \geq 7$ the coalescence point involved three sub-branches — this is not the case, as the better resolution of the plots demonstrates.

The lower sub-branch of the $n = 3$ branch is the lowest lying. In figure 5 we followed this branch all the way to $b = 1$, correspondingly to $\ln\frac{H^2}{\Lambda^2} = 1$, see (4.1). In figure 7 we switch the computational scheme to that of (4.2), and follow this sub-branch for $H < \Lambda$, represented by the magenta dots. This mode becomes marginal at

$$\ln\frac{H^2_{\text{crit}_3}}{\Lambda^2} = -0.1636(3)\,, \tag{4.6}$$

represented by the vertical red line, reproducing the critical Hubble constant H_{crit_3}, corresponding to the origin of the TypeA$_b$ dynamical fixed point with the spontaneously broken chiral symmetry, originally reported in [17]. Note that for $H < H_{\text{crit}_3}$ this mode becomes unstable. This establishes our first main result:

> *The chirally symmetric TypeA$_s$ DFP of the cascading gauge theory is perturbative unstable when $H < H_{\text{crit}_3}$, given by* (4.6).

4.2 Chiral symmetry preserving sector

Chiral symmetry preserving fluctuations about TypeA$_s$ DFP activate the cascading gauge theory operators of conformal dimensions $\Delta = \{4, 6, 8\}$. Thus, in the near conformal limit,

[17] Our numerical work, not reported here, established joining of $n = 5$ and $n = 4$, as well as $n = 6$ and $n = 5$ sub-branches.

JHEP01(2023)130

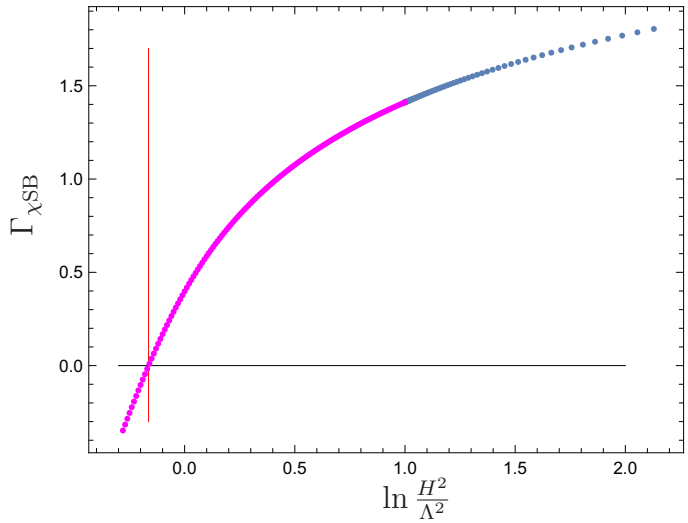

Figure 7. The lower sub-branch of the $n = 3$ branch of chiral symmetry breaking fluctuations about TypeA$_s$ DFP of the cascading gauge theory becomes unstable for $H < H_{\text{crit}_3}$ (4.6), represented by the red vertical line.

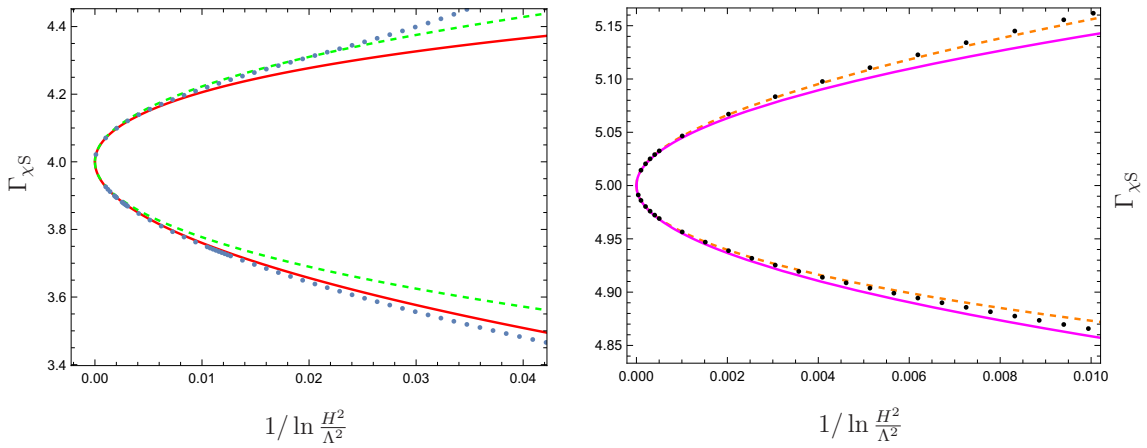

Figure 8. Attenuation $\Gamma^{(n)}_{\chi\text{SB}} \equiv -\mathfrak{Im}[\mathfrak{w}^{(n)}_{\chi\text{SB}}]$ of the chirally symmetric fluctuations about cascading gauge theory TypeA$_s$ DFP for $H \gg \Lambda$. Dashed and solid curves are correspondingly the leading and the first subleading order corrections to the conformal spectra, see (4.8).

i.e., for $H \gg \Lambda$, we expect [29] discrete branches indexed with $n \in \mathbb{Z}_{\geq 4}$ and

$$\mathfrak{Re}[\mathfrak{w}^{(n)}_{\chi\text{S}}] = 0\,, \qquad \mathfrak{Im}[\mathfrak{w}^{(n)}_{\chi\text{SB}}] \equiv -\Gamma^{(n)}_{\chi\text{S}} \neq 0\,. \tag{4.7}$$

We use the subscript $_{\chi\text{S}}$ to indicate that the fluctuations are chirally symmetric.. We find that the branches with $n = \{4, 5\}$ are doubly degenerate in the limit $b \to 0$, while those with $n \geq 6$ are triple degenerate in the conformal limit. In figure 8 dots represent the attenuation $\Gamma^{(n)}_{\chi\text{S}}$ as a function of $\ln^{-1} \frac{H^2}{\Lambda^2}$ for the lowest $n = 4$ mode (the left panel) and the $n = 4$ mode (the right panel). The dashed curves indicate $\mathcal{O}(\sqrt{b})$ analytic leading order corrections, see

JHEP01(2023)130

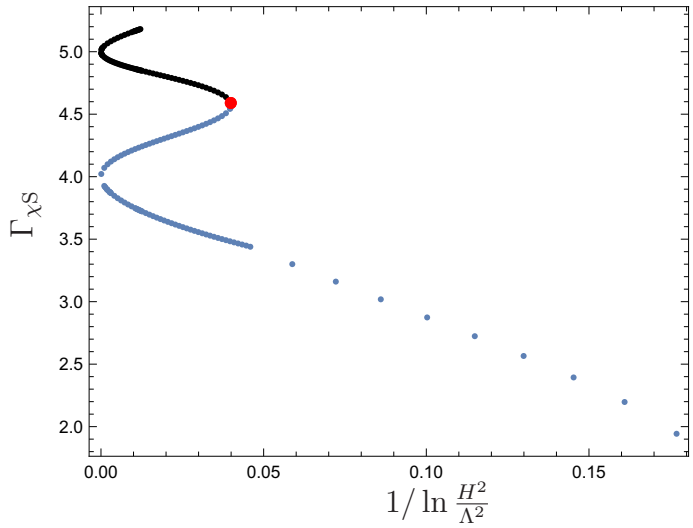

Figure 9. Sub-branches of the distinct in the conformal limit branches of the fluctuations coalesce as $\frac{H}{\Lambda}$ is lowered. The red dot, see (4.9), highlights this phenomenon for $n = 5$ and $n = 4$ sub-branches.

appendix C.1.1, and the solid lines include next-to-leading $\mathcal{O}(b)$ order corrections:

$$\begin{aligned}\Gamma^{(4)}_{\chi\mathrm{S}} &= 4 \pm \frac{\sqrt{130b}}{5} - 1.79(1)\cdot b \pm \mathcal{O}(b^{3/2})\,,\\ \Gamma^{(5)}_{\chi\mathrm{S}} &= 5 \pm \sqrt{2b} + 1.45(6)\cdot b \pm \mathcal{O}(b^{3/2})\,,\end{aligned} \tag{4.8}$$

where b is related to $\frac{H}{\Lambda}$ as in (4.1).

As in section 4.1, as b increases, the distinct branches of the fluctuations coalesce, see figure 9. Specifically we find that the lower sub-branch of the $n = 5$ branch and the upper sub-branch of the $n = 4$ branch combine at

$$\ln^{-1}\frac{H^2}{\Lambda^2} = 0.039(9)\,, \tag{4.9}$$

represented by the red dot, and are removed from the spectrum.

In figure 10 we present leading order correction to the conformal spectra for $n = \{4, 5\}$ (the left panel) and for $5 \leq n \leq 8$ (the right panel). Note that the non-analytic sub-branches, see appendix C, (perturbatively) combine — the red dot (the left panel) is replotted from figure 9.

In figure 11 we show that the lowest lying mode in the chiral symmetry preserving sector of fluctuations about TypeA$_s$ DFP remains perturbatively stable, at least for $H > H_{\mathrm{crit}_3}$, represented by the vertical red line (the right panel). The solid green curve is the perturbative approximation to the mode, see $\Gamma^{(4)}_{\chi\mathrm{S}}$ in (4.8). The blue dots are obtained in the computation scheme (4.1), and the magenta dots are obtained in the computation scheme (4.2).

This establishes our second main result:

> *The chirally symmetric TypeA$_s$ DFP of the cascading gauge theory is perturbative stable when $H > H_{\mathrm{crit}_3}$, given by (4.6).*

JHEP01(2023)130

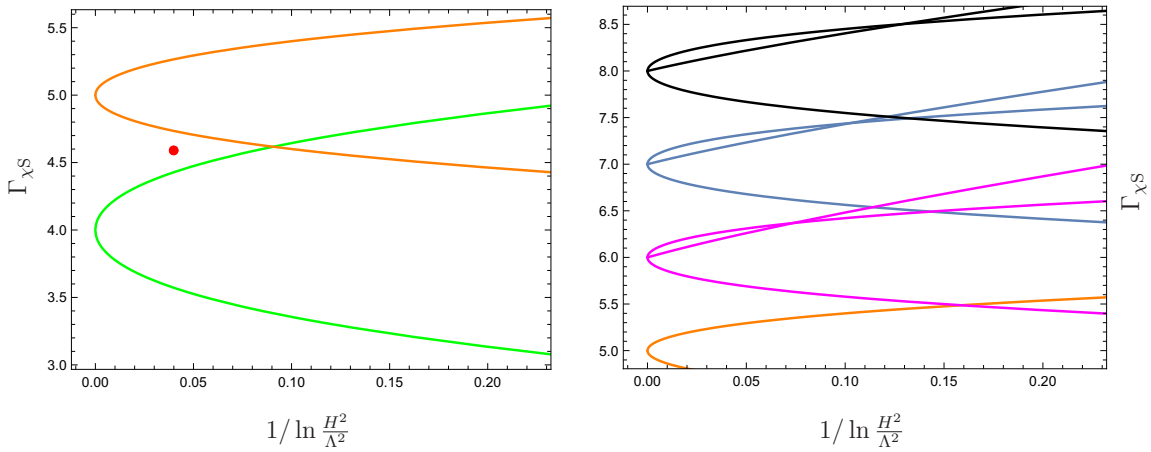

Figure 10. Leading order correction to the conformal spectra for the chiral symmetry breaking fluctuations at higher n. Note that the (perturbative) coalescence of various sub-branches is quite generic. The red dot (the left panel) is a replot of the red dot from figure 9.

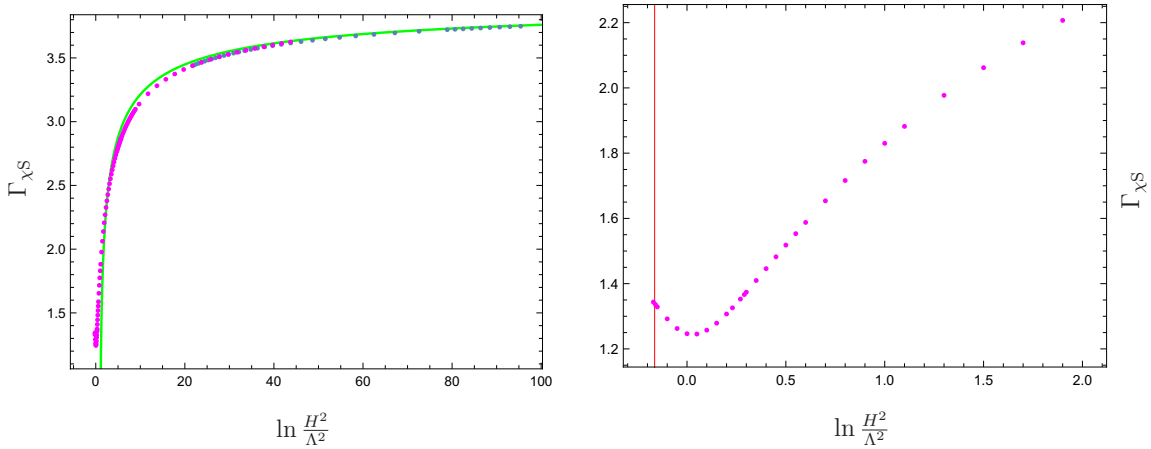

Figure 11. The lower sub-branch of the $n = 4$ branch of chirally symmetric fluctuations about TypeA$_s$ DFP of the cascading gauge theory remains perturbatively stable for $H > H_{\text{crit}_3}$ (4.6), represented by the red vertical line.

5 Stability analysis of TypeA$_b$ DFP

TypeA$_b$ dynamical fixed point of the cascading gauge theory with spontaneous broken chiral symmetry [17] exists only for $H > H_{\text{crit}_3}$, given by (4.6). Exactly at $H = H_{\text{crit}_3}$ TypeA$_s$ and TypeA$_b$ DFPs are indistinguishable. Additionally, at this critical value of the Hubble constant, the DFP has a marginal chiral symmetry breaking mode — this is the lower sub-branch of the $n = 3$ fluctuations about TypeA$_s$ DFP, see figure 7. In figure 12 we present the attenuation of this mode, as a fluctuation about TypeA$_b$ DFP. Note that the mode is *always* unstable. In the left panel we present $\Gamma_{\chi\text{SB}}$ with TypeA$_b$ DFP parameterized using the chiral symmetry breaking order parameter A of this DFP, see (D.2). This is useful, as it provides a ready comparison with the perturbative results of appendix D, see (D.1), represented by a solid red curve. The translation between the order

JHEP01(2023)130

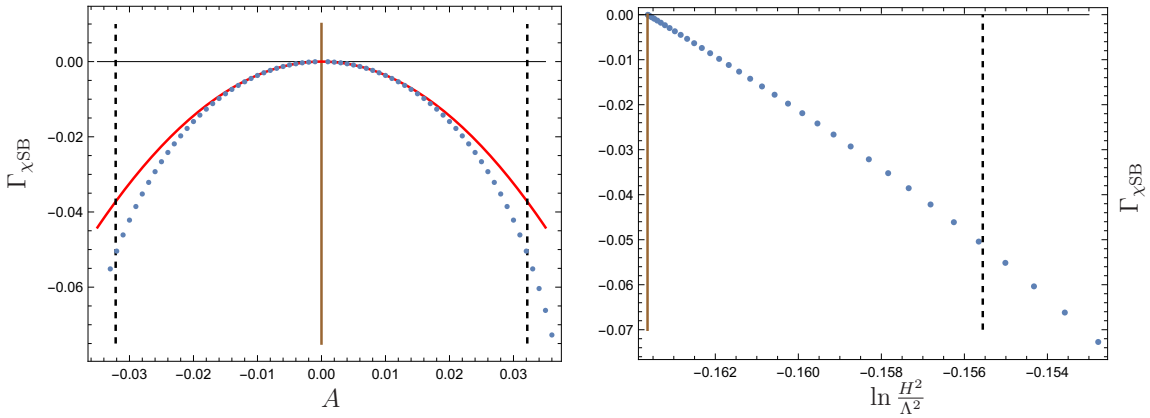

Figure 12. The marginal at $H = H_{\text{crit}_3}$ chiral symmetry breaking mode becomes unstable in TypeA$_b$ DFP. In the left panel we parameterize this mode with the order parameter A of the chiral symmetry breaking of TypeA$_b$ DFP, see (D.2). In the right panel we show the attenuation $\Gamma_{\chi\text{SB}}$ of this mode as a function of $\ln \frac{H^2}{\Lambda^2}$. The solid red curve represent perturbative approximation, close to criticality, see (D.1). The vertical brown lines represent $H = H_{\text{crit}_3}$, and the vertical dashed black lines represent $H = H_{\text{crit}_2}$.

parameter A and the physical label (4.2) of TypeA$_b$ DFP is shown in figure 13; the latter is further used to generate the plot in the right panel of figure 12. The vertical solid brown lines correspond to $H = H_{\text{crit}_3}$, and the vertical dashed black lines correspond $H = H_{\text{crit}_2}$ — recall that for $H > H_{\text{crit}_2}$, chirally symmetric TypeA$_s$ DFP is the preferred dynamical attractor compare to the symmetry broken TypeA$_b$ DFP, see figure 3.

Our final main result is:

TypeA$_b$ DFP of the cascading gauge theory is perturbative unstable.

6 Future directions and speculations

In this paper we presented comprehensive stability analysis of the de Sitter dynamical fixed points of the cascading gauge theory. The late-time attractor of the theory is determined by the ratio of the de Sitter Hubble constant H and the strong coupling scale Λ of the theory. We presented strong evidence that for $H > H_{\text{crit}_2}$, an arbitrary initial state of the gauge theory would evolve to a chirally symmetric DFP, TypeA$_s$. On the other hand, an arbitrary state of the theory with $H < H_{\text{crit}_1}$ is expected to evolve to a de Sitter vacuum, with vanishing comoving entropy density production rate asymptotically. Since $H_{\text{crit}_1} < H_{\text{crit}_2}$, what is the late-time dynamics of the cascading gauge theory state in de Sitter with the Hubble constant in the range $H \in (H_{\text{crit}_1}, H_{\text{crit}_2})$ is unknown. In our view, this is the biggest open question.

Note that all the dynamical fixed points of the cascading gauge theory identified in [17] have unbroken SU(2) × SU(2) global symmetry. The reason for this limitation is simple: we do not know the dual holographic description of the cascading gauge theory outside of this SU(2) × SU(2) symmetric sector (2.1). It is possible that for $H < \Lambda$, the above global symmetry is spontaneously broken as well, and the new DFPs are stable. We can only imagine how horrendously complicated it would be to analyze such DFPs!

JHEP01(2023)130

Another interesting question is the role confinement plays in producing de Sitter DFPs of non-conformal field theories in the first place. In other non-conformal holographic models, as discussed in [27] and [19], the late time attractor of the de Sitter evolution of these models is *always* a dynamical fixed point, i.e., the state with the non-vanishing comoving entropy production rate.[18] In other words, there is no analogue of the cascading gauge theory TypeB de Sitter vacuum. Intuitively, the holographic description of confinement in de Sitter is fairly robust, at least when $H \ll \Lambda$, and thus it is natural to expect that with a large hierarchy of scales between the confinement scale and the Hubble constant, as it is in our Universe, there is no dynamical fixed point at late times. Can we find a holographic model where a dynamical fixed point exists in the limit $\frac{H}{m} \to 0$? Can the idea that a dynamical fixed point requires deconfinement of the gauge theory be made precise, or shown to be false?

Clearly it is interesting to explore other holographic models in de Sitter and analyze the corresponding DFPs.

Acknowledgments

Research at Perimeter Institute is supported in part by the Government of Canada through the Department of Innovation, Science and Economic Development Canada and by the Province of Ontario through the Ministry of Colleges and Universities. This work is further supported by a Discovery Grant from the Natural Sciences and Engineering Research Council of Canada.

A Symmetry broken DFP — TypeA$_b$

In this appendix we discuss the linearized fluctuations about TypeA_b dynamical fixed point of the cascading gauge theory. In section A.1 we apply a straightforward generalization of the *master equation* formalism [29] to derive the equations of motion for the fluctuations. The final equations are too long/complicated to be collected in the paper — they are available as a Maple worksheet in [31]. In section A.2 we discuss the boundary conditions, both for the background geometry and for the fluctuations.

A.1 Equations of motion

As explained in section 3, we consider the cascading gauge theory DFPs and linearized fluctuations about them in ten-dimensional Type IIB supergravity. The detailed discussion of the uplift can be found in [17].

For the Fefferman-Graham metric ansatz (with spatially homogeneous and isotropic background metric of the cascading gauge theory $\propto d\boldsymbol{x}^2$) we take

$$ds_{10}^2 = -\hat{c}_1^2\, d\tau^2 + \hat{c}_2^2\, d\boldsymbol{x}^2 + \hat{c}_3^2\, d\rho^2 + \underbrace{\hat{\Omega}_1^2\, g_5^2 + \hat{\Omega}_2^2\, \left(g_3^2 + g_4^2\right) + \hat{\Omega}_3^2\, \left(g_1^2 + g_2^2\right)}_{\text{new compare to master formalism}}, \tag{A.1}$$

[18] We expect that DFPs discussed there will become unreliable then $H \ll m$, where m is the mass-scale of the models.

JHEP01(2023)130

with

$$\begin{aligned}
\hat{c}_1 &= \frac{\sqrt{\hat{G}_{tt}}}{\rho\,\hat{h}^{1/4}}\,, & \hat{c}_2 &= \frac{\sqrt{\hat{G}_{\boldsymbol{xx}}}}{\rho\,\hat{h}^{1/4}}\,, & \hat{c}_3 &= \frac{\hat{h}^{1/4}}{\rho}\,,\\
\hat{\Omega}_1 &= \frac{1}{3}\,\hat{f}_c^{1/2}\left(\hat{h}\right)^{1/4}\,, & \hat{\Omega}_2 &= \frac{1}{\sqrt{6}}\,\hat{f}_a^{1/2}\left(\hat{h}\right)^{1/4}\,, & \hat{\Omega}_3 &= \frac{1}{\sqrt{6}}\,\hat{f}_b^{1/2}\left(\hat{h}\right)^{1/4}\,,
\end{aligned} \tag{A.2}$$

where we highlighted the part of the metric new compare to the general ansatz of [29]. Additionally we set

$$\hat{h}_1 = \frac{1}{P}\left(\frac{\hat{K}_1}{12} - 36\Omega_0\right)\,, \qquad \hat{h}_2 = \frac{P}{18}\hat{K}_2\,, \qquad \hat{h}_3 = \frac{1}{P}\left(\frac{\hat{K}_3}{12} - 36\Omega_0\right)\,, \qquad \hat{g} = e^{\hat{\Phi}}\,, \tag{A.3}$$

where we use $\hat{}$ to indicate that the corresponding functions depend on ρ and τ. In (A.1), g_i (for $i = 1, \cdots, 5$) are the usual one-forms defined on the warped-squashed $T^{1,1}$ [33].

Following [29], we introduced linearized fluctuation, $\delta\cdots$, on top of the background solution specified by [17]

$$\{f_{a,b,c}\,,\ h\,,\ K_{1,2,3}\,,\ g\}\,, \tag{A.4}$$

specifically,

$$\begin{aligned}
\sqrt{\hat{G}_{tt}} &= 1 + \delta\hat{g}_{11}\,, & \sqrt{\hat{G}_{\boldsymbol{xx}}} &= e^{H\tau}\,(1 + \delta\hat{g}_{22})\,, & \hat{f}_{a,b,c} &= f_{a,b,c}(\rho) + \delta\hat{f}_{a,b,c}\,,\\
\hat{h} &= h(\rho) + \delta\hat{h}\,, & \hat{K}_{1,2,3} &= K_{1,2,3}(\rho) + \delta K_{1,2,3}\,, & \hat{g} &= g(\rho) + \delta\hat{g}\,.
\end{aligned} \tag{A.5}$$

Notice that the h factor enters both in the definition of the background DFP metric, e.g., see $\hat{c}_1$ in (A.2), and the five-dimensional bulk scalars Ω_i (A.2). This is necessary to produce equations of motion without the fractional powers of h [3].

Assuming the harmonic time-dependence for the fluctuations, i.e.,

$$\begin{aligned}
\delta\hat{g}_{11} &= e^{-i\omega\tau}H_1(\rho)\,, & \delta\hat{g}_{22} &= e^{-i\omega\tau}H_2(\rho)\,, & \delta\hat{f}_{a,b,c} &= e^{-i\omega\tau}H_{a,b,c}(\rho)\,,\\
\delta\hat{h} &= e^{-i\omega\tau}H_h(\rho)\,, & \delta\hat{K}_{1,2,3} &= e^{-i\omega\tau}H_{K_{1,2,3}}(\rho)\,, & \delta\hat{g} &= e^{-i\omega\tau}H_g(\rho)\,,
\end{aligned} \tag{A.6}$$

we derive 11 equations[19] for 10 fluctuations:

$$\left\{H_{a,b,c}\,,\ H_{1,2}\,,\ H_h\,,\ H_g\,,\ H_{K_{1,2,3}}\,.\right\} \tag{A.7}$$

These equations are collected in [31]. It is convenient to further introduce

$$\omega = -iHs\,, \tag{A.8}$$

effectively measuring all energy scales in Hubble units. To declutter the formulas we set from now on the Hubble constant to unity $H = 1$.

The master formalism of [29] allowed to eliminate algebraically — solve their corresponding equations — the fluctuations H_1 and H_2 as

$$\text{master}: \qquad H_1 = H_2 = \left.\frac{(d-2)H_h}{4(d-1)h}\right|_{d=3\,,\,\text{in our case}} = \frac{H_h}{8h}\,. \tag{A.9}$$

[19] The 11's equation is the Einstein equation with coordinate indices $_{\rho\tau}$.

JHEP01(2023)130

Such substitution will not work for the cascading gauge theory gravitational dual: from the 5d perspective because the Einstein-Hilbert term in the Kaluza-Klein reduced effective action is warped (3.4), or from the 10d perspective because of extra contributions in the metric (A.1). Instead, we find that a substitution

$$H_1 = H_2 = -\frac{H_h}{2h} - \frac{H_a}{2f_a} - \frac{H_b}{2f_b} - \frac{H_c}{4f_c} \tag{A.10}$$

solves the equations for $H_{1,2}$. Furthermore, much like in [29], the equation for H_h is of the first-order, and can be solved algebraically in terms of the other fluctuations and their first-order (radial coordinate) derivatives.

As explained in [29], while the boundary conditions for the fluctuations in the EF coordinate frame are natural, they are less obvious in the FG coordinate frame:

- first, near the boundary we require that the fluctuations are normalizable;

- second, the EF frame bulk regularity condition is replaced in the FG frame with the requirement that all fluctuations behave as

$$H_{\dots} \sim \rho^{s/2} \times \text{finite} \qquad \text{as} \qquad \rho \to \infty \,. \tag{A.11}$$

It is thus convenient to extract this singularity from the radial profiles of the fluctuations,

$$\begin{aligned} H_{a,b,c} &= (1+\rho)^{s/2}\ fl_{a,b,c}(\rho)\,, & H_{K_{1,2,3}} &= (1+\rho)^{s/2}\ fl_{K_{1,2,3}}(\rho)\,, \\ H_g &= (1+\rho)^{s/2}\ fl_g(\rho)\,, & H_h &= (1+\rho)^{s/2}\ fl_h(\rho)\,, \end{aligned} \tag{A.12}$$

where we modified $\rho \to (1+\rho)$ to avoid introduction of the spurious singularity near the boundary, i.e., as $\rho \to 0$. As for H_h, the expression for fl_h is algebraic,

$$fl_h = fl_h\left[fl_{a,b,c}, \frac{d}{d\rho} fl_{a,b,c}\,;\ fl_{K_{1,2,3}}, \frac{d}{d\rho} fl_{K_{1,2,3}}\,;\ fl_g, \frac{d}{d\rho} fl_g\,;\ s\right]. \tag{A.13}$$

We collected the equations for

$$\left\{\ fl_{a,b,c}\,,\ fl_{K_{1,2,3}}\,,\ fl_g\,,\ fl_h\ \right\}, \tag{A.14}$$

along with the algebraic expression (A.13) in [31]. These final equations, solved subject to normalizability of the fluctuations at the boundary, and their regularity in the bulk $\rho \in [0, \infty)$, would determine the spectrum $\{\omega\}$. We would like to stress that the regularity condition as $\rho \to \infty$ is much more stronger than the requirement that the modes $fl_{\dots}$ are finite in this limit; rather, the regularity mandates [29] that we have a standard Maclaurin series expansion for the profiles $fl_{\dots}$ in variable $y \equiv \frac{1}{\rho}$, e.g., the terms $\rho^{-17/2}$ or $\rho^{-7}\ln\rho$ are not allowed. This is necessary so that the fluctuations can be properly transformed to the EF coordinate frame in the vicinity of $y \propto (r - r_0) \to 0$ (see (2.22)), and further extended in the EF coordinate frame all the way to the apparent horizon, $r \in [r_{AH}, r_0]$.

JHEP01(2023)130

A.2 Asymptotics

In this section we discuss the asymptotics of the DFP background functions (A.4), and the fluctuations (A.14). Keep in find that the equations of motion for $\{f_{a,b},\, h,\, K_{1,2,3},\, g\}$ are of the second-order in ρ, the equation for f_c is of the first-order; and the equations of motion for $\{fl_{a,b,c},\, fl_{K_{1,2,3}},\, fl_g\}$ are of the second-order. The first-order equation for fl_h is not independent, see (A.13). All the equations are nonlinear and coupled. To find a solution to a DFP background, one needs a single label, corresponding to $\frac{H}{\Lambda}$ (2.10), and $7\times 2+1\times 1=15$ parameters (from counting the total order of the background equations of motion). Likewise, to solve the fluctuation equations, assuming that the radial profile functions $fl_{\ldots}$ are real and $\mathfrak{Re}[\mathfrak{w}]=0$, one needs $7\times 2+0\times 1=14$ parameters; one of these parameters must be s (A.8). It is possible to have fluctuations about a DFP which are not purely imaginary [27]. Their analysis, using the equations of motion derived in this paper, are straightforward, but it will not be performed here: TypeA$_b$ DFP is found to be unstable to a mode with $\mathfrak{Re}[\mathfrak{w}]=0$ already; instabilities of TypeA$_s$ DFP are anticipated by the marginal modes, that can be identified independently as in section 5.1 of [17]. Besides the marginal mode responsible for a branching of TypeA$_b$ DFP away from TypeA$_s$ DFP discussed in section 4.1, none exists. Thus, we do not expect any of TypeA$_s$ fluctuations with $\mathfrak{Re}[\mathfrak{w}]\neq 0$, if exist, would become unstable, at least for $H>H_{\text{crit}_3}$.

A.2.1 Background

The general UV (as $\rho\to 0$) asymptotic solution of the background equations of motion describing the phase of the cascading gauge theory with spontaneously broken chiral symmetry takes the form

$$f_c=1+f_{a,1,0}\;\rho+\sum_{n=2}^{\infty}\sum_{k}f_{c,n,k}\;\rho^n\ln^k\rho\,, \tag{A.15}$$

$$f_a=1+f_{a,1,0}\;\rho+\sum_{n=2}^{\infty}\sum_{k}f_{a,n,k}\;\rho^n\ln^k\rho\,, \tag{A.16}$$

$$f_b=1+f_{a,1,0}\;\rho+\sum_{n=2}^{\infty}\sum_{k}f_{b,n,k}\;\rho^n\ln^k\rho\,, \tag{A.17}$$

$$h=\frac{1}{8}b+\frac{1}{4}K_0-\frac{1}{2}b\ln\rho+\left(b\ln\rho-\frac{1}{2}K_0\right)f_{a,1,0}\;\rho+\sum_{n=2}^{\infty}\sum_{k}h_{n,k}\;\rho^n\ln^k\rho\,, \tag{A.18}$$

$$K_1=K_0-2b\ln\rho+bf_{a,1,0}\;\rho+\sum_{n=2}^{\infty}\sum_{k}k_{1,n,k}\;\rho^n\ln^k\rho\,, \tag{A.19}$$

$$K_2=1+\left(k_{2,3,0}+\frac{3}{4}f_{a,1,0}b\ln\rho+3f_{a,3,0}\ln\rho\right)\rho^3+\sum_{n=4}^{\infty}\sum_{k}k_{2,n,k}\;\rho^n\ln^k\rho\,, \tag{A.20}$$

$$K_3=K_0-2b\ln\rho+bf_{a,1,0}\;\rho+\sum_{n=2}^{\infty}\sum_{k}k_{3,n,k}\;\rho^n\ln^k\rho\,, \tag{A.21}$$

$$g=1-\frac{1}{2}b\;\rho^2+\sum_{n=3}^{\infty}\sum_{k}g_{n,k}\;\rho^n\ln^k\rho\,. \tag{A.22}$$

JHEP01(2023)130

It is characterized by 9 parameters:

$$\{K_0\,,\ f_{a,1,0}\,,\ \underbrace{f_{a,3,0}\,,\ k_{2,3,0}}_{\mathcal{O}_3^\alpha}\,,\ \underbrace{g_{4,0}\,,\ f_{c,4,0}}_{\mathcal{O}_4^\beta}\,,\ \underbrace{f_{a,6,0}}_{\mathcal{O}_6}\,,\ \underbrace{f_{a,7,0}}_{\mathcal{O}_7}\,,\ \underbrace{f_{a,8,0}}_{\mathcal{O}_8}\}\,, \tag{A.23}$$

where we indicated the dual cascading gauge theory operators which expectation values these parameters characterize. K_0 is related to strong coupling scale Λ of the cascading gauge theory as (2.10). Finally, $f_{a,1,0}$ corresponds to a diffeomorphism parameter that ensures the range of the radial coordinate as in (2.8).

To study the infrared asymptotics, i.e., as $y \equiv \frac{1}{\rho} \to 0$, we redefine

$$h^h \equiv y^{-2}\ h\,, \qquad f^h_{a,b,c} \equiv y\ f_{a,b,c}\,. \tag{A.24}$$

The IR asymptotic expansions

$$\begin{aligned} f^h_{a,b,c} &= \sum_{n=0} f^h_{a,b,c,n} y^n\,, & h^h &= \frac{1}{4} + \sum_{n=1} h^h_n y^n\,, \\ K_{1,2,3} &= \sum_{n=0} K^h_{1,2,3,n} y^n\,, & g &= \sum_{n=0} g^h_n y^n\,, \end{aligned} \tag{A.25}$$

are characterized by 7 parameters:

$$\left\{f^h_{a,0}\,,\ f^h_{b,0}\,,\ f^h_{c,0}\,,\ K^h_{1,0}\,,\ K^h_{2,0}\,,\ K^h_{3,0}\,,\ g^h_0\right\}\,. \tag{A.26}$$

Notice that in total we have, (A.23) and (A.26), $9 + 7 = 16 = 1 + 15$ parameters, as expected.

A.2.2 Fluctuations

The general UV (as $\rho \to 0$) asymptotic solution of the fluctuation equations of motion is much more complicated:

$$\begin{aligned} fl_{a,b,c} &= \sum_{n=2}^{\infty} \rho^n\ F_{a,b,c;n}(z)\,, & fl_{K_{1,3}} &= \sum_{n=2}^{\infty} \rho^n\ F_{K_{1,3};n}(z) \\ fl_{K_2} &= \sum_{n=3}^{\infty} \rho^n\ F_{K_2;n}(z)\,, & fl_g &= \sum_{n=4}^{\infty} \rho^n\ F_{g;n}(z)\,, & fl_h &= \sum_{n=2}^{\infty} \rho^n\ F_{h;n}(z)\,, \end{aligned} \tag{A.27}$$

where $z \equiv \ln \rho$. At each fixed order n we have a coupled system of 7 second-order ODEs for

$$\left\{\ F_{a,b,c;n}(z)\,,\ F_{K_{1,2,3};n}(z)\,,\ F_{g;n}(z)\ \right\}\,, \tag{A.28}$$

along with the first-order constraint involving $F_{h;n}(z)$. The complexity of these equations grows with n. Since the cascading gauge theory has a gravitational scalar dual to a dimension $\Delta = 8$ operator, at the very least the series expansions must be developed to order $n = 8$ inclusive.

JHEP01(2023)130

We present here the simplest set of the equations, i.e., for $n = 2$:

$$
\begin{aligned}
0 = {} & F''_{a;2} - \frac{b}{b-4bz+2K_0}\left(2F'_{a;2} + F'_{c;2} + 2F'_{b;2}\right) - \frac{4}{b-4bz+2K_0}\left(F'_{K_1;2} + 3F'_{K_3;2}\right) \\
& + \frac{1}{(4bz-2K_0-b)^3}\left(\left(6144z^2 - 768z + 256\right)b^2 + (-6144z+384)\,K_0 b + 1536K_0^2\right)F_{h;2} \\
& + \frac{1}{2\,(4bz-2K_0-b)^2}\Big(\left(\left(-1296z^2 + 264z - 97\right)b^2 + (1296z-132)\,K_0 b - 324K_0^2\right)F_{a;2} \\
& + \left(\left(-1264z^2 - 8z - 31\right)b^2 + (1264z+4)\,K_0 b - 316K_0^2\right)F_{b;2} + \left(\left(-512z^2 - 24\right)b^2 \\
& + 512bzK_0 - 128K_0^2\Big)F_{c;2} + \left((-320z-32)\,b + 160K_0\right)F_{K_1;2} + \Big((128z-32)\,b^2 \\
& - 64bK_0\Big)F_{K_2;2} - 192F_{K_3;2}\left(\left(z+\frac{1}{3}\right)b - \frac{K_0}{2}\right)\Big), \qquad \text{(A.29)} \\
0 = {} & F''_{b;2} - \frac{b}{b-4bz+2K_0}\left(2F'_{b;2} + F'_{c;2} + 2F'_{a;2}\right) - \frac{4}{b-4bz+2K_0}\left(F'_{K_3;2} + 3F'_{K_1;2}\right) \\
& + \frac{1}{(4bz-2K_0-b)^3}\left(\left(6144z^2 - 768z + 256\right)b^2 + (-6144z+384)\,K_0 b + 1536K_0^2\right)F_{h;2} \\
& + \frac{1}{2\,(4bz-2K_0-b)^2}\Big(\left(\left(-1296z^2 + 264z - 97\right)b^2 + (1296z-132)\,K_0 b - 324K_0^2\right)F_{b;2} \\
& + \left(\left(-1264z^2 - 8z - 31\right)b^2 + (1264z+4)\,K_0 b - 316K_0^2\right)F_{a;2} + \left(\left(-512z^2 - 24\right)b^2 \\
& + 512bzK_0 - 128K_0^2\Big)F_{c;2} + \left((-320z-32)\,b + 160K_0\right)F_{K_3;2} - \Big((128z-32)\,b^2 \\
& - 64bK_0\Big)F_{K_2;2} - 192F_{K_1;2}\left(\left(z+\frac{1}{3}\right)b - \frac{K_0}{2}\right)\Big), \qquad \text{(A.30)} \\
0 = {} & F''_{c;2} - \frac{b}{b-4bz+2K_0}\left(2F'_{a;2} + F'_{c;2} + 2F'_{b;2}\right) - \frac{4}{b-4bz+2K_0}\left(F'_{K_3;2} + F'_{K_1;2}\right) \\
& + \frac{1}{(4bz-2K_0-b)^3}\left(\left(6144z^2 - 768z + 256\right)b^2 + (-6144z+384)\,K_0 b + 1536K_0^2\right)F_{h;2} \\
& + \frac{1}{(4bz-2K_0-b)^2}\Big(\left(\left(-512z^2 + 160z - 36\right)b^2 + (512z-80)\,K_0 b - 128K_0^2\right)F_{c;2} \\
& + \left(\left(-512z^2 - 24\right)b^2 + 512bzK_0 - 128K_0^2\right)F_{a;2} + \left(\left(-512z^2 - 24\right)b^2 + 512bzK_0 \\
& - 128K_0^2\Big)F_{b;2} + \left((-160z-16)\,b + 80K_0\right)F_{K_1;2} + \left((-160z-16)\,b + 80K_0\right)F_{K_3;2} \\
& - 64F_{g;2}b\left(\left(z-\frac{1}{4}\right)b - \frac{K_0}{2}\right)\Big), \qquad \text{(A.31)} \\
0 = {} & F''_{K_1;2} + \frac{4b}{b-4bz+2K_0}F'_{K_1;2} + b\left(2F'_{g;2} - F'_{a;2} - \frac{1}{2}F'_{c;2} + 3F'_{b;2}\right) \\
& + \frac{320b\,(-2bz+K_0)}{(b-4bz+2K_0)^2}F_{h;2} + \frac{1}{b-4bz+2K_0}\Big(4b\,(5K_0-10bz-b)\,(2F_{a;2}+F_{c;2}) \\
& + 24b\,(K_0-2bz)\,F_{b;2} + 4b\,(4bz-2K_0+b)\,F_{g;2} + \left(34bz - 17K_0 - \frac{41}{2}b\right)F_{K_1;2} \\
& + 16b\,(K_0-2bz)\,F_{K_2;2} + \left(-18bz + 9K_0 - \frac{31}{2}b\right)F_{K_3;2}\Big), \qquad \text{(A.32)}
\end{aligned}
$$

$$0 = F''_{K_2;2} + \frac{4b}{b-4bz+2K_0} F'_{K_2;2} + 9\left(F_{b;2} - F_{a;2}\right) + \frac{1}{b-4bz+2K_0}\left(\frac{18}{b}\left(K_0-2bz\right)\left(F_{K_1;2}-F_{K_3;2}\right) + \left(52bz-26K_0-5b\right)F_{K_2;2}\right), \tag{A.33}$$

$$0 = F''_{K_3;2} + \frac{4b}{b-4bz+2K_0} F'_{K_3;2} + b\left(2F'_{g;2} + 3F'_{a;2} - F'_{b;2} - \frac{1}{2}F'_{c;2}\right) + \frac{320b\left(-2bz+K_0\right)}{\left(b-4bz+2K_0\right)^2} F_{h;2} + \frac{1}{b-4bz+2K_0}\Big(4b\left(5K_0-10bz-b\right)\left(2F_{b;2}+F_{c;2}\right) + 24b\left(K_0-2bz\right)F_{a;2} + 4b\left(4bz-2K_0+b\right)F_{g;2} + \left(34bz-17K_0-\frac{41}{2}b\right)F_{K_3;2} - 16b\left(K_0-2bz\right)F_{K_2;2} + \left(-18bz+9K_0-\frac{31}{2}b\right)F_{K_1;2}\Big), \tag{A.34}$$

$$0 = F''_{g;2} - \frac{4}{b-4bz+2K_0+b}\left(F'_{K_3;2}+F'_{K_1;2}\right) - \frac{4}{b-4bz+2K_0}\Big(F_{g;2}\left(-4bz+2K_0+5b\right) - 2F_{c;2}b + 2F_{K_1;2} + 2F_{K_3;2}\Big), \tag{A.35}$$

$$0 = F'_{h;2} + \frac{6b}{b-4bz+2K_0} F_{h;2} + \frac{b-4bz+2K_0}{32}\left(2F'_{a;2}+F'_{c;2}+2F'_{b;2}\right) + \frac{1}{4}\left(F_{K_1;2}+F_{K_3;2}\right) + \frac{b}{8}\left(2F_{b;2}+2F_{a;2}+F_{c;2}\right). \tag{A.36}$$

It is straightforward to verify that (A.36) is solved using the algebraic expression for $F_{h,2}$, derived from (A.13),

$$F_{h;2} = -\frac{\left(b-4bz+2K_0\right)^2}{640(K_0-2bz)}\left(2F'_{a;2}+2F'_{b;2}+F'_{c;2}+\frac{4}{b}\left(F'_{K_1;2}+F'_{K_3;2}\right)\right) - \frac{4}{5b(K_0-2bz)}\Bigg(\left(\frac{b}{4}(z+1)-\frac{1}{8}K_0\right)\left(F_{K_1;2}+F_{K_3;2}\right) + b\Bigg(\left(\left(z+\frac{1}{16}\right)b-\frac{1}{2}K_0\right) \times \left(F_{a;2}+F_{b;2}\right) + \left(\left(\frac{1}{4}z+\frac{3}{32}\right)b-\frac{1}{8}K_0\right)F_{c;2} + \frac{1}{2}F_{g;2}\left(\left(z-\frac{1}{4}\right)b-\frac{1}{2}K_0\right)\Bigg)\Bigg) \times \left(\left(z-\frac{1}{4}\right)b-\frac{1}{2}K_0\right). \tag{A.37}$$

Remarkably, above equations can be solved analytically,

$$F_{a,b,c;2} = -\frac{2A(3b-4bz+2K_0)}{b(b-4bz+2K_0)^2}, \qquad F_{K_{1,3};2} = -\frac{A}{b-4bz+2K_0}, \qquad F_{K_2;2} = F_{g;2} = 0, \qquad F_{h;2} = \frac{A(5b-8bz+4K_0)}{4b(b-4bz+2K_0)}, \tag{A.38}$$

where A is an arbitrary constant, characterizing an overall normalization of the linearized fluctuations.

JHEP01(2023)130

n	$M_{a;n}=M_{b;n}$	$M_{c;n}$	$M_{K_1;n}=M_{K_3;n}$	$M_{K_2;n}$	$M_{g;n}$	$M_{h;n}$
2	1	1	0	–	–	1
3	3	2	3	1	–	2
4	4	4	4	1	2	4
5	6	5	6	3	3	5
6	8	8	7	4	5	7
7	10	9	10	7	6	8
8	12	12	11	8	9	12

Table 1. Upper limits of summation in (A.39).

In general, we find that the differential equations for (A.28) are solved with the ansatz

$$\begin{aligned}
F_{a,b,c;n}(z) &= \frac{1}{(b-4bz+2K_0)^n}\sum_{m=0}^{M_{a,b,c;n}} fl_{a,b,c;n;m}\, z^m\,, && n\geq 2\,,\\
F_{K_{1,3};n}(z) &= \frac{1}{(b-4bz+2K_0)^{n-1}}\sum_{m=0}^{M_{K_{1,3};n}} fl_{K_{1,3};n;m}\, z^m\,, && n\geq 2\,,\\
F_{K_2;3}(z) &= fl_{K_2;3;0}+fl_{K_2;3;1}\, z\,,\\
F_{K_2;n}(z) &= \frac{1}{(b-4bz+2K_0)^{n-4}}\sum_{m=0}^{M_{K_2;n}} fl_{K_2;n;m}\, z^m\,, && n\geq 4\,,\\
F_{g;n}(z) &= \frac{1}{(b-4bz+2K_0)^{n-3}}\sum_{m=0}^{M_{g;n}} fl_{g;n;m}\, z^m\,, && n\geq 4\,,\\
F_{h;n}(z) &= \frac{1}{(b-4bz+2K_0)^{n-1}}\sum_{m=0}^{M_{h;n}} fl_{h;n;m}\, z^m\,, && n\geq 2\,,
\end{aligned} \tag{A.39}$$

where $fl_{\dots;n;m}$ are constants, and the orders of z-polynomials in the numerators of $F_{\dots;n}$, i.e., $M_{\dots;n}$, are collected in the table 1 : The set of independent constants, fully determining the remaining coefficients $fl_{\dots;n;m}$, is given by

$$\{\ A;\, fl_{a;3;0}\,,\ fl_{K_2;3;0}\,,\ fl_{g;4;0}\,,\ fl_{K_3;6;5}\,,\ fl_{K_2;7;0}\,,\ fl_{g;8;0};\, s\ \}\,, \tag{A.40}$$

where we also included the frequency parameter s, see (A.8). In the IR, i.e., as $y\equiv\frac{1}{\rho}\to 0$, it is convenient to redefine some of the fluctuations as

$$fl_{a,b,c}\equiv y^{-1}\, fl^h_{a,b,c}\,,\qquad fl_h\equiv y^2\, fl^h_h\,. \tag{A.41}$$

Note that this redefinition mimic the corresponding redefinitions of the related background scalars $f_{a,b,c}$ and h in (A.24). The IR asymptotic expansions take form:

$$\begin{aligned}
fl^h_{a,b,c} &= \sum_{m=0}^{\infty} fl^h_{a,b,c;m}\, y^m\,, & fl_{K_{1,2,3}} &= \sum_{m=0}^{\infty} fl^h_{K_{1,2,3};m}\, y^m\,,\\
fl_g &= \sum_{m=0}^{\infty} fl^h_{g;m}\, y^m\,, & fl^h_h &= \sum_{m=0}^{\infty} fl^h_{h;m}\, y^m\,.
\end{aligned} \tag{A.42}$$

JHEP01(2023)130

They are uniquely characterized by

$$\left\{\ fl^h_{a;0}\,,\ fl^h_{b;0}\,,\ fl^h_{c;0}\,,\ fl^h_{K_1;0}\,,\ fl^h_{K_2;0}\,,\ fl^h_{K_3;0}\,,\ fl^h_{g;0}\ \right\}. \tag{A.43}$$

Notice that in total we have, (A.40) and (A.43), $8+7=15=14+1$, i.e., we have the expected number of parameters, $=14$ (corresponding to the total order of the non-redundant differential equations of motion for the fluctuations), and a single arbitrary overall normalization amplitude A. We are free to fix A as we wish. We find it convenient to fix A differently for different branches of the fluctuations.

B Chirally symmetric DFP — TypeA$_s$, χSB fluctuations

In this appendix we discuss the linearized fluctuations about TypeA$_s$ dynamical fixed point of the cascading gauge theory, spontaneously breaking the U(1)$_R$ chiral symmetry of this DFP to $\mathbb{Z}_2$. The corresponding background and the fluctuation equations of motion are the special case, a consistent truncation, of the general equations discussed in appendix A. Specifically,

- for the background we find [17]:

$$f_c\equiv f_2\,,\qquad f_a=f_b\equiv f_3\,,\qquad K_1=K_3\equiv K\,,\qquad K_2\equiv 1\,; \tag{B.1}$$

- for the fluctuations, note the rescaling of the $fl_a=-fl_b$ modes, we find:

$$\begin{array}{lll} fl_a=-fl_b\equiv f_3\cdot F\,, & fl_{K_1}=-fl_{K_3}\equiv\chi_1\,, & fl_{K_2}\equiv\chi_2\,,\\ fl_c\equiv 0\,, & fl_g\equiv 0\,, & fl_h\equiv 0\,. \end{array} \tag{B.2}$$

This particular mode, i.e., $\{F,\,\chi_1,\,\chi_2\}$, is featured prominently throughout the paper, so we discuss it in some details. The corresponding equations of motion are given by:

$$\begin{aligned}
0=&F''+\frac{1}{16bf_3^3f_2g^2h^2\rho\,(1+\rho)\,(f_3'\rho-2f_3)}\Big(f_3^2hf_2g\rho^2\,(1+\rho)\,(K')^2\\
&+2h^2f_2f_3^4b\rho^2\,(1+\rho)\,(g')^2+2g^2f_3^4f_2b\rho^2\,(1+\rho)\,(h')^2+20g^2h^2f_3^2f_2b\rho^2\,(1+\rho)\,(f_3')^2\\
&+16f_3^3h^2f_2g^2b\rho\,(\rho s-3\rho-3)\,f_3'+16hg^2f_3^4f_2b\rho\,(1+\rho)\,h'-4g^3f_3^2h\,(1+\rho)\,b^2\\
&+2g^2b\Big(-8h^2f_3^2\,(\rho+1)\,f_2^2+24h^2\Big(\Big(\rho^2\,(\rho+1)\,h+1+\Big(-\frac{2}{3}s+1\Big)\rho\Big)f_3+2\rho+2\Big)f_3^3f_2\\
&-K^2\,(\rho+1)\Big)\Big)F'-\frac{K'}{2f_3^2hgb}\kappa_1'+\frac{1}{32\,(\rho+1)^2\rho^2h^2g^2f_2f_3^3b\,(f_3'\rho-2f_3)}\\
&\times\Big(20b\rho^3sg^2h^2f_2f_3^2\,(\rho+1)\,(f_3')^2-64g\Big(\frac{1}{4}\rho^2f_2\,(\rho+1)^2\,(K')^2+g\Big(\Big(\Big(\rho^2sf_2\,(\rho+1)^2\,(s-3)\,h\\
&-((-6+(s-8)\,\rho)\,s\rho f_2)\,\frac{1}{4}+9\,(\rho+1)^2\Big)hf_3^2\Big)\frac{1}{2}-6hf_2\,(\rho+1)^2\,f_3+bg\,(\rho+1)^2\Big)b\Big)f_3\rho hf_3'\\
&+((s+32)\,\rho+32)\,gf_3^2f_2\,(\rho+1)\,\rho^2h\,(K')^2-4b\Big(-\rho^3sg^2f_2f_3^4\,(\rho+1)\,(h')^2\,\frac{1}{2}\\
&-4\rho^2sg^2hf_2f_3^4\,(\rho+1)\,h'-\rho^3sh^2f_2f_3^4\,(\rho+1)\,(g')^2\,\frac{1}{2}
\end{aligned}$$

JHEP01(2023)130

$$
\begin{aligned}
&+g^2\Big(-16\Big(\Big(\Big(s-\frac{9}{4}\Big)\rho+s-3\Big)f_2 s\,(\rho+1)\,\rho^2 h-((-3+(s-5)\,\rho)\,s\rho f_2)\,\frac{1}{4}+9\,(\rho+1)^2\Big)h^2 f_3^4\\
&-24\,((s-8)\,\rho-8)\,f_2\,(\rho+1)\,h^2 f_3^3+(\rho+1)\,h\Big(((s-32)\,\rho-32)\,bg+4\rho s h f_2^2\Big)f_3^2\\
&+\rho s K^2\,(\rho+1)\,\frac{1}{2}\Big)\Big)\Big)F-\frac{\kappa_1 f_2\,(K')\,\rho^2 s+8\kappa_2 g^2 b^2\,(\rho+1)}{4\,(\rho+1)\,hg f_3^2\rho^2 f_2 b}\,,
\end{aligned}
\tag{B.3}
$$

$$
\begin{aligned}
0=\kappa_1''+&\frac{1}{16\rho\,(f_3'\rho-2f_3)\,bf_3^3 f_2 g^2 h^2\,(\rho+1)}\Big(-12b\rho^2 g^2 h^2 f_2 f_3^2\,(\rho+1)\,(f_3')^2\\
&-16gbf_3^3 f_2\Big(\rho h\,(\rho+1)\,g'+\Big(\Big(\rho^2+\rho\Big)h'-h\,(1+(s+1)\,\rho)\Big)g\Big)\rho h f_3'\\
&+2b\rho^2 h^2 f_2 f_3^4\,(\rho+1)\,(g')^2+32b\rho g h^2 f_2 f_3^4\,(\rho+1)\,g'-4g\Big(-b\rho^2 g f_2 f_3^4\,(\rho+1)\,(h')^2\,\frac{1}{2}\\
&-12b\rho g h f_2 f_3^4\,(\rho+1)\,h'-\rho^2 h f_2 f_3^2\,(\rho+1)\,(K')^2\,\frac{1}{4}+\Big(-12f_2\Big(\rho^2\,(\rho+1)\,h+1\\
&+\Big(-\frac{2}{3}s+1\Big)\rho\Big)h^2 f_3^4-24h^2 f_2\,(\rho+1)\,f_3^3+h\,(\rho+1)\Big(4hf_2^2+bg\Big)f_3^2+K^2\,(\rho+1)\,\frac{1}{2}\Big)gb\Big)\Big)\kappa_1'\\
&+2K'F'+\frac{1}{32\,(\rho+1)^2\rho^2 h^2 g^2 f_2 f_3^3 b\,(f_3'\rho-2f_3)}\Big(-12br^3 s g^2 h^2 f_2 f_3^2\,(\rho+1)\,(f_3')^2\\
&-16gb\Big(\rho^2 s h f_2\,(\rho+1)\,g'+g\Big(\rho^2 s f_2\,(\rho+1)\,h'+2\Big(\rho^2 s f_2\,(\rho+1)^2\,(s-3)\,h-\rho s\,(\rho s+2)\,f_2\,\frac{1}{4}\\
&+9\,(\rho+1)^2\Big)h\Big)\Big)f_3^3\rho h f_3'+2b\rho^3 s h^2 f_2 f_3^4\,(\rho+1)\,(g')^2+32b\rho^2 s g h^2 f_2 f_3^4\,(\rho+1)\,g'\\
&-4g\Big(-b\rho^3 s g f_2 f_3^4\,(\rho+1)\,(h')^2\,\frac{1}{2}-12b\rho^2 s g h f_2 f_3^4\,(\rho+1)\,h'-\rho^3 s h f_2 f_3^2\,(\rho+1)\,(K')^2\,\frac{1}{4}\\
&+gb\Big(-16\Big(\Big(\Big(s-\frac{9}{4}\Big)\rho+s-3\Big)f_2 s\,(\rho+1)\,\rho^2 h-((-3+(s-5)\,\rho)\,s\rho f_2)\,\frac{1}{4}\\
&+9\,(\rho+1)^2\Big)h^2 f_3^4-24\rho s h^2 f_2\,(\rho+1)\,f_3^3+\rho s h\,(\rho+1)\Big(4hf_2^2+bg\Big)f_3^2\\
&+\rho s K^2\,(\rho+1)\,\frac{1}{2}\Big)\Big)\Big)\kappa_1+\frac{F f_3^2 h f_2 K'\rho^2 s+2bKg\,(\rho+1)\,(\kappa_2+2F)}{(\rho+1)\,h f_3^2\rho^2 f_2}\,,
\end{aligned}
\tag{B.4}
$$

$$
\begin{aligned}
0=\kappa_2''+&\frac{1}{16\rho\,(f_3'\rho-2f_3)\,bf_3^3 f_2 g^2 h^2\,(\rho+1)}\Big(-12b\rho^2 g^2 h^2 f_2 f_3^2\,(\rho+1)\,(f_3')^2\\
&+16gbf_3^3 f_2\rho h\Big(\rho h\,(\rho+1)\,g'-\Big(\Big(\rho^2+\rho\Big)h'-h\,(1+(s+1)\,\rho)\Big)g\Big)f_3'\\
&+2b\rho^2 h^2 f_2 f_3^4\,(\rho+1)\,(g')^2-32b\rho g h^2 f_2 f_3^4\,(\rho+1)\,g'-4g\Big(-b\rho^2 g f_2 f_3^4\,(\rho+1)\,(h')^2\,\frac{1}{2}\\
&-12b\rho g h f_2 f_3^4\,(\rho+1)\,h'-\rho^2 h f_2 f_3^2\,(\rho+1)\,(K')^2\,\frac{1}{4}+\Big(-12f_2\Big(\rho^2\,(\rho+1)\,h+1\\
&+\Big(-\frac{2}{3}s+1\Big)\rho\Big)h^2 f_3^4-24h^2 f_2\,(\rho+1)\,f_3^3+h\,(\rho+1)\Big(4hf_2^2+bg\Big)f_3^2+K^2\,(\rho+1)\,\frac{1}{2}\Big)gb\Big)\Big)\kappa_2'\\
&+\frac{1}{32\,(\rho+1)^2\rho^2 h^2 g^2 f_2 f_3^3 b\,(f_3'\rho-2f_3)}\Big(-12b\rho^3 s g^2 h^2 f_2 f_3^2\,(\rho+1)\,(f_3')^2\\
&+16g\Big(\rho^2 s h f_2\,(\rho+1)\,g'-g\Big(\rho^2 s f_2\,(\rho+1)\,h'+2\Big(\rho^2 s f_2\,(\rho+1)^2\,(s-3)\,h-\rho s\,(\rho s+2)\,f_2\,\frac{1}{4}\\
&+9\,(\rho+1)^2\Big)h\Big)\Big)bf_3^3\rho h f_3'+2b\rho^3 s h^2 f_2 f_3^4\,(\rho+1)\,(g')^2-32b\rho^2 s g h^2 f_2 f_3^4\,(\rho+1)\,g'
\end{aligned}
$$

JHEP01(2023)130

$$
\begin{aligned}
&-4g\Big(-b\rho^3 s g f_2 f_3^4 (\rho+1) (h')^2 \frac{1}{2} - 12 b\rho^2 s g h f_2 f_3^4 (\rho+1) h' - \rho^3 s h f_2 f_3^2 (\rho+1) (K')^2 \frac{1}{4} \\
&+gb\Big(-16\Big(\Big(\Big(s-\frac{9}{4}\Big)\rho+s-3\Big) f_2 s (\rho+1) \rho^2 h - ((-3+(s-5)\rho) s\rho f_2) \frac{1}{4} \\
&+9(\rho+1)^2\Big) h^2 f_3^4 - 24\rho s h^2 f_2 (\rho+1) f_3^3 + \rho s h (\rho+1) \Big(4h f_2^2 + bg\Big) f_3^2 \\
&+\rho s K^2 (\rho+1) \frac{1}{2}\Big)\Big)\Big)\kappa_2 - \frac{18F}{\rho^2 f_2} + \frac{9\kappa_1 K}{2b\rho^2 f_2 g h f_3^2} \,.
\end{aligned}
\tag{B.5}
$$

Since in this sector the fluctuations of fl_h are not activated (B.2), the asymptotics are much simpler compare to the general case of section A.2. In the UV, i.e., as $\rho \to 0$,

$$
F = f_{3,0}\rho^3 + \sum_{n=4}^{\infty} \rho^n \cdot \sum_m f_{n,m} \ \ln^m \rho \,, \tag{B.6}
$$

$$
\kappa_1 = \Big(\frac{2}{3} b (f_{3,0} + \kappa_{2;3,0}) + 2 f_{3,0} b \ln\rho\Big) \rho^3 + \sum_{n=4}^{\infty} \rho^n \cdot \sum_m \kappa_{1;n,m} \ \ln^m \rho \,, \tag{B.7}
$$

$$
\kappa_2 = (\kappa_{2;3,0} + 3 f_{3,0} \ln\rho) \rho^3 + \sum_{n=4}^{\infty} \rho^n \cdot \sum_m \kappa_{2;n,m} \ \ln^m \rho \,. \tag{B.8}
$$

In the IR, i.e., as $y \equiv \frac{1}{\rho} \to 0$,

$$
F = \sum_{n=0}^{\infty} f_n^h \ y^n \,, \qquad \kappa_1 = \sum_{n=0}^{\infty} \kappa_{1;n}^h \ y^n \,, \qquad \kappa_2 = \sum_{n=0}^{\infty} \kappa_{2;n}^h \ y^n \,. \tag{B.9}
$$

The mode asymptotics

$$
\begin{aligned}
\text{UV}: &\qquad \{\ s\,,\ f_{3,0}\,,\ \kappa_{2;3,0}\,,\ \kappa_{2;7,0}\ \}\,, \\
\text{IR}: &\qquad \{\ f_0^h\,,\ \kappa_{1;0}^h\,,\ \kappa_{2,0}^h\}\,,
\end{aligned}
\tag{B.10}
$$

are completely specified by $4+3 = 1+6$ parameters. One of the parameters from the set $\{f_{3,0},\, k_{2,3,0},\, k_{2,7,0}\}$, plays the role of the overall normalization A in (A.40), and the number of the remaining ones match the total order of the coupled differential equations for the fluctuations (B.3)–(B.5): $3 \times 2 = 6$. One of the physical parameter, i.e., s, determines the frequency of this χSB mode about TypeA$_s$ DFP, see (A.8).

In the rest of this appendix we analyze the near-conformal $b \to 0$, equivalently $H \gg \Lambda$, limit of this mode. Strictly at $b = 0$ the cascading gauge theory is conformal, and the spectra can be computed analytically [29]. We discover multiple spectral branches of the fluctuations. On some branches we are able to compute analytically the leading $\mathcal{O}(\sqrt{b})$, and numerically the first $\mathcal{O}(b)$ subleading, corrections to the conformal spectra, sections B.1.1 and B.1.2. On the remaining branches we compute numerically the leading $\mathcal{O}(b)$ corrections to the conformal spectra, section B.1.3. Perturbative results obtained here provide a valuable check of the finite $\frac{H}{\Lambda}$ spectra in the near-conformal limit, see figure 4.

JHEP01(2023)130

B.1 Near-conformal limit: $b \to 0$

In the near-conformal limit the background of TypeA$_s$ DFP is represented by

$$f_2 = (1+\rho)\left(1+\sum_{n=1}^{\infty} b^n\ f_{2;n}(\rho)\right), \qquad f_3 = (1+\rho)\left(1+\sum_{n=1}^{\infty} b^n\ f_{3;n}(\rho)\right),$$
$$h = \frac{1}{4(1+\rho)^2}\left(1+\sum_{n=1}^{\infty} b^n\ h_n(\rho)\right), \qquad K = 1+\sum_{n=1}^{\infty} b^n\ k_n(\rho), \qquad g = 1+\sum_{n=1}^{\infty} b^n\ g_n(\rho). \tag{B.11}$$

Explicit equations for $\{f_{2n}, f_{3n}, h_n, k_n, g_n\}$ for $n = 1, 2$ along with the UV/IR asymptotics are presented in appendix D.1 of [17]. There is a useful analytical solution for k_1:

$$k_1 = \frac{\rho}{4} + \frac{1}{4+4\rho} - \frac{1}{4} - 4\ln 2 + \frac{\rho^3 - 6\rho^2 - 24\rho - 16}{8(1+\rho)^{3/2}}\ \ln\frac{\sqrt{1+\rho}-1}{\sqrt{1+\rho}+1}. \tag{B.12}$$

The coupled system of the linearized fluctuations (B.3)–(B.5) can be simplified introducing

$$\kappa_1 = \frac{b}{3}(q_3 - q_7), \qquad \kappa_2 = \frac{1}{2}(q_3 + q_7). \tag{B.13}$$

To leading order in b, we find from (B.3)–(B.5):

$$\begin{aligned}
0 &= F'' + \frac{2\rho s - \rho - 6}{2\rho(\rho+1)}\ F' - \frac{3(\rho s - 2\rho - 2)}{2(\rho+1)^2\rho^2}\ F, \\
0 &= q_3'' + \frac{2\rho s - \rho - 6}{2\rho(\rho+1)}\ q_3' - \frac{3(\rho s - 2\rho - 2)}{2(\rho+1)^2\rho^2}\ q_3 + 3k_1'\ F' + \frac{3(k_1'\rho^2 s + 4)}{2\rho^2(\rho+1)}\ F, \\
0 &= q_7'' + \frac{2\rho s - \rho - 6}{2\rho(\rho+1)}\ q_7' - \frac{3(\rho s + 14\rho + 14)}{2(\rho+1)^2\rho^2}\ q_7 - 3k_1'\ F' - \frac{3(k_1'\rho^2 s + 28)}{2(\rho+1)\rho^2}\ F.
\end{aligned} \tag{B.14}$$

Solving the decoupled equation for F, we find (up to an overall normalization A_F)

$$F = A_F\ \frac{\rho^3}{(1+\rho)^s}\ {}_2F_1\left(\frac{3}{2}, 3-s; 3; -\rho\right), \qquad s = 3, 4, \cdots. \tag{B.15}$$

Given (B.15), and using (B.12), it is straightforward to see that it is impossible to solve the equation for q_3 in (B.14), so that this mode is both normalizable as $\rho \to 0$ and analytic as $\rho \to \infty$ — this means that the amplitude of F must always vanish in the limit $b \to 0$. This is precisely what we find, see (B.18) and (B.19).

With $F \equiv 0$, we find from (B.14) the following leading order as $b \to 0$ solutions:

$$q_3 = A_3\ \frac{\rho^3}{(1+\rho)^s}\ {}_2F_1\left(\frac{3}{2}, 3-s; 3; -\rho\right), \qquad s = 3, 4, \cdots, \tag{B.16}$$

and

$$q_7 = A_7\ \frac{\rho^7}{(1+\rho)^s}\ {}_2F_1\left(\frac{11}{2}, 7-s; 11; -\rho\right), \qquad s = 7, 8, \cdots. \tag{B.17}$$

Extending the leading order solutions (B.16), (B.17) perturbatively in b we identify three branches:

JHEP01(2023)130

- A pair of non-analytic[20] in b branches, (A_b) and (B_b),

$$\begin{aligned} s\Big|_{A,B} &= n + \sum_{k=1}^{\infty} (\pm)^k s_{n;k}\, b^{k/2}\,, \quad n \in \mathbb{N} \geq 3\,, & q_3\Big|_{A,B} &= \sum_{k=0}^{\infty} (\pm)^k q_{3;n;k}\, b^{k/2}\,, \\ F\Big|_{A,B} &= \sum_{k=1}^{\infty} (\pm)^k F_{n;k}\, b^{k/2}\,, & q_7\Big|_{A,B} &= \sum_{k=0}^{\infty} (\pm)^k q_{7;n;k}\, b^{k/2}\,, \end{aligned} \tag{B.18}$$

with $q_{3;n;0}$ given by (B.16) and $q_{7;n\geq 7;0}$ given by (B.17) with $s = n$. $q_{7;n;0} \equiv 0$ for $3 \leq n < 7$.

- An analytic in b branch (C_b),

$$\begin{aligned} s\Big|_{C} &= n + \sum_{k=1}^{\infty} s_{n;k}\, b^{k}\,, \quad n \in \mathbb{N} \geq 7\,, & q_3\Big|_{C} &= \sum_{k=0}^{\infty} q_{3;n;k}\, b^{k}\,, \\ F\Big|_{C} &= \sum_{k=1}^{\infty} F_{n;k}\, b^{k}\,, & q_7\Big|_{C} &= \sum_{k=0}^{\infty} q_{7;n;k}\, b^{k}\,, \end{aligned} \tag{B.19}$$

where $q_{7;n;0}$ is given by (B.17) and $q_{3;n;0}$ is given by (B.16) with $s = n$.

B.1.1 Details of $s = 3 \pm \mathcal{O}(\sqrt{b})$ branches: $(\mathbf{A_b})$ and $(\mathbf{B_b})$

From (B.16), here

$$s_{3;0} = 3\,, \qquad q_{3;3;0} = \boxed{1} \cdot \frac{\rho^3}{(1+\rho)^s}\, {}_2F_1\left(\frac{3}{2}, 3-s; 3; -\rho\right)\Big|_{s=s_{3;0}} = \frac{\rho^3}{(1+\rho)^3}\,, \tag{B.20}$$

where we highlighted the (fixed) overall normalization of the linearized fluctuations; the latter implies that in the UV, i.e., $\rho \to 0$, expansion of $q_{3;3;k\geq 1}$ the order $\mathcal{O}(\rho^3)$ terms are absent. Because the leading order fluctuation spectra (B.15) and (B.16) are degenerate, the equations for $F_{3;k}$ will necessarily contain zero modes; specifically, if $F_{3;k\geq 1}$ is a solution, so is $(F_{3;k} + \alpha_k \cdot q_{3;3;0})$ for an arbitrary set of constants α_k. As we will see shortly, the zero modes at order k will be completely fixed at order $k+1$. We find it convenient to set

$$F_{3;k} \equiv \boxed{\alpha_k} \cdot\ q_{3;3;0} + \hat{F}_{3;k}\,, \tag{B.21}$$

with the understanding that in the UV expansion of $\hat{F}_{3;k}$ the order $\mathcal{O}(\rho^3)$ terms are absent.

Using (B.20), (B.21), the perturbative ansatz (B.11) and (B.18), we find from (B.3) the leading order equation for $\hat{F}_{3;1}$,

$$0 = \hat{F}''_{3;1} + \frac{5\rho - 6}{2\rho(\rho+1)}\, \hat{F}'_{3;1} - \frac{3(\rho-2)}{2(\rho+1)^2\rho^2}\, \hat{F}_{3;1}\,. \tag{B.22}$$

The most general solution to (B.22) is specified by two integration constants C_1 and C_2:

$$\hat{F}_{3;1} = C_1 \cdot \frac{\rho^3}{(1+\rho)^3} + C_2 \cdot \frac{\rho}{(1+\rho)^3}\left(\rho^2\, \ln\frac{\sqrt{1+\rho}+1}{\sqrt{1+\rho}-1} - 2(\rho+2)\sqrt{1+\rho}\right). \tag{B.23}$$

[20] Related phenomenon was observed earlier in [15] and [34].

JHEP01(2023)130

Normalizability of the fluctuations sets $C_2 = 0$; the boundary condition imposed by (B.21) further sets $C_1 = 0$, resulting in

$$\hat{F}_{3,1} \equiv 0\,. \tag{B.24}$$

Likewise, we find

$$q_{7;3;0} = 0\,. \tag{B.25}$$

The subleading set of equations involving constants α_1, $s_{3;1}$, and functions $\{q_{3;3;1}, q_{7;3;1}, \hat{F}_{3;2}\}$ reads:

$$0 = q''_{3;3;1} + \frac{5\rho-6}{2(1+\rho)\rho} q'_{3;3;1} - \frac{3(\rho-2)q_{3;3;1}}{2\rho^2(1+\rho)^2} + \frac{9\alpha_1\rho^2(\rho+2)}{2(1+\rho)^4} k'_1 + \frac{3(4\alpha_1(\rho+1)+\rho s_{3;1})\rho}{2(1+\rho)^5}\,, \tag{B.26}$$

$$0 = q''_{7;3;1} + \frac{5\rho-6}{2(1+\rho)\rho} q'_{7;3;1} - \frac{3(17\rho+14)}{2\rho^2(1+\rho)^2} q_{7;3;1} - \frac{9\alpha_1\rho^2(\rho+2)}{2(1+\rho)^4} k'_1 - \frac{42\alpha_1\rho}{(1+\rho)^4}\,, \tag{B.27}$$

$$0 = \hat{F}''_{3;2} + \frac{5\rho-6}{2(1+\rho)\rho} \hat{F}'_{3;2} - \frac{3(\rho-2)}{2\rho^2(1+\rho)^2} \hat{F}_{3;2} - \frac{\rho^2(\rho+2)}{(1+\rho)^4} k'_1 + \frac{(3\alpha_1\rho s_{3;1} - 8(\rho+1))\rho}{2(1+\rho)^5}\,. \tag{B.28}$$

Above set can be solved numerically — and we explain how to do it for the set of equations at the next order — here instead we show that the most important constant, i.e., $s_{3;1}$ can be computed analytically:

- Substituting

$$\hat{F}_{3;2} = q_{3;3;0}\, G_{3;2}\,, \tag{B.29}$$

and using (B.12), we find a general analytic solution for $G'_{3;2}$,

$$\begin{aligned} G'_{3;2} = &-\frac{\rho^3}{16(1+\rho)^{5/2}} \ln\frac{\sqrt{1+\rho}+1}{\sqrt{1+\rho}-1} + \frac{\sqrt{1+\rho}}{\rho^3} C_1 - \frac{(3\rho^2+12\rho+8)}{\rho^3(1+\rho)}\, \alpha_1 s_{3;1} \\ &+ \frac{(\rho+2)(3\rho^4-8\rho^3+56\rho^2+128\rho+64)}{24(1+\rho)^2\rho^3}\,. \end{aligned} \tag{B.30}$$

Normalizability of $\hat{F}_{3;2}$ sets

$$C_1 = -\frac{16}{3} + 8\alpha_1 s_{3;1}\,. \tag{B.31}$$

As $\rho \to \infty$,

$$G'_{3;2} = -\frac{1}{48}\left(-\frac{384}{5} + 144\alpha_1 s_{3;1}\right)\rho^{-2} - \frac{1}{48}\left(-384\alpha_1 s_{3;1} + 256\right)\rho^{-5/2} + \mathcal{O}(\rho^{-3})\,, \tag{B.32}$$

thus analyticity of $\hat{F}_{3;2}$, and thus $G'_{3;2}$, in this limit requires

$$\alpha_1 = \frac{2}{3 s_{3;1}} \qquad \Longrightarrow \qquad C_1 = 0\,, \tag{B.33}$$

which is also evident from (B.30).

JHEP01(2023)130

- We continue with (B.26), setting

$$q_{3;3;1} = \frac{1}{s_{3;1}}\, q_{3;3;0}\, J_{3;3;1}\,, \tag{B.34}$$

allows to solve analytically for $J'_{3;3;1}$,

$$\begin{aligned} J'_{3;3;1} = {} & \frac{3\rho^3}{16(1+\rho)^{5/2}} \ln\frac{\sqrt{1+\rho}+1}{\sqrt{1+\rho}-1} - \frac{3\rho^2+12\rho+8}{\rho^3(1+\rho)}\, s_{3;1}^2 + \frac{\sqrt{1+\rho}}{\rho^3}\, C_1 \\ & - \frac{(\rho+2)(3\rho^4-8\rho^3-72\rho^2-128\rho-64)}{8(1+\rho)^2\rho^3}\,. \end{aligned} \tag{B.35}$$

Normalizability of $q_{3;3;1}$ sets

$$C_1 = 8s_{3;1}^2 - 16\,, \tag{B.36}$$

and analyticity of $q_{3;3;1}$, and thus $J'_{3;3;1}$, in the limit $\rho \to \infty$ requires

$$s_{3;1}^2 = 2 \qquad \Longrightarrow \qquad s_{3;1} = \pm\sqrt{2}\,. \tag{B.37}$$

Note that to determine $s_{3;1}$, there is no need to solve for $q_{7;3;1}$ — of course, this solution is needed for the computation of the higher order corrections $s_{3;k\geq 2}$.

The sub-subleading set of equations involving constants α_2, $s_{3;2}$, and functions $\{q_{3;3;2}, \hat{F}_{3;3}\}$ reads (we omit the equation for $q_{7;3;2}$ as it is not need to compute $s_{3;2}$; it is required for the computation of $s_{3;k\geq 3}$):

$$\begin{aligned} 0 = {} & q''_{3;3;2} + \frac{5\rho-6}{2(1+\rho)\rho} q'_{3;3;2} - \frac{3(\rho-2)}{2\rho^2(1+\rho)^2} q_{3;3;2} + \frac{s_{3;1} q'_{3;3;1}}{1+\rho} - \frac{3 s_{3;1} q_{3;3;1}}{2\rho(1+\rho)^2} + 3k'_1 \hat{F}'_{3;2} \\ & + \frac{3(3k'_1\rho^2+4)}{2(1+\rho)\rho^2}\hat{F}_{3;2} + \frac{3\rho\alpha_2(3\rho k'_1(\rho+2)+4)}{2(1+\rho)^4} + \frac{3\rho^2 s_{3;2}}{2(1+\rho)^5} - \frac{3\rho^3(k'_1)^2}{8(1+\rho)^3} + \frac{\rho^3 k'_1}{(1+\rho)^4} \\ & - \frac{3\rho^2(\rho+2)f'_{3;1}}{(1+\rho)^4} - \frac{9\rho^2(\rho+2)h'_1}{4(1+\rho)^4} + \frac{3\rho}{8(1+\rho)^5}\Big(-3h_1(\rho^2+16\rho+16) \\ & + 4(1+\rho)(12k_1 - 3f_{2;1} - 20f_{3;1} + 1)\Big)\,, \end{aligned} \tag{B.38}$$

$$\begin{aligned} 0 = {} & \hat{F}''_{3;3} + \frac{5\rho-6}{2(1+\rho)\rho}\hat{F}'_{3;3} - \frac{3(\rho-2)}{2\rho^2(1+\rho)^2}\hat{F}_{3;3} + \frac{s_{3;1}}{1+\rho}\hat{F}'_{3;2} - \frac{3 s_{3;1}\hat{F}_{3;2}}{2\rho(1+\rho)^2} - \frac{2}{3}k'_1 q'_{3;3;1} \\ & - \frac{k'_1\rho^2+4}{(1+\rho)\rho^2} q_{3;3;1} + \frac{2}{3}k'_1 q'_{7;3;1} + \frac{k'_1\rho^2-4}{(1+\rho)\rho^2} q_{7;3;1} + \frac{\rho^2 s_{3;2}}{s_{3;1}(1+\rho)^5} - \frac{19\rho^3(k'_1)^2}{12 s_{3;1}(1+\rho)^3} \\ & - \frac{\rho^3 s_{3;1} k'_1}{3(1+\rho)^4} - \frac{\rho^2(\rho+2)h'_1}{2s_{3;1}(1+\rho)^4} + \frac{3\rho^2 s_{3;1}\alpha_2}{2(1+\rho)^5} + \frac{\rho}{12 s_{3;1}(1+\rho)^5}\Big(-3h_1(\rho+4)(3\rho+4) \\ & + 4(1+\rho)(12k_1 + 15f_{2;1} - 36f_{3;1} - 13)\Big)\,. \end{aligned} \tag{B.39}$$

Eqs. (B.38) and (B.39) are solved subject to the asymptotic expansions,

- in the UV, i.e., as $\rho \to 0$,

$$\begin{aligned} q_{3;3;2} = {} & \Big(\boxed{0} + 6\alpha_2 \ln\rho\Big)\rho^3 + \Big(-3\alpha_2 - \frac{3}{2}f_{2,1,0;1} - \frac{1}{2}s_{3;2} + (-3\alpha_1 s_{3;1} - 18\alpha_2)\ln\rho\Big)\rho^4 \\ & + \mathcal{O}(\rho^5 \ln\rho)\,, \\ \hat{F}_{3;3} = {} & \boxed{0}\,\rho^3 + \Big(-\frac{3}{2}\alpha_1 f_{2,1,0;1} - \frac{1}{2}\alpha_1 s_{3;2} - \frac{1}{2}s_{3;1}\alpha_2\Big) r^4 + \mathcal{O}(\rho^5 \ln\rho)\,, \end{aligned} \tag{B.40}$$

JHEP01(2023)130

it is completely specified by $\{\alpha_2, s_{3;2}\}$; we further highlighted arbitrary constants, fixed to zero by the overall normalization (B.20) and the extraction of the zero mode in $F_{3;3}$ (B.21);

- in the IR, i.e., as $y \equiv \frac{1}{\rho} \to 0$,

$$q_{3;3;2} = q^h_{3;3;2;0} + \mathcal{O}(y)\,, \qquad \hat{F}_{3;3} = \hat{F}^h_{3;3;0} + \mathcal{O}(y)\,, \tag{B.41}$$

it is completely specified by

$$\left\{q^h_{3;3;2;0}\,,\, \hat{F}^h_{3;3;0}\,,\, \alpha_2\,,\, s_{3;2}\right\}\,. \tag{B.42}$$

In total, the UV and IR expansions are completely determined by the parameters (B.42), which is precisely what is needed to find a unique solution for a pair of second order ODEs (B.38) and (B.39). Solving these equations we find

$$s_{3;2} = -1.5748(9)\,, \qquad \alpha_2 = 0.7936(8)\,, \qquad q^h_{3;3;2;0} = 4.174(3)\,, \qquad \hat{F}^h_{3;3;0} = \mp 0.40398(7)\,. \tag{B.43}$$

Once the numerical solution for $\{q_{3;3;2}, \hat{F}_{3;3}\}$ is found, the second order ODE for $q_{7;3;2}$ — necessary to determine $s_{3;k\geq 3}$ — is solved adjusting two parameters,

$$\left\{q_{7;3;2;7,0}\,,\, q^h_{7;3;2;0}\right\}\,, \tag{B.44}$$

that completely determines its UV and IR asymptotics.

B.1.2 Details of $s = 7 \pm \mathcal{O}(\sqrt{b})$ branches: $(\mathbf{A}_b)$ and $(\mathbf{B}_b)$

From (B.16), here

$$\begin{aligned} s_{7;0} = 7\,, \qquad q_{3;7;0} =& \boxed{1} \cdot \frac{\rho^3}{(1+\rho)^s}\, {}_2F_1\left(\frac{3}{2}, 3-s; 3; -\rho\right)\Big|_{s=s_{7;0}} \\ =& \frac{\rho^3(21\rho^4 + 112\rho^3 + 240\rho^2 + 256\rho + 128)}{128(1+\rho)^7}\,, \end{aligned} \tag{B.45}$$

where we highlighted the (fixed) overall normalization of the linearized fluctuations; the latter implies that in the UV, i.e., $\rho \to 0$, expansion of $q_{3;7;k\geq 1}$ the order $\mathcal{O}(\rho^3)$ terms are absent. Because the leading order fluctuation spectra (B.15), (B.16) and (B.17) are degenerate at $s_{7;0}$, the equations for $F_{7;k}$ and $q_{7;7;k}$ will necessarily contain zero modes; specifically, if $F_{7;k\geq 1}$ and $q_{7;7;k\geq 1}$ are solutions, so are $(F_{7;k} + \alpha_k \cdot q_{3;7;0})$ and $(q_{7;7;k} + \frac{\beta_k}{\beta_0} \cdot q_{7;7;0})$,

$$q_{7;7;0} = \beta_0 \cdot \frac{\rho^7}{(1+\rho)^s}\, {}_2F_1\left(\frac{11}{2}, 7-s; 11; -\rho\right)\Big|_{s=s_{7;0}} = \beta_0 \cdot \frac{\rho^7}{(1+\rho)^7}\,, \tag{B.46}$$

for an arbitrary set of constants $\{\alpha_k, \beta_k\}$. As in section B.1.1, the zero modes at order k will be completely fixed at order $k+1$. We find it convenient to set

$$F_{7;k\geq 1} \equiv \boxed{\alpha_k} \cdot q_{3;7;0} + \hat{F}_{7;k}\,, \qquad q_{7;7;k\geq 1} \equiv \boxed{\beta_k} \cdot \frac{1}{\beta_0} q_{7;7;0} + \hat{q}_{7;7;k}\,, \tag{B.47}$$

JHEP01(2023)130

with the understanding that in the UV expansion of $\hat{F}_{7;k}$ the order $\mathcal{O}(\rho^3)$ terms are absent, and in the UV expansion of $\hat{q}_{7;7;k}$ the order $\mathcal{O}(\rho^7)$ terms are absent.

As in section B.1.1, the equation for $\hat{F}_{7;1}$ is homogeneous, and the boundary condition implied by (B.47) sets

$$\hat{F}_{7,1} \equiv 0\,. \tag{B.48}$$

The subleading set of equations involving constants α_1, β_0, $s_{7;1}$, and functions $\{q_{3;3;1}$, $q_{3;7;1}$, $\hat{F}_{3;2}\}$ reads:

$$\begin{aligned}0 = {} & q''_{3;7;1} + \frac{13\rho-6}{2(1+\rho)\rho} q'_{3;7;1} - \frac{3(5\rho-2)}{2\rho^2(1+\rho)^2} q_{3;7;1} + \frac{3\rho^2(\rho+2)\alpha_1 k'_1}{256(1+\rho)^8}\Big(147\rho^4+560\rho^3 \\ & + 944\rho^2+768\rho+384\Big) + \frac{\rho}{256(1+\rho)^9}\Big(\rho(7\rho^4+48\rho^3+144\rho^2+256\rho+384)s_{7;1} \\ & + 12\alpha_1(1+\rho)(21\rho^4+112\rho^3+240\rho^2+256\rho+128)\Big)\,,\end{aligned} \tag{B.49}$$

$$\begin{aligned}0 = {} & \hat{q}''_{7;7;1} + \frac{13\rho-6}{2(1+\rho)\rho} \hat{q}'_{7;7;1} - \frac{21(3\rho+2)}{2\rho^2(1+\rho)^2} \hat{q}_{7;7;1} - \frac{3\rho^2(\rho+2)\alpha_1 k'_1}{256(1+\rho)^8}\Big(147\rho^4+560\rho^3 \\ & + 944\rho^2+768\rho+384\Big) - \frac{21\rho\alpha_1}{64(1+\rho)^8}\Big(21\rho^4+112\rho^3+240\rho^2+256\rho+128\Big) \\ & + \frac{11 s_{7;1}\beta_0\rho^6}{2(1+\rho)^9}\,,\end{aligned} \tag{B.50}$$

$$\begin{aligned}0 = {} & \hat{F}''_{7;2} + \frac{13\rho-6}{2(1+\rho)\rho} \hat{F}'_{7;2} - \frac{3(5\rho-2)}{2\rho^2(1+\rho)^2} \hat{F}_{7;2} - \frac{(\rho+2)\rho^2 k'_1}{384(1+\rho)^8}\Big(147\rho^4+560\rho^3+944\rho^2 \\ & + 768\rho+384\Big) + \frac{\rho}{256(1+\rho)^9}\Big(\alpha_1 s_{7;1}\rho(7\rho^4+48\rho^3+144\rho^2+256\rho+384) - 8(1+\rho) \\ & \times(21\rho^4+112\rho^3+240\rho^2+256\rho+128)\Big) + \frac{\rho^5\beta_0(7\rho(\rho+2)k'_1-12)}{3(1+\rho)^8}\,.\end{aligned} \tag{B.51}$$

We show here that the most important constant, i.e., $s_{7;1}$ can be computed analytically:

- Substituting

$$\beta_0 = \frac{\alpha_1}{s_{7;1}}\, p\,, \qquad \hat{q}_{7;7;1} = \alpha_1 \cdot \frac{1}{\beta_0} q_{7;7;0} \cdot B_{7;7;1}\,, \tag{B.52}$$

and using (B.12), we find a general analytic solution for $B'_{7;7;1}$,

$$\begin{aligned}B'_{7;7;1} = {} & -\frac{3(315\rho^4+1400\rho^3+2552\rho^2+2304\rho+1152)}{20480\rho(1+\rho)^{5/2}} \ln\frac{\sqrt{1+\rho}+1}{\sqrt{1+\rho}-1} \\ & - \frac{p}{63\rho^{11}(1+\rho)}\Big(77\rho^{10}-220\rho^9+792\rho^8-4224\rho^7+59136\rho^6+709632\rho^5 \\ & + 2365440\rho^4+3784704\rho^3+3244032\rho^2+1441792\rho+262144\Big) + \frac{(1+\rho)^{9/2}}{\rho^{11}} C_1 \\ & + \frac{1}{51200(1+\rho)^2\rho^{11}}\Big(4725\rho^{13}+17850\rho^{12}+42480\rho^{11}+193440\rho^{10}+599424\rho^9 \\ & + 985856\rho^8+277504\rho^7-5945344\rho^6-24600576\rho^5-49201152\rho^4-56229888\rho^3 \\ & - 37486592\rho^2-13631488\rho-2097152\Big)\,.\end{aligned} \tag{B.53}$$

JHEP01(2023)130

Normalizability of $\hat{q}_{7;7;1}$ sets

$$C_1 = \frac{1024}{25} + \frac{262144}{63}\, p\,. \tag{B.54}$$

As $\rho \to \infty$,

$$\begin{aligned} B'_{7;7;1} = &\left(\frac{49}{160} - \frac{11}{9}p\right)\rho^{-2} + \left(\frac{45}{16} + \frac{33}{7}p\right)\rho^{-3} + \left(\frac{141}{25} - \frac{121}{7}p\right)\rho^{-4} \\ &+ \left(\frac{30242}{5775} + \frac{253}{3}p\right)\rho^{-5} + \left(-\frac{268984}{25025} - 1023p\right)\rho^{-6} \\ &+ \left(\frac{1024}{25} + \frac{262144}{63}p\right)\rho^{-13/2} + \mathcal{O}(\rho^{-7})\,, \end{aligned} \tag{B.55}$$

thus analyticity of $\hat{q}_{7;7;1}$, and thus $B'_{7;7;1}$, in this limit requires

$$p = -\frac{63}{6400} \qquad \Longrightarrow \qquad C_1 = 0\,, \tag{B.56}$$

which is also evident from (B.53).

- We continue with (B.49), setting

$$\alpha_1 = s_{7;1} v\,, \qquad q_{3;7;1} = \alpha_1 \cdot q_{3;7;0} \cdot J_{3;7;1}\,, \tag{B.57}$$

allows to solve analytically for $J'_{3;7;1}$,

$$\begin{aligned} J'_{3;7;1} = &\frac{9\rho^3}{32(1+\rho)^{5/2}} \ln\frac{\sqrt{1+\rho}+1}{\sqrt{1+\rho}-1} + \frac{(1+\rho)^{9/2} C_1}{(21\rho^4+112\rho^3+240\rho^2+256\rho+128)^2\rho^3} \\ &- \frac{1}{15v\rho^3(21\rho^4+112\rho^3+240\rho^2+256\rho+128)^2(1+\rho)}\Big(245\rho^{10}+3140\rho^9 \\ &+ 18936\rho^8 + 73088\rho^7 + 243968\rho^6 + 715776\rho^5 + 1505280\rho^4 + 2015232\rho^3 \\ &+ 1622016\rho^2 + 720896\rho + 131072\Big) \\ &- \frac{\rho+2}{80(1+\rho)^2(21\rho^4+112\rho^3+240\rho^2+256\rho+128)^2\rho^3}\Big(19845\rho^{12}+158760\rho^{11} \\ &+ 353640\rho^{10} - 900480\rho^9 - 7755456\rho^8 - 23990272\rho^7 - 45821952\rho^6 \\ &- 60620800\rho^5 - 57819136\rho^4 - 39976960\rho^3 - 19529728\rho^2 - 6291456\rho \\ &- 1048576\Big)\,. \end{aligned} \tag{B.58}$$

Normalizability of $q_{3;7;1}$ sets

$$C_1 = -\frac{131072}{15}\,\frac{3v-1}{v}\,, \tag{B.59}$$

and analyticity of $q_{3;7;1}$, and thus $J'_{3;7;1}$, in the limit $\rho \to \infty$ requires

$$v = \frac{1}{3} \qquad \Longrightarrow \qquad C_1 = 0\,. \tag{B.60}$$

JHEP01(2023)130

- Consider now (B.51): introducing

$$\hat{F}_{7;2} = q_{3;7;0} \cdot G_{7;2}\,, \tag{B.61}$$

we solve for $G'_{7;2}$,

$$\begin{aligned}
G'_{7;2} = &-\frac{\rho^3}{4000(1+\rho)^{5/2}(21\rho^4+112\rho^3+240\rho^2+256\rho+128)^2}\Big(112455\rho^8\\
&+1189720\rho^7+5688536\rho^6+16165632\rho^5+30098816\rho^4+37888000\rho^3\\
&+31744000\rho^2+16384000\rho+4096000\Big)\ln\frac{\sqrt{1+\rho}+1}{\sqrt{1+\rho}-1}\\
&-\frac{s_{7;1}^2}{45\rho^3(21\rho^4+112\rho^3+240\rho^2+256\rho+128)^2(1+\rho)}\Big(245\rho^{10}+3140\rho^9\\
&+18936\rho^8+73088\rho^7+243968\rho^6+715776\rho^5+1505280\rho^4+2015232\rho^3\\
&+1622016\rho^2+720896\rho+131072\Big)+\frac{(1+\rho)^{9/2}C_1}{(21\rho^4+112\rho^3+240\rho^2+256\rho+128)^2\rho^3}\\
&+\frac{\rho+2}{90000(1+\rho)^2(21\rho^4+112\rho^3+240\rho^2+256\rho+128)^2\rho^3}\Big(5060475\rho^{12}\\
&+40042800\rho^{11}+110307120\rho^{10}+27525120\rho^9-600006144\rho^8-1699570688\rho^7\\
&-1994001408\rho^6+24739840\rho^5+3575996416\rho^4+5505679360\rho^3+4226940928\rho^2\\
&+1704984576\rho+284164096\Big)\,.
\end{aligned} \tag{B.62}$$

Normalizability of $\hat{F}_{7;2}$ sets

$$C_1 = -\frac{35520512}{5625}+\frac{131072}{45}\,s_{7;1}^2\,, \tag{B.63}$$

and analyticity of $\hat{F}_{7;2}$, and thus $G'_{7;2}$, in the limit $\rho\to\infty$ requires

$$s_{7;1}^2 = \frac{271}{125} \qquad \Longrightarrow \qquad s_{7;1} = \pm\frac{\sqrt{1355}}{25}\,. \tag{B.64}$$

B.1.3 Details of $s = 7 + \mathcal{O}(b)$ branch: ($\mathbf{C}_b$)

From (B.17), here

$$s_{7;0} = 7\,, \qquad q_{7;7;0} = 1\cdot\frac{\rho^7}{(1+\rho)^s}\,{}_2F_1\left(\frac{11}{2},7-s;11;-\rho\right)\Big|_{s=s_{7;0}} = \frac{\rho^7}{(1+\rho)^7}\,, \tag{B.65}$$

where we highlighted the (fixed) overall normalization of the linearized fluctuations; the latter implies that in the UV, i.e., $\rho\to 0$, expansion of $q_{7;7;k\geq 1}$ the order $\mathcal{O}(\rho^7)$ terms are absent. Because the leading order spectra (B.15), (B.16) and (B.17) are degenerate at $s_{7;0}$, the equations for $F_{7;k}$ and $q_{3;7;k}$ will necessarily contain zero modes; specifically, if $F_{7;k\geq 1}$ and $q_{7;7;k\geq 1}$ are solutions, so are $(F_{7;k}+\frac{\beta_k}{\alpha_0}\cdot q_{3;7;0})$ and $(q_{3;7;k}+\frac{\alpha_k}{\alpha_0}\cdot q_{3;7;0})$,

$$q_{3;7;0} = \alpha_0\cdot{}_2F_1\left(\frac{3}{2},3-s;3;-\rho\right)\Big|_{s=s_{7;0}} = \alpha_0\cdot\frac{\rho^3(21\rho^4+112\rho^3+240\rho^2+256\rho+128)}{128(1+\rho)^7}\,, \tag{B.66}$$

JHEP01(2023)130

for an arbitrary set of constants $\{\alpha_k, \beta_k\}$. As in section B.1.1, the zero modes at order k will be completely fixed at order $k+1$. We find it convenient to set

$$F_{7;k\geq 1} \equiv \beta_k \cdot \frac{1}{\alpha_0} q_{3;7;0} + \hat{F}_{7;k}\,, \qquad q_{3;7;k\geq 1} \equiv \alpha_k \cdot \frac{1}{\alpha_0} q_{3;7;0} + \hat{q}_{3;7;k}\,, \tag{B.67}$$

with the understanding that in the UV expansion of $\hat{F}_{7;k}$ and $\hat{q}_{3;7;k}$ the order $\mathcal{O}(\rho^3)$ terms are absent.

The subleading set of equations involving constants α_0, β_1, $s_{7;1}$, and functions $\{\hat{q}_{3;7;1}$, $q_{7;7;1}$, $\hat{F}_{7;1}\}$ reads:

$$\begin{aligned}
0 = {} & \hat{q}''_{3;7;1} + \frac{13\rho-6}{2(1+\rho)\rho}\hat{q}'_{3;7;1} - \frac{3(5\rho-2)}{2\rho^2(1+\rho)^2}\hat{q}_{3;7;1} + 3k_1'\hat{F}'_{7;1} + \frac{21k_1'\hat{F}_{7;1}}{2(1+\rho)} + \frac{7\rho^6(\rho+2)g_1'}{2(1+\rho)^8} \\
& + \frac{6\hat{F}_{7;1}}{\rho^2(1+\rho)} + \frac{12\rho^5 g_1}{(1+\rho)^8} - \frac{\alpha_0\rho}{168(1+\rho)^9}\Big(\rho^2(147\rho^4+560\rho^3+944\rho^2+768\rho \\
& + 384)(1+\rho)^2(k_1')^2 + 2\rho(\rho+2)(1+\rho)(147\rho^4+560\rho^3+944\rho^2+768\rho+384)(3h_1' \\
& + 4f_{3;1}') - 4\rho(7\rho^4+48\rho^3+144\rho^2+256\rho+384)s_{7;1} - 16(1+\rho)(273\rho^4+1232\rho^3 \\
& + 2384\rho^2+2304\rho+1152)k_1 + (1617\rho^6+12320\rho^5+40352\rho^4+74496\rho^3+83328\rho^2 \\
& + 55296\rho+18432)h_1 + 4(1+\rho)((273\rho^4+1232\rho^3+2384\rho^2+2304\rho+1152)f_{2;1} \\
& + (1596\rho^4+7616\rho^3+15296\rho^2+15360\rho+7680)f_{3;1} - (147\rho^4+560\rho^3+944\rho^2+768\rho \\
& + 384))\Big) + \frac{\beta_1\rho}{14(1+\rho)^8}\Big(k_1'\rho(\rho+2)(147\rho^4+560\rho^3+944\rho^2+768\rho+384) + 84\rho^4 \\
& + 448\rho^3+960\rho^2+1024\rho+512\Big)\,,
\end{aligned} \tag{B.68}$$

$$\begin{aligned}
0 = {} & q''_{7;7;1} + \frac{13\rho-6}{2(1+\rho)\rho}q'_{7;7;1} - \frac{21(3\rho+2)}{2\rho^2(1+\rho)^2}q_{7;7;1} - \frac{7\rho^7(k_1')^2}{8(1+\rho)^7} - 3k_1'\hat{F}'_{7;1} \\
& - \frac{21(\rho^2k_1'+4)}{2\rho^2(1+\rho)}\hat{F}_{7;1} - \frac{7\rho^6(\rho+2)f_{3;1}'}{(1+\rho)^8} + \frac{\alpha_0\rho^2(\rho+2)g_1'}{42(1+\rho)^8}\Big(147\rho^4+560\rho^3+944\rho^2+768\rho \\
& + 384\Big) - \frac{21\rho^6(\rho+2)h_1'}{4(1+\rho)^8} + \frac{11\rho^6 s_{7;1}}{2(1+\rho)^9} + \frac{\rho}{56(1+\rho)^9}\Big(-32g_1(1+\rho)(21\rho^4+112\rho^3 \\
& + 240\rho^2+256\rho+128)\alpha_0 + \rho^4(28(1+\rho)(35f_{2;1}+4k_1+20f_{3;1}+7) - 7(77\rho^2+16\rho \\
& + 16)h_1)\Big) - \frac{\beta_1\rho}{14(1+\rho)^8}\Big(k_1'\rho(\rho+2)(147\rho^4+560\rho^3+944\rho^2+768\rho+384) + 6720\rho^2 \\
& + 7168\rho+3584+588\rho^4+3136\rho^3\Big)\,,
\end{aligned} \tag{B.69}$$

$$\begin{aligned}
0 = {} & \hat{F}''_{7;1} + \frac{13\rho-6}{2(1+\rho)\rho}\hat{F}'_{7;1} - \frac{3(5\rho-2)}{2\rho^2(1+\rho)^2}\hat{F}_{7;1} - \frac{\rho^2(\rho+2)k_1'}{63(1+\rho)^8}\Big(\Big(147\rho^4+560\rho^3+944\rho^2 \\
& + 768\rho+384\Big)\alpha_0 - 147\rho^4\Big) - \frac{4\rho}{21(1+\rho)^8}\Big(\alpha_0\left(21\rho^4+112\rho^3+240\rho^2+256\rho+128\right) \\
& + 21\rho^4\Big)\,.
\end{aligned} \tag{B.70}$$

Eqs. (B.68)—(B.70) are solved subject to the asymptotic expansions,

- in the UV, i.e., as $\rho \to 0$,

$$\begin{aligned}
\hat{q}_{3;7;1} = {} & \left(0 + \frac{256}{7}\beta_1\ln\rho\right)\rho^3 - \left(\frac{128}{7}\beta_1 + \frac{64}{7}\alpha_0 f_{2,1,0;1} + \frac{64}{21}\alpha_0 s_{7;1} + \frac{1280}{7}\beta_1\ln\rho\right)\rho^4 \\
& + \mathcal{O}(\rho^5\ln\rho)\,,
\end{aligned} \tag{B.71}$$

JHEP01(2023)130

$$q_{7;7;1} = -\frac{128}{21}\beta_1\rho^3 + \frac{640}{21}\beta_1\rho^4 + \left(-\frac{1966}{21}\beta_1 + \frac{46}{21}\alpha_0\right)\rho^5 + \left(\frac{4756}{21}\beta_1 - \frac{92}{7}\alpha_0\right)\rho^6 + \Big(\\ 0 + \left(-2 - \frac{256}{35}\alpha_0 k_{4,0;1} + \frac{768}{35}\beta_1 k_{4,0;1} + \frac{457}{350}\alpha_0 - \frac{191}{350}\beta_1\right)\ln\rho \\ + \left(\frac{18}{35}\beta_1 - \frac{6}{35}\alpha_0\right)\ln^2\rho\Big)\rho^7 + \mathcal{O}(\rho^8\ln^2\rho)\,, \tag{B.72}$$

$$\hat{F}_{7;1} = 0\,\rho^3 + 0\,\rho^4 - \frac{88}{63}\alpha_0\rho^5 + \frac{176}{21}\alpha_0\rho^6 + \mathcal{O}(\rho^7\ln\rho)\,, \tag{B.73}$$

it is completely specified by $\{\beta_1, \alpha_0, s_{7;1}\}$; we further highlighted arbitrary constants, fixed to zero by the overall normalization (B.65), and the extraction of the zero modes in $F_{7;1}$ and $q_{3;7;1}$ (B.67);

- in the IR, i.e., as $y \equiv \frac{1}{\rho} \to 0$,

$$\hat{q}_{3;7;1} = \hat{q}^h_{3;7;1;0} + \mathcal{O}(y)\,, \qquad q_{7;7;1} = q^h_{7;7;1;0} + \mathcal{O}(y)\,, \qquad \hat{F}_{7;1} = \hat{F}^h_{7;1;0} + \mathcal{O}(y)\,, \tag{B.74}$$

it is completely specified by

$$\left\{\hat{q}^h_{3;7;1;0}\,,\, q^h_{7;7;1;0}\,,\, \hat{F}^h_{7;1;0}\,,\, \beta_1\,,\, \alpha_0\,,\, s_{7;1}\right\}. \tag{B.75}$$

In total, the UV and IR expansions are completely determined by the parameters (B.75), which is precisely what is needed to find a unique solution for three second order ODEs (B.68)–(B.70). Solving these equations we find

$$\begin{aligned} s_{7;1} &= 4.3945(5)\,, & \beta_1 &= -3.5047(8)\,, & \alpha_0 &= 4.2000(0)\,, \\ \hat{q}^h_{3;7;1;0} &= -4.4179(7)\,, & q^h_{7;7;1;0} &= -1850.3(4)\,, & \hat{F}^h_{7;1;0} &= -1.2222(2)\,. \end{aligned} \tag{B.76}$$

Note that equation (B.70) for $\hat{F}_{7;1}$ is decoupled, and involves k_1 for which the analytic expression is available (B.12); solving this equation using the techniques of section B.1.1, we find

$$\begin{aligned} \hat{F}_{7;1} &= \frac{\rho^3(21\rho^4+112\rho^3+240\rho^2+256\rho+128)}{21(1+\rho)^7}\,G_{7;1}\,, \qquad \alpha_0 = \frac{21}{5}\,, \\ G'_{7;1} &= -\frac{7\rho^3}{10(1+\rho)^{5/2}(21\rho^4+112\rho^3+240\rho^2+256\rho+128)^2}\Big(126\rho^8+1519\rho^7+7903\rho^6 \\ &\quad +23520\rho^5+44784\rho^4+56832\rho^3+47616\rho^2+24576\rho+6144\Big)\ln\frac{\sqrt{1+\rho}+1}{\sqrt{1+\rho}-1} \\ &\quad +\frac{7(\rho+2)\rho}{5(1+\rho)^2(21\rho^4+112\rho^3+240\rho^2+256\rho+128)^2}\Big(126\rho^8+1183\rho^7+4375\rho^6+4976\rho^5 \\ &\quad -12296\rho^4-49280\rho^3-68992\rho^2-45056\rho-11264\Big)\,, \end{aligned} \tag{B.77}$$

where the analytic expression for α_0 is in perfect agreement with the numerical result (B.76).

JHEP01(2023)130

n	$s^{(A)\&(B)}_{n;1}$	$s^{(C)}_{n;1}$
3	$\pm\sqrt{2}$	–
4	$\pm\sqrt{2}$	–
5	$\pm\sqrt{2}$	–
6	$\pm\sqrt{2}$	–
7	$\pm\frac{\sqrt{1355}}{25}$	4.39(5)
8	$\pm\frac{\sqrt{73163}}{175}$	4.95(1)
9	$\pm\frac{\sqrt{1276274}}{700}$	5.32(3)
10	$\pm\frac{\sqrt{604049698}}{14700}$	did not compute

Table 2. Leading corrections to the conformal spectra on branches (A_b), (B_b) and (C_b).

B.1.4 Select values of $s_{3\leq n\leq 10;1}$

Extending the computations of sections B.1.1 and B.1.3, we collect in the table 2 leading corrections to the conformal spectra on branches (A_b), (B_b) and (C_b) for $3 \leq n \leq 10$. These results are used to highlight the features of the spectra presented in figure 6. Notice that the leading correction to the conformal spectra on branches (A_b), (B_b) is unchanged for $n \leq 6$,

$$-\,\mathfrak{Im}[\mathfrak{w}]\Big|_{(A_b)\&(B_b)} = n \pm \sqrt{2b} + \mathcal{O}(b)\,. \tag{B.78}$$

C Chirally symmetric DFP — TypeA$_s$, chirally symmetric fluctuations

In this appendix we discuss the linearized fluctuations about TypeA$_s$ dynamical fixed point of the cascading gauge theory, preserving the U(1)$_R$ chiral symmetry of this DFP. The corresponding background and the fluctuation equations of motion are the special case, a consistent truncation, of the general equations discussed in appendix A. Specifically,

- for the background we find [17]:

$$f_c \equiv f_2\,, \qquad f_a = f_b \equiv f_3\,, \qquad K_1 = K_3 \equiv K\,, \qquad K_2 \equiv 1\,; \tag{C.1}$$

- for the fluctuations: we keep $\{fl_g\,,\, fl_h\}$ modes, and further restrict

$$fl_a = fl_b \equiv fl_3\,, \qquad fl_{K_1} = fl_{K_3} \equiv fl_K\,, \qquad fl_{K_2} \equiv 0\,, \qquad fl_c \equiv fl_2\,. \tag{C.2}$$

Given (C.1) and (C.2), the corresponding equations for the fluctuations and the boundary conditions can be deduced from those of the symmetry broken DFP discussed in appendix A.

In the rest of this appendix we analyze the near-conformal $b \to 0$, equivalently $H \gg \Lambda$, limit of the chiral symmetry preserving fluctuations in TypeA$_s$ DFP. Strictly at $b = 0$ the cascading gauge theory is conformal, and the spectra can be computed analytically [29].

JHEP01(2023)130

We discover multiple spectral branches of the fluctuations. On some branches we are able to compute analytically the leading $\mathcal{O}(\sqrt{b})$, and numerically the first $\mathcal{O}(b)$ subleading, corrections to the conformal spectra, sections C.1.1, C.1.2 and C.1.4. On the remaining branches we compute numerically the leading $\mathcal{O}(b)$ corrections to the conformal spectra, sections C.1.3 and C.1.5. Perturbative results obtained here provide a valuable check of the finite $\frac{H}{\Lambda}$ spectra in the near-conformal limit, see figure 8.

C.1 Near-conformal limit: $b \to 0$

Introducing

$$fl_2 = (1+\rho)\,(fl_f + 4fl_w)\,, \qquad fl_3 = (1+\rho)(fl_f - fl_w)\,, \tag{C.3}$$

to leading order in b, we find[21]

$$\begin{aligned}
0 &= fl_K'' + \frac{(2s-1)\rho - 6}{2(1+\rho)\rho}\, fl_K' - \frac{3s}{2\rho(1+\rho)^2}\, fl_K\,,\\
0 &= fl_g'' + \frac{(2s-1)\rho - 6}{2(1+\rho)\rho}\, fl_g' - \frac{3s}{2\rho(1+\rho)^2}\, fl_g + 2k_1' fl_K' + \frac{k_1' s fl_K}{1+\rho}\,,\\
0 &= fl_w' + \frac{(2s-1)\rho - 6}{2\rho(1+\rho)}\, fl_w' - \frac{3(\rho s + 8\rho + 8)}{2(1+\rho)^2\rho^2}\, fl_w - \frac{2}{5}k_1' fl_K' - \frac{k_1' s fl_K}{5(1+\rho)}\,,\\
0 &= fl_f'' + \frac{(2s-1)\rho - 6}{2\rho(1+\rho)}\, fl_f' - \frac{3\rho s + 64\rho + 64}{2\rho^2(1+\rho)^2}\, fl_f + \frac{8k_1' fl_K'}{5\rho^2(s-4)(1+s)}\Big(\rho^2 s^2 - 3\rho^2 s\\
&\quad - 9\rho^2 - 120\rho - 120\Big) + \frac{4fl_K}{5(1+\rho)\rho^4(s-4)(1+s)}\Big(\rho k_1'\Big(\rho^3 s(s+6)(s-4) + 10\rho s(\rho s\\
&\quad - 15\rho - 12) + 480(\rho+2)(\rho+1)\Big) + 80\rho^2 s^2 - 240\rho^2 s - 240\rho^2 + 1920\rho + 1920\Big)\,.
\end{aligned} \tag{C.4}$$

Solving the decoupled equation for fl_K, we find (up to an overall normalization A_K)

$$fl_K = A_K\, \frac{\rho^4}{(1+\rho)^s}\, {}_2F_1\left(\frac{5}{2}, 4-s; 5; -\rho\right)\,, \qquad s = 4, 5, \cdots\,. \tag{C.5}$$

Given (C.5), and using (B.12), it is straightforward to see that it is impossible to solve the equation for fl_g in (C.4), so that this mode is both normalizable as $\rho \to 0$ and analytic as $\rho \to \infty$ — this means that the amplitude of fl_K must always vanish in the limit $b \to 0$. This is precisely what we find, see (C.9) and (C.10).

With $fl_K \equiv 0$, we find from (C.4) the following leading order as $b \to 0$ solutions:

$$fl_g = A_g\, \frac{\rho^4}{(1+\rho)^s}\, {}_2F_1\left(\frac{5}{2}, 4-s; 5; -\rho\right)\,, \qquad s = 4, 5, \cdots\,, \tag{C.6}$$

$$fl_w = A_w\, \frac{\rho^6}{(1+\rho)^s}\, {}_2F_1\left(\frac{9}{2}, 6-s; 9; -\rho\right)\,, \qquad s = 6, 7, \cdots\,, \tag{C.7}$$

$$fl_f = A_f\, \frac{\rho^8}{(1+\rho)^s}\, {}_2F_1\left(\frac{13}{2}, 8-s; 13; -\rho\right)\,, \qquad s = 8, 9, \cdots\,. \tag{C.8}$$

[21] Note (see the equation for fl_f) that the leading $s = 4$ mode is more subtle; it will be discussed in details in section C.1.1.

JHEP01(2023)130

Extending the leading order solutions (C.6), (C.7) and (C.8) perturbatively in b we identify three branches:

- A pair of non-analytic in b branches, (A_s) and (B_s),

$$\begin{aligned} s\Big|_{A,B} &= n + \sum_{k=1}^{\infty} (\pm)^k s_{n;k}\, b^{k/2}\,, \quad n \in \mathbb{N} \geq 4\,, & fl_g\Big|_{A,B} &= \sum_{k=0}^{\infty} (\pm)^k fl_{g;n;k}\, b^{k/2}\,, \\ fl_K\Big|_{A,B} &= \sum_{k=1}^{\infty} (\pm)^k fl_{K;n;k}\, b^{k/2}\,, & fl_w\Big|_{A,B} &= \sum_{k=0}^{\infty} (\pm)^k fl_{w;n;k}\, b^{k/2}\,, \\ fl_f\Big|_{A,B} &= \sum_{k=0}^{\infty} (\pm)^k fl_{f;n;k}\, b^{k/2}\,, \end{aligned} \tag{C.9}$$

with $fl_{g;n;0}$ given by (C.6), $fl_{w;n\geq 6;0}$ given by (C.7), and $fl_{f;n\geq 8;0}$ given by (C.8) with $s = n$. $fl_{w;n;0} \equiv 0$ for $4 \leq n < 6$, $fl_{f;n;0} \equiv 0$ for $4 < n < 8$, and $fl_{f;4;0} \neq 0$, see (C.15).

- An analytic in b branch (C_s),

$$\begin{aligned} s\Big|_{C} &= n + \sum_{k=1}^{\infty} s_{n;k}\, b^{k}\,, \quad n \in \mathbb{N} \geq 6\,, & fl_g\Big|_{C} &= \sum_{k=0}^{\infty} fl_{g;n;k}\, b^{k}\,, \\ fl_K\Big|_{C} &= \sum_{k=1}^{\infty} fl_{K,n;k}\, b^{k}\,, & fl_w\Big|_{C} &= \sum_{k=0}^{\infty} fl_{w;n;k}\, b^{k}\,, \quad fl_f\Big|_{C} = \sum_{k=0}^{\infty} fl_{f;n;k}\, b^{k}\,, \end{aligned} \tag{C.10}$$

where $fl_{w;n;0}$ is given by (C.7), $fl_{g;n;0}$ is given by (C.6), and $fl_{f;n\geq 8;0}$ given by (C.8) with $s = n$. $fl_{f;n;0} \equiv 0$ for $6 \leq n < 8$.

C.1.1 Details of $s = 4 \pm \mathcal{O}(\sqrt{b})$ branches: $(\mathbf{A}_s)$ and $(\mathbf{B}_s)$

From (C.6), here

$$s_{4;0} = 4\,, \qquad fl_{g;4;0} = \boxed{1} \cdot \frac{\rho^4}{(1+\rho)^s}\, {}_2F_1\left(\frac{5}{2}, 4-s; 5; -\rho\right)\Big|_{s=s_{4;0}} = \frac{\rho^4}{(1+\rho)^4}\,, \tag{C.11}$$

where we highlighted the (fixed) overall normalization of the linearized fluctuations; the latter implies that in the UV, i.e., $\rho \to 0$, expansion of $fl_{g;4;k\geq 1}$ the order $\mathcal{O}(\rho^4)$ terms are absent. Because the leading order fluctuation spectra (C.5) and (C.6) are degenerate, the equations for $fl_{K;4;k}$ will necessarily contain zero modes; specifically, if $fl_{K;4;k\geq 1}$ is a solution, so is $(fl_{K;4;k} + \alpha_k \cdot fl_{g;4;0})$ for an arbitrary set of constants α_k. As in section B.1.1, the zero modes at order k will be completely fixed at order $k+1$. We find it convenient to set

$$fl_{K;4;k} \equiv \boxed{\alpha_k} \cdot\ fl_{g;4;0} + \hat{fl}_{K;4;k}\,, \tag{C.12}$$

with the understanding that in the UV expansion of $\hat{fl}_{K;4;k}$ the order $\mathcal{O}(\rho^4)$ terms are absent.

As in section B.1.1, the equation for $\hat{fl}_{K;4;1}$ is homogeneous, and the boundary condition implied by (C.12) sets

$$\hat{fl}_{K;4;1} \equiv 0\,. \tag{C.13}$$

JHEP01(2023)130

The leading order equation for $fl_{f;4;0}$ takes form

$$0 = fl''_{f;4;0} + \frac{7\rho-6}{2\rho(1+\rho)}\, fl'_{f;4;0} - \frac{2(19\rho+16)}{\rho^2(1+\rho)^2}\, fl_{f;4;0} + \frac{64(\rho^2+24\rho+24)\alpha_1}{5(1+\rho)^5 s_{4;1}}\,, \tag{C.14}$$

and can be solved analytically,

$$f_{f;4;0} = \frac{128\alpha_1\rho^2}{15 s_{4;1}(1+\rho)^3}\,. \tag{C.15}$$

The subleading set of equations involving constants α_1, $s_{4;1}$, and functions $\{fl_{g;4;1}, \hat{fl}_{K;4;2}, fl_{w;4;1}\}$ reads:

$$0 = fl''_{g;4;1} + \frac{7\rho-6}{2\rho(1+\rho)}\, fl'_{g;4;1} - \frac{6}{\rho(1+\rho)^2}\, fl_{g;4;1} + \frac{4\alpha_1(\rho+2)\rho^3 k_1'}{(1+\rho)^5} + \frac{5\rho^3 s_{4;1}}{2(1+\rho)^6}\,, \tag{C.16}$$

$$\begin{aligned} 0 = {} & \hat{fl}''_{K;4;2} + \frac{7\rho-6}{2\rho(1+\rho)}\hat{fl}'_{K;4;2} - \frac{6}{\rho(1+\rho)^2}\hat{fl}_{K;4;2} + \frac{2k_1'(\rho+2)(32\alpha_1(\rho+1)-5\rho^2 s_{4;1})\rho}{5(1+\rho)^5 s_{4;1}} \\ & + \frac{1}{30(1+\rho)^6 s_{4;1}}\Big(75\alpha_1\rho^3 s_{4;1}^2 - 240\rho^3 s_{4;1} + 2048\alpha_1(1+\rho)^2 - 240\rho^2 s_{4;1}\Big)\,, \end{aligned} \tag{C.17}$$

$$0 = fl''_{w;4;1} + \frac{7\rho-6}{2\rho(1+\rho)}\, fl'_{w;4;1} - \frac{6(3\rho+2)}{\rho^2(1+\rho)^2}\, fl_{w;4;1} - \frac{4(\rho+2)\rho^3 k_1'\alpha_1}{5(1+\rho)^5}\,. \tag{C.18}$$

Above set can be solved numerically — and we explain how to do it for the set of equations at the next order — here instead we show that the most important constant, i.e., $s_{4;1}$ can be computed analytically:

- Substituting

$$\alpha_1 = s_{4;1} v\,, \qquad fl_{g;4;1} = s_{4;1}\cdot fl_{g;4;0}\cdot\ G_{g;4;1}\,, \tag{C.19}$$

and using (B.12), we find a general analytic solution for $G'_{g;4;1}$,

$$\begin{aligned} G'_{g;4;1} = {} & \frac{3v\rho^3}{16(1+\rho)^{5/2}}\ln\frac{\sqrt{1+\rho}+1}{\sqrt{1+\rho}-1} + \frac{(1+\rho)^{3/2}}{\rho^5}C_1 - \frac{1}{24(1+\rho)^2\rho^5}\Big((\rho+2) \\ & \times(9\rho^6 - 24\rho^5 - 152\rho^4 + 768\rho^3 + 2944\rho^2 + 3072\rho + 1024)v + 8(1+\rho)(5\rho^4 \\ & - 40\rho^3 - 240\rho^2 - 320\rho - 128)\Big)\,. \end{aligned} \tag{C.20}$$

Analyticity of $fl_{g;4;1}$, and thus $G'_{g;4;1}$, as $\rho\to\infty$ sets

$$C_1 = 0\,, \tag{C.21}$$

and normalizability of $fl_{g;4;1}$ identifies

$$v = \frac{1}{2}\,. \tag{C.22}$$

- We continue with (C.17), setting

$$\hat{fl}_{K;4;2} = fl_{g;4;0}\cdot H_{K;4;2}\,, \tag{C.23}$$

JHEP01(2023)130

allows to solve analytically for $H'_{K;4;2}$,

$$H'_{K;4;2} = -\frac{\rho(15\rho^2-64\rho-64)}{160(1+\rho)^{5/2}}\ln\frac{\sqrt{1+\rho}+1}{\sqrt{1+\rho}-1} + \frac{(1+\rho)^{3/2}}{\rho^5}\,C_1 - \frac{s_{4;1}^2}{6(1+\rho)\rho^5}\Big(5\rho^4 - 40\rho^3 - 240\rho^2 - 320\rho - 128\Big) + \frac{\rho+2}{240(1+\rho)^2\rho^5}\Big(45\rho^6 - 312\rho^5 + 840\rho^4 - 11008\rho^3 - 38784\rho^2 - 39936\rho - 13312\Big)\,. \tag{C.24}$$

Analyticity of $\hat{fl}_{K;4;2}$, and thus $H'_{K;4;2}$, in the limit $\rho\to\infty$ requires

$$C_1 = 0\,, \tag{C.25}$$

while normalizability of $\hat{fl}_{K;4;2}$ sets

$$s_{4;1}^2 = \frac{26}{5} \qquad \Longrightarrow \qquad s_{4;1} = \pm\frac{\sqrt{130}}{5}\,. \tag{C.26}$$

Note that to determine $s_{4;1}$, there is no need to solve for $fl_{w;4;1}$ — of course, this solution is needed for the computation of higher order corrections $s_{4;k\geq 2}$.

The sub-subleading set of equations involving constants α_2, $s_{4;2}$, and functions $\{fl_{f;4;1}$, $fl_{g;4;2}$ and $\hat{fl}_{K;4;3}\}$ reads (we omit the equation for $fl_{w;4;2}$ as it is not need to compute $s_{4;2}$; it is required for the computation of $s_{4;k\geq 3}$):

$$\begin{aligned}
0 = {} & fl''_{f;4;1} + \frac{7\rho-6}{2\rho(1+\rho)}\,fl'_{f;4;1} - \frac{2(19\rho+16)}{\rho^2(1+\rho)^2}\,fl_{f;4;1} - \frac{8(\rho^2+24\rho+24)k_1'\hat{fl}'_{K;4;2}}{5\rho^2 s_{4;1}} \\
& + \frac{32(\rho^2+24\rho+24)(\rho k_1'+2)\hat{fl}_{K;4;2}}{5s_{4;1}\rho^4(1+\rho)} - \frac{4(\rho^2+24\rho+24)(64\alpha_1(\rho+1)-5\rho^2 s_{4;1})(k_1')^2}{25s_{4;1}^2(1+\rho)^4} \\
& + \frac{8\alpha_1\rho^2(4\rho^2-3\rho-12)k_1'}{5(1+\rho)^5} - \frac{2048(\rho+2)(\rho^2+24\rho+24)\alpha_1}{75s_{4;1}^2(1+\rho)^4\rho}\left(f'_{3;1}+\frac{1}{4}f'_{2;1}+\frac{1}{4}h_1'\right) \\
& - \frac{64\alpha_1(\rho^2+24\rho+24)s_{4;2}}{5(1+\rho)^5 s_{4;1}^2} + \frac{64(\rho^2+24\rho+24)\alpha_2}{5(1+\rho)^5 s_{4;1}} + \frac{1}{75(1+\rho)^5 s_{4;1}^2\rho^2}\Big(-768(\rho^2 \\
& + 24\rho+24)\alpha_1\left(\rho+\frac{4}{3}\right)(\rho+4)h_1 - 1024\alpha_1(1+\rho)(\rho^2+24\rho+24)(f_{2;1}+4f_{3;1}-4k_1) \\
& + (24576 + 3968\rho^4 s_{4;1}^2 + (-4288 s_{4;1}^2+1024)\rho^3 + (-4608 s_{4;1}^2+25600)\rho^2 + 49152\rho)\alpha_1 \\
& + 240\rho^2 s_{4;1}(\rho^2+24\rho+24)\Big)\,,
\end{aligned} \tag{C.27}$$

$$\begin{aligned}
0 = {} & fl''_{g;4;2} + \frac{7\rho-6}{2\rho(1+\rho)}\,fl'_{g;4;2} - \frac{6}{\rho(1+\rho)^2}\,fl_{g;4;2} + 2k_1'\hat{fl}'_{K;4;2} + \frac{4k_1'\hat{fl}_{K;4;2}}{1+\rho} \\
& + \frac{s_{4;1}fl'_{g;4;1}}{1+\rho} + \frac{4k_1'\rho^3(\rho+2)\alpha_2}{(1+\rho)^5} + \frac{4(\rho+2)(16\alpha_1(\rho+1)-5\rho^2 s_{4;1})\rho g_1'}{5(1+\rho)^5 s_{4;1}} + \frac{\alpha_1\rho^4 s_{4;1}k_1'}{(1+\rho)^5} \\
& + \frac{(\rho+2)\rho^3(f'_{2;1}+4f'_{3;1})}{(1+\rho)^5} - \frac{3s_{4;1}fl_{g;4;1}}{2\rho(1+\rho)^2} + \frac{1}{30s_{4;1}(1+\rho)^6}\Big(1024\alpha_1(2\rho+1) - 30h_1\rho^4 s_{4;1} \\
& + (75s_{4;2}-240)s_{4;1}\rho^3 + (-240s_{4;1}+1024\alpha_1)\rho^2\Big)\,,
\end{aligned} \tag{C.28}$$

JHEP01(2023)130

$$
\begin{aligned}
0 = {} & \hat{fl}''_{K;4;3} + \frac{7\rho-6}{2\rho(1+\rho)}\,\hat{fl}'_{K;4;3} - \frac{6}{\rho(1+\rho)^2}\,\hat{fl}_{K;4;3} - \frac{3}{4}k_1' fl'_{f;4;1} - \frac{12\hat{fl}'_{K;4;2}}{5(1+\rho)s_{4;1}\rho^2}\Big(\rho(\rho \\
& + 2)(1+\rho)^2(k_1')^2 - \frac{8}{3}(1+\rho)^2 k_1' - \frac{5}{12}\rho^2 s_{4;1}^2\Big) + \frac{48\hat{fl}_{K;4;2}}{5s_{4;1}(1+\rho)^2\rho^4}\Big(\rho^2(\rho+2)(1+\rho)^2(k_1')^2 \\
& + 2\left(\rho+\frac{2}{3}\right)\rho(1+\rho)^2 k_1' - \frac{5}{32}\rho^3 s_{4;1}^2 - \frac{16}{3}(1+\rho)^2\Big) + \frac{1}{2(1+\rho)\rho^2}\Big(-2\rho^2\Big((1+\rho) \\
& \times (fl'_{g;4;1} - 2fl_{w;4;1}) + \frac{3}{2}fl_{f;4;1} - 4fl_{w;4;1}\Big)k_1' + 28fl_{f;4;1} + 32fl_{w;4;1} - 4(\rho^2 k_1' \\
& + 4)fl_{g;4;1}\Big) + \frac{192\rho(\rho+2)(1+\rho)^2 k_1' + 25\rho^3 s_{4;1}^2 - 512(1+\rho)^2}{10s_{4;1}(1+\rho)^6}\alpha_2 - \frac{96\alpha_1 s_{4;2}}{5(1+\rho)^6 s_{4;1}^2}\Big(\\
& \rho(\rho+2)(1+\rho)^2 k_1' - \frac{25}{192}\rho^3 s_{4;1}^2 - \frac{8}{3}(1+\rho)^2\Big) + \frac{\alpha_1}{75\rho^2(1+\rho)^6 s_{4;1}^2}\Big(-1152\rho^3(\rho+2) \\
& \times (1+\rho)^4(k_1')^3 - 315\rho^2\left(\rho^4 s_{4;1}^2 + \frac{4}{7}\rho^3 s_{4;1}^2 - \frac{1024}{105}(1+\rho)^2\right)(1+\rho)^2(k_1')^2 - 768(\rho+2) \\
& \times \Big(\rho(\rho+2)(\rho+1)(f'_{2;1} + h_1' + 4f'_{3;1}) + \left(\frac{3}{2}\rho^2 + 8\rho + 8\right)h_1 + 2(\rho+1)(f_{2;1} + 4f_{3;1} \\
& - 4k_1 - 1) + \frac{3}{8}\rho^2 s_{4;1}^2\Big)\rho(1+\rho)^2 k_1' + 75(\rho+2)\rho(1+\rho)\Big(\left(\rho^4 s_{4;1}^2 + \frac{2048}{75}(1+\rho)^2\right)f'_{2;1} \\
& - 2\left(\rho^4 s_{4;1}^2 - \frac{1024}{75}(1+\rho)^2\right)h_1'\Big) - 2\rho(\rho+2)(1+\rho)(75\rho^5 s_{4;1}^2 g_1' - 4096(1+\rho)^2 f'_{3;1}) \\
& + (-75\rho^6 s_{4;1}^2 + 1024(\rho+4)(3\rho+4)(1+\rho)^2)h_1 - 600(1+\rho)\Big(-\frac{512}{75}(1+\rho)^2(f_{2;1} \\
& + 4f_{3;1} - 4k_1 - 1) + s_{4;1}^2\left(\rho^4 - \frac{32}{25}\rho^2(\rho+1)\right)\Big)\Big) + \frac{1}{10(1+\rho)^5 s_{4;1}}\Big(4\rho^2(1+\rho)^2(k_1')^2 \\
& \times (3\rho(2+\rho)k_1' - 8) + (-5\rho^4 s_{4;1}^2 + 48\rho(\rho+2)(1+\rho))k_1' - 128(1+\rho)\Big)\,. \qquad \text{(C.29)}
\end{aligned}
$$

Eqs. (C.27)–(C.29) are solved subject to the asymptotic expansions,

- in the UV, i.e., as $\rho \to 0$,

$$
\begin{aligned}
fl_{f;4;1} = {} & \left(-\frac{128(\alpha_1 s_{4;1}^2 + 5\alpha_1 s_{4;2} - 5\alpha_2 s_{4;1})}{75 s_{4;1}^2} - \frac{46592\alpha_1}{225 s_{4;1}^2} + \frac{64}{15 s_{4;1}}\right)\rho^2 + \cdots \\
& + \rho^8\left(fl_{f;4;1;8;0} + \alpha_1\left(\frac{17}{200} - \frac{32}{15}k_{4;0;1}\right)\ln\rho - \frac{1}{20}\alpha_1\ln^2\rho\right) + \mathcal{O}(\rho^9\ln^2\rho)\,, \qquad \text{(C.30)}
\end{aligned}
$$

$$
fl_{g;4;2} = \left(\boxed{0} + \left(4\alpha_2 + 2 - \frac{1456\alpha_1}{15 s_{4;1}}\right)\ln\rho\right)\rho^4\ln\rho + \mathcal{O}(\rho^5\ln\rho)\,, \qquad \text{(C.31)}
$$

$$
\begin{aligned}
\hat{fl}_{K;4;3} = {} & \left(-\frac{64(\alpha_1 s_{4;1}^2 + 5\alpha_1 s_{4;2} - 5\alpha_2 s_{4;1})}{75 s_{4;1}^2} - \frac{23296\alpha_1}{225 s_{4;1}^2} + \frac{32}{15 s_{4;1}}\right)\rho^2 \\
& + \cdots + \left(\boxed{0} - 4\alpha_1\right)\rho^4\ln\rho + \mathcal{O}(\rho^5\ln\rho)\,, \qquad \text{(C.32)}
\end{aligned}
$$

JHEP01(2023)130

it is completely specified by $\{\alpha_2, s_{4;2}, fl_{f;4;1;8;0}\}$; we further highlighted arbitrary constants, fixed to zero by the overall normalization (C.11) and the extraction of the zero mode in $fl_{K;4;3}$ (C.12);

- in the IR, i.e., as $y \equiv \frac{1}{\rho} \to 0$,

$$fl_{f;4;1} = fl^h_{f;4;1;0} + \mathcal{O}(y)\,, \qquad fl_{g;4;2} = fl^h_{g;4;2;0} + \mathcal{O}(y)\,, \qquad \hat{fl}_{K;4;3} = \hat{fl}^h_{K;4;3;0} + \mathcal{O}(y)\,, \tag{C.33}$$

it is completely specified by

$$\left\{ fl^h_{f;4;1;0}\,,\ fl^h_{g;4;2;0}\,,\ \hat{fl}^h_{K;4;3;0}\,,\ \alpha_2\,,\ s_{4;2} \right\}. \tag{C.34}$$

In total, the UV and IR expansions are completely determined by the parameters (C.34) and $fl_{f;4;1;8;0}$, which is precisely what is needed to find a unique solution for three second order ODEs (C.27)–(C.29). Solving these equations we find

$$s_{4;2} = -1.7907(6)\,. \tag{C.35}$$

Once the numerical solution for $\{fl_{f;4;1}, fl_{g;4;2}, \hat{fl}_{K;4;3}\}$ is found, the second order ODE for $fl_{w;4;2}$ — necessary to determine $s_{4;k\geq 3}$ — is solved adjusting two parameters

$$\left\{ fl_{w;4;2;6,0}\,,\ fl^h_{w;4;2;0} \right\}, \tag{C.36}$$

that completely determine its UV and IR asymptotics.

C.1.2 Details of $s = 6 \pm \mathcal{O}(\sqrt{b})$ branches: $(\mathbf{A}_s)$ and $(\mathbf{B}_s)$

From (C.6), here

$$s_{6;0} = 6\,,\ fl_{g;6;0} = \boxed{1}\cdot \frac{\rho^4}{(1+\rho)^s}\,{}_2F_1\left(\frac{5}{2}, 4-s; 5; -\rho\right)\Big|_{s=s_{6;0}} = \frac{\rho^4(7\rho^2+24\rho+24)}{24(1+\rho)^6}\,, \tag{C.37}$$

where we highlighted the (fixed) overall normalization of the linearized fluctuations; the latter implies that in the UV, i.e., $\rho \to 0$, expansion of $fl_{g;6;k\geq 1}$ the order $\mathcal{O}(\rho^4)$ terms are absent. Because the leading order fluctuation spectra (C.5), (C.6) and (C.7) are degenerate at $s_{6;0}$, the equations for $fl_{K;6;k}$ and $fl_{w;6;k}$ will necessarily contain zero modes; specifically, if $fl_{K;6;k\geq 1}$ and $fl_{w;6;k\geq 1}$ are solutions, so are $(fl_{K;6;k} + \alpha_k \cdot fl_{g;6;0})$ and $(fl_{w;6;k} + \frac{\beta_k}{\beta_0} \cdot fl_{w;6;0})$,

$$fl_{w;6;0} = \beta_0 \cdot \frac{\rho^6}{(1+\rho)^s}\,{}_2F_1\left(\frac{9}{2}, 6-s; 9; -\rho\right)\Big|_{s=s_{6;0}} = \beta_0 \cdot \frac{\rho^6}{(1+\rho)^6}\,, \tag{C.38}$$

for an arbitrary set of constants $\{\alpha_k, \beta_k\}$. As in section B.1.1, the zero modes at order k will be completely fixed at order $k+1$. We find it convenient to set

$$fl_{K;6;k\geq 1} \equiv \boxed{\alpha_k} \cdot fl_{g;6;0} + \hat{fl}_{K;6;k}\,, \qquad fl_{w;6;k\geq 1} \equiv \boxed{\beta_k} \cdot \frac{1}{\beta_0} fl_{w;6;0} + \hat{fl}_{w;6;k}\,, \tag{C.39}$$

JHEP01(2023)130

with the understanding that in the UV expansion of $\hat{fl}_{K;6;k}$ the order $\mathcal{O}(\rho^4)$ terms are absent, and in the UV expansion of $\hat{fl}_{w;6;k}$ the order $\mathcal{O}(\rho^6)$ terms are absent.

As in section B.1.1, the equation for $\hat{fl}_{K;6;1}$ is homogeneous, and the boundary condition implied by (C.39) sets

$$\hat{fl}_{K;6,1} \equiv 0\,. \tag{C.40}$$

The subleading set of equations involving constants α_1, β_0, $s_{6;1}$, and functions $\{fl_{g;6;1}$, $\hat{fl}_{K;6;2}$, $\hat{fl}_{w;6;1}$, $fl_{f;6;1}\}$ reads:

$$\begin{aligned}0 = {} & fl''_{g;6;1} + \frac{11\rho-6}{2\rho(1+\rho)}\, fl'_{g;6;1} - \frac{9}{(1+\rho)^2\rho}\, fl_{g;6;1} + \frac{\rho^3 s_{6;1}(5\rho^2+24\rho+40)}{16(1+\rho)^8} \\ & + \frac{\alpha_1\rho^3(\rho+2)(7\rho^2+16\rho+16)k'_1}{4(1+\rho)^7}\,,\end{aligned} \tag{C.41}$$

$$\begin{aligned}0 = {} & \hat{fl}''_{K;6;2} + \frac{11\rho-6}{2\rho(1+\rho)}\, \hat{fl}'_{K;6;2} - \frac{9}{(1+\rho)^2\rho}\, \hat{fl}_{K;6;2} - \frac{(\rho+2)(7\rho^2+16\rho+16)\rho^3 k'_1}{8(1+\rho)^7} \\ & + \frac{(3\alpha_1\rho s_{6;1}(5\rho^2+24\rho+40) - (16(7\rho^2+24\rho+24))(1+\rho))\rho^2}{48(1+\rho)^8} \\ & + \frac{2\beta_0\rho^4(3\rho k'_1(\rho+2)+8)}{(1+\rho)^7}\,,\end{aligned} \tag{C.42}$$

$$\begin{aligned}0 = {} & \hat{fl}''_{w;6;1} + \frac{11\rho-6}{2\rho(1+\rho)}\, \hat{fl}'_{w;6;1} - \frac{3(7\rho+4)}{(1+\rho)^2\rho^2}\, \hat{fl}_{w;6;1} + \frac{9\rho^5\beta_0 s_{6;1}}{2(1+\rho)^8} \\ & - \frac{\alpha_1\rho^3(\rho+2)(7\rho^2+16\rho+16)k'_1}{20(1+\rho)^7}\,,\end{aligned} \tag{C.43}$$

$$\begin{aligned}0 = {} & fl''_{f;6;1} + \frac{11\rho-6}{2\rho(1+\rho)}\, fl'_{f;6;1} - \frac{41\rho+32}{(1+\rho)^2\rho^2}\, fl_{f;6;1} \\ & + \frac{4(5\rho^2+8\rho+8)(7\rho^2+24\rho+24)\alpha_1}{7(1+\rho)^7} + \frac{4\alpha_1\rho^3(\rho+2)(3\rho^2+4\rho+4)k'_1}{5(1+\rho)^7}\,.\end{aligned} \tag{C.44}$$

We show here that the most important constant, i.e., $s_{6;1}$ can be computed analytically:

- Substituting

$$\alpha_1 = s_{6;1}\cdot v\,, \qquad fl_{g;6;1} = s_{6;1}\cdot fl_{g;6;0}\cdot J_{g;6;1}\,, \tag{C.45}$$

and using (B.12), we find a general analytic solution for $J'_{g;6;1}$,

$$\begin{aligned}J'_{g;6;1} = {} & \frac{3\rho^3 v}{16(1+\rho)^{5/2}}\ln\frac{\sqrt{1+\rho}+1}{\sqrt{1+\rho}-1} + \frac{(1+\rho)^{7/2}}{\rho^5(7\rho^2+24\rho+24)^2}\, C_1 \\ & - \frac{1}{40\rho^5(1+\rho)^2(7\rho^2+24\rho+24)^2}\Big((\rho+2)(735\rho^{10}+3080\rho^9-6200\rho^8-63104\rho^7 \\ & -151104\rho^6-100864\rho^5+233984\rho^4+622592\rho^3+647168\rho^2+327680\rho \\ & +65536)v+8(\rho+1)(75\rho^8+624\rho^7+1968\rho^6-576\rho^5-20160\rho^4-53760\rho^3 \\ & -64512\rho^2-36864\rho-8192)\Big)\,.\end{aligned} \tag{C.46}$$

JHEP01(2023)130

Analyticity of $fl_{g;6;1}$, and thus $J'_{g;6;1}$, in the limit $\rho \to \infty$ requires

$$C_1 = 0\,, \tag{C.47}$$

while normalizability of $fl_{g;6;1}$ sets

$$v = \frac{1}{2}\,. \tag{C.48}$$

- We continue with (C.43), setting

$$\hat{fl}_{w;6;1} = s_{6;1} \cdot \frac{1}{\beta_0} fl_{w;6;0} \cdot H_{w;6;1}\,, \tag{C.49}$$

allows to solve analytically for $H'_{w;6;1}$,

$$\begin{aligned} H'_{w;6;1} = &-\frac{\rho(35\rho^2+96\rho+96)}{6400(1+\rho)^{5/2}} \ln\frac{\sqrt{1+\rho}+1}{\sqrt{1+\rho}-1} + \frac{(1+\rho)^{7/2}}{\rho^9}\, C_1 \\ &-\frac{1}{336000(1+\rho)^2\rho^9}\Big((9600(1+\rho))(45\rho^8-144\rho^7+672\rho^6-8064\rho^5-80640\rho^4 \\ &-215040\rho^3-258048\rho^2-147456\rho-32768)\beta_0-7(\rho+2)(525\rho^{10}+40\rho^9 \\ &-7000\rho^8-11008\rho^7-14208\rho^6+74752\rho^5+560128\rho^4+1245184\rho^3 \\ &+1294336\rho^2+655360\rho+131072)\Big)\,. \end{aligned} \tag{C.50}$$

Analyticity of $\hat{fl}_{w;6;1}$, and thus $H'_{w;6;1}$, in the limit $\rho \to \infty$ requires

$$C_1 = 0\,, \tag{C.51}$$

while normalizability of $\hat{fl}_{w;6;1}$ sets

$$\beta_0 = -\frac{7}{1200}\,. \tag{C.52}$$

- Consider now (C.42): introducing

$$\hat{fl}_{K;6;2} = fl_{g;6;0} \cdot G_{K;6;2}\,, \tag{C.53}$$

we solve for $G'_{K;6;2}$,

$$\begin{aligned} G'_{K;6;2} = &-\frac{3\rho^3(3185\rho^4+21504\rho^3+57504\rho^2+72000\rho+36000)}{2000(1+\rho)^{5/2}(7\rho^2+24\rho+24)^2} \ln\frac{\sqrt{1+\rho}+1}{\sqrt{1+\rho}-1} \\ &+\frac{(1+\rho)^{7/2}}{\rho^5(7\rho^2+24\rho+24)^2}\, C_1 + \frac{1}{5000\rho^5(1+\rho)^2(7\rho^2+24\rho+24)^2}\Big((\rho+2)(47775\rho^{10} \\ &+195160\rho^9+166200\rho^8-164672\rho^7+220128\rho^6-2597632\rho^5-19464448\rho^4 \\ &-43270144\rho^3-44978176\rho^2-22773760\rho-4554752)-500(1+\rho)(75\rho^8+624\rho^7 \\ &+1968\rho^6-576\rho^5-20160\rho^4-53760\rho^3-64512\rho^2-36864\rho-8192)s_{6;1}^2\Big)\,. \end{aligned} \tag{C.54}$$

JHEP01(2023)130

Analyticity of $\hat{fl}_{K;6;2}$, and thus $G'_{K;6;2}$, in the limit $\rho \to \infty$ requires

$$C_1 = 0\,, \tag{C.55}$$

while normalizability of $\hat{fl}_{K;6;2}$ sets

$$s_{6;1}^2 = \frac{278}{125} \qquad \Longrightarrow \qquad s_{6;1} = \pm\frac{\sqrt{1390}}{25}\,. \tag{C.56}$$

The remaining equation, i.e., (C.44), does not constrain $s_{6;1}$ — it is required to determine the higher-order corrections $s_{6,k\geq 2}$.

C.1.3 Details of $s = 6 + \mathcal{O}(b)$ branch: $(\mathbf{C}_s)$

From (C.7), here

$$s_{6;0} = 6\,, \qquad fl_{w;6;0} = 1 \cdot \frac{\rho^6}{(1+\rho)^s}\, {}_2F_1\left(\frac{9}{2}, 6-s; 9; -\rho\right)\Big|_{s=s_{6;0}} = \frac{\rho^6}{(1+\rho)^6}\,, \tag{C.57}$$

where we highlighted the (fixed) overall normalization of the linearized fluctuations; the latter implies that in the UV, i.e., $\rho \to 0$, expansion of $fl_{w;6;k\geq 1}$ the order $\mathcal{O}(\rho^6)$ terms are absent. Because the leading order fluctuation spectra of (C.5), (C.6) and (C.7) are degenerate at $s_{6;0}$, the equations for $fl_{g;6;k}$ and $fl_{K;6;k}$ will necessarily contain zero modes; specifically, if $fl_{g;6;k\geq 1}$ and $fl_{K;6;k\geq 1}$ are solutions, so are $(fl_{g;6;k} + \frac{\alpha_k}{\alpha_0} \cdot fl_{g;6;0})$ and $(fl_{K;6;k} + \frac{\beta_k}{\alpha_0} \cdot fl_{g;6;0})$,

$$fl_{g;6;0} = \alpha_0 \cdot {}_2F_1\left(\frac{5}{2}, 4-s; 5; -\rho\right)\Big|_{s=s_{6;0}} = \alpha_0 \cdot \frac{\rho^4(7\rho^2+24\rho+24)}{24(1+\rho)^6}\,, \tag{C.58}$$

for an arbitrary set of constants $\{\alpha_k, \beta_k\}$. As in section B.1.1, the zero modes at order k will be completely fixed at order $k+1$. We find it convenient to set

$$fl_{g;6;k\geq 1} \equiv \alpha_k \cdot \frac{1}{\alpha_0} fl_{g;6;0} + \hat{fl}_{g;6;k}\,, \qquad fl_{K;6;k\geq 1} \equiv \beta_k \cdot \frac{1}{\alpha_0} fl_{g;6;0} + \hat{fl}_{K;6;k}\,, \tag{C.59}$$

with the understanding that in the UV expansion of $\hat{fl}_{g;6;k}$ and $\hat{fl}_{K;6;k}$ the order $\mathcal{O}(\rho^4)$ terms are absent.

The subleading set of equations involving constants α_0, β_1, $s_{6;1}$, and functions $\{\hat{fl}_{g;6;1}$, $\hat{fl}_{K;6;1}$, $fl_{w;6;1}\}$ reads (we do not discuss the equation for $fl_{f;6;1}$ — it is needed to determine $s_{6;k\geq 2}$, but it does not affect the computation of $s_{6;1}$):

$$\begin{aligned} 0 = {} & \hat{fl}''_{g;6;1} + \frac{11\rho-6}{2\rho(1+\rho)}\,\hat{fl}'_{g;6;1} - \frac{9}{\rho(1+\rho)^2}\,\hat{fl}_{g;6;1} + 2k'_1\hat{fl}'_{K;6;1} + \frac{6k'_1\hat{fl}_{K;6;1}}{1+\rho} \\ & + \frac{\rho^3 k'_1(\rho+2)(7\rho^2+16\rho+16)\beta_1}{4(1+\rho)^7} + \frac{2\rho^6(k'_1)^2}{(1+\rho)^6} + \frac{8\rho^4}{(1+\rho)^7} - \frac{\rho^2\alpha_0}{48(1+\rho)^8}\Big(-3\rho(\rho+2) \\ & \times (1+\rho)(7\rho^2+16\rho+16)(f'_{2;1}+4f'_{3;1}-4g'_1) + 9\rho^2(7\rho^2+24\rho+24)h_1 - 3\rho(5\rho^2+24\rho \\ & + 40)s_{6;1} + 16(1+\rho)(7\rho^2+24\rho+24)\Big)\,, \end{aligned} \tag{C.60}$$

JHEP01(2023)130

$$0 = \hat{f}l''_{K;6;1} + \frac{11\rho-6}{2\rho(1+\rho)}\,\hat{f}l'_{K;6;1} - \frac{9}{\rho(1+\rho)^2}\,\hat{f}l_{K;6;1} + \frac{2(3k_1'\rho(\rho+2)+8)\rho^4}{(1+\rho)^7} - \frac{\rho^2(3k_1'\rho(\rho+2)(7\rho^2+16\rho+16)+56\rho^2+192\rho+192)\alpha_0}{24(1+\rho)^7}\,, \tag{C.61}$$

$$\begin{aligned}0 = {} & fl''_{w;6;1} + \frac{11\rho-6}{2\rho(1+\rho)}\,fl'_{w;6;1} - \frac{3(7\rho+4)}{\rho^2(1+\rho)^2}\,fl_{w;6;1} - \frac{2}{5}k_1'\hat{f}l'_{K;6;1} - \frac{6k_1'\hat{f}l_{K;6;1}}{5(1+\rho)} \\ & + \frac{9\rho^5 s_{6;1}}{2(1+\rho)^8} - \frac{19\rho^6(k_1')^2}{20(1+\rho)^6} + \frac{(7\rho^2+24\rho+24)((k_1')^2\rho^2(1+\rho)+4)\rho^2\alpha_0}{120(1+\rho)^7} \\ & - \frac{\rho^3 k_1'(\rho+2)(7\rho^2+16\rho+16)\beta_1}{20(1+\rho)^7} - \frac{\rho^4}{20(1+\rho)^8}\Big(2\rho(\rho+2)(\rho+1)(33f'_{2;1}-48f'_{3;1} \\ & - 5h_1') + 5(7\rho+4)(3\rho-4)h_1 + 80(\rho+1)\left(k_1 + \frac{19}{4}f_{2;1} - 11f_{3;1} - \frac{3}{20}\right)\Big)\,.\end{aligned} \tag{C.62}$$

Eqs. (C.60)—(C.62) are solved subject to the asymptotic expansions,

- in the UV, i.e., as $\rho \to 0$,

$$\hat{f}l_{g;6;1} = \Big(0 + (2\alpha_0 + 4\beta_1)\ln\rho\Big)\rho^4 + \mathcal{O}(\rho^5\ln\rho)\,, \tag{C.63}$$

$$\hat{f}l_{K;6;1} = 0\,\rho^4 + 0\,\rho^5 + \left(\frac{2}{3} - \frac{1}{72}\alpha_0\right)\rho^6 + \mathcal{O}(\rho^7)\,, \tag{C.64}$$

$$\begin{aligned}fl_{w;6;1} = {} & \left(\frac{2}{15}\alpha_0 + \frac{4}{15}\beta_1\right)\rho^4 + \left(-\frac{2}{3}\alpha_0 - \frac{4}{3}\beta_1\right)\rho^5 + \left(0 + \left(\frac{7}{120}\alpha_0 - \frac{1}{120}\beta_1\right)\ln\rho\right)\rho^6 \\ & + \mathcal{O}(\rho^7\ln\rho)\,,\end{aligned} \tag{C.65}$$

it is completely specified by $\{\alpha_0, \beta_1, s_{6;1}\}$; we further highlighted arbitrary constants, fixed to zero by the overall normalization (C.57), and the extraction of the zero modes in $fl_{g;6;1}$ and $fl_{K;6;1}$ (C.59);

- in the IR, i.e., as $y \equiv \frac{1}{\rho} \to 0$,

$$\hat{f}l_{g;6;1} = \hat{f}l^h_{g;6;1;0} + \mathcal{O}(y)\,, \qquad \hat{f}l_{K;6;1} = \hat{f}l^h_{K;6;1;0} + \mathcal{O}(y)\,, \qquad fl_{w;6;1} = fl^h_{w;6;1;0} + \mathcal{O}(y)\,, \tag{C.66}$$

it is completely specified by

$$\{\hat{f}l^h_{g;6;1;0}\,,\ \hat{f}l^h_{K;6;1;0}\,,\ fl^h_{w;6;1;0}\,,\ \alpha_0\,,\ \beta_1\,,\ s_{6;1}\}\,. \tag{C.67}$$

In total, the UV and IR expansions are completely determined by the parameters (C.67), which is precisely what is needed to find a unique solution for three second order ODEs (C.60)–(C.62). Solving these equations we find

$$s_{6;1} = 6.0318(6)\,. \tag{C.68}$$

C.1.4 Details of $s = 8 \pm \mathcal{O}(\sqrt{b})$ branches: $(\mathbf{A}_s)$ and $(\mathbf{B}_s)$

From (C.6), here

$$\begin{aligned}s_{8;0} = 8\,,\ fl_{g;8;0} = {} & 1\cdot\frac{\rho^4}{(1+\rho)^s}\,{}_2F_1\left(\frac{5}{2}, 4-s; 5; -\rho\right)\Big|_{s=s_{8;0}} \\ = {} & \frac{\rho^4(33\rho^4+192\rho^3+448\rho^2+512\rho+256)}{256(1+\rho)^8}\,,\end{aligned} \tag{C.69}$$

JHEP01(2023)130

where we highlighted the (fixed) overall normalization of the linearized fluctuations; the latter implies that in the UV, i.e., $\rho \to 0$, expansion of $fl_{g;8;k\geq 1}$ the order $\mathcal{O}(\rho^4)$ terms are absent. Because the leading order fluctuation spectra (C.5), (C.6), (C.7) and (C.8) are degenerate at $s_{8;0}$, the equations for $fl_{K;8;k}$, $fl_{w;8;k}$ and $fl_{f;8;k}$ will necessarily contain zero modes; specifically, if $fl_{K;8;k\geq 1}$, $fl_{w;8;k\geq 1}$ and $fl_{f;8;k\geq 1}$ are solutions, so are $(fl_{K;8;k} + \alpha_k \cdot fl_{g;8;0})$, $(fl_{w;8;k} + \frac{\beta_k}{\beta_0} \cdot fl_{w;8;0})$ and $(fl_{f;8;k} + \frac{\gamma_k}{\gamma_0} \cdot fl_{f;8;0})$,

$$\begin{aligned} fl_{w;8;0} &= \beta_0 \cdot \frac{\rho^6}{(1+\rho)^s}\, {}_2F_1\left(\frac{9}{2}, 6-s; 9; -\rho\right)\Big|_{s=s_{8;0}} = \beta_0 \cdot \frac{\rho^6(11\rho^2+40\rho+40)}{40(1+\rho)^8}\,, \\ fl_{f;8;0} &= \gamma_0 \cdot \frac{\rho^8}{(1+\rho)^s}\, {}_2F_1\left(\frac{13}{2}, 8-s; 13; -\rho\right)\Big|_{s=s_{8;0}} = \gamma_0 \cdot \frac{\rho^8}{(1+\rho)^8}\,, \end{aligned} \tag{C.70}$$

for an arbitrary set of constants $\{\alpha_k, \beta_k, \gamma_k\}$. As in section B.1.1, the zero modes at order k will be completely fixed at order $k+1$. We find it convenient to set

$$\begin{aligned} fl_{K;8;k\geq 1} &\equiv \alpha_k \cdot fl_{g;8;0} + \hat{fl}_{K;8;k}\,, \qquad fl_{w;8;k\geq 1} \equiv \beta_k \cdot \frac{1}{\beta_0} fl_{w;8;0} + \hat{fl}_{w;8;k}\,, \\ fl_{f;8;k\geq 1} &\equiv \gamma_k \cdot \frac{1}{\gamma_0} fl_{f;8;0} + \hat{fl}_{f;8;k}\,, \end{aligned} \tag{C.71}$$

with the understanding that in the UV expansion of $\hat{fl}_{K;8;k}$ the order $\mathcal{O}(\rho^4)$ terms are absent, in the UV expansion of $\hat{fl}_{w;8;k}$ the order $\mathcal{O}(\rho^6)$ terms are absent, and in the UV expansion of $\hat{fl}_{f;8;k}$ the order $\mathcal{O}(\rho^8)$ terms are absent.

As in section B.1.1, the equation for $\hat{fl}_{K;8;1}$ is homogeneous, and the boundary condition implied by (C.71) sets

$$\hat{fl}_{K;8,1} \equiv 0\,. \tag{C.72}$$

The subleading set of equations involving constants α_1, β_0, γ_0, $s_{8;1}$, and functions $\{fl_{g;8;1}, \hat{fl}_{K;8;2}, \hat{fl}_{w;8;1}, \hat{fl}_{f;8;1}\}$ reads:

$$\begin{aligned} 0 = {} & fl''_{g;8;1} + \frac{3(5\rho-2)}{2(1+\rho)\rho}\, fl'_{g;8;1} - \frac{12}{\rho(1+\rho)^2}\, fl_{g;8;1} + \frac{s_{8;1}\rho^3}{512(1+\rho)^{10}}\Big(45\rho^4+320\rho^3+960\rho^2 \\ & + 1536\rho + 1280\Big) + \frac{k'_1\alpha_1\rho^3(\rho+2)(33\rho^4+144\rho^3+272\rho^2+256\rho+128)}{32(1+\rho)^9}\,, \end{aligned} \tag{C.73}$$

$$\begin{aligned} 0 = {} & \hat{fl}''_{K;8;2} + \frac{3(5\rho-2)}{2\rho(1+\rho)}\, \hat{fl}'_{K;8;2} - \frac{12}{\rho(1+\rho)^2}\, \hat{fl}_{K;8;2} - \frac{(\rho+2)\rho^3 k'_1}{64(1+\rho)^9}\Big(33\rho^4+144\rho^3 \\ & + 272\rho^2+256\rho+128\Big) + \frac{\alpha_1 s_{8;1}\rho^3(45\rho^4+320\rho^3+960\rho^2+1536\rho+1280)}{512(1+\rho)^{10}} \\ & + \frac{\rho^4(\rho k'_1(\rho+2)(11\rho^2+30\rho+30)+22\rho^2+80\rho+80)\beta_0}{5(1+\rho)^9} - \frac{\gamma_0\rho^6(3\rho k'_1(\rho+2)-14)}{(1+\rho)^9} \\ & - \frac{\rho^2(33\rho^4+192\rho^3+448\rho^2+512\rho+256)}{32(1+\rho)^9}\,, \end{aligned} \tag{C.74}$$

$$\begin{aligned} 0 = {} & \hat{fl}''_{w;8;1} + \frac{3(5\rho-2)}{2\rho(1+\rho)}\, \hat{fl}'_{w;8;1} - \frac{12(2\rho+1)}{\rho^2(1+\rho)^2}\, \hat{fl}_{w;8;1} + \frac{(63\rho^2+280\rho+360)\beta_0\rho^5 s_{8;1}}{80(1+\rho)^{10}} \\ & - \frac{k'_1\alpha_1(\rho+2)(33\rho^4+144\rho^3+272\rho^2+256\rho+128)\rho^3}{160(1+\rho)^9}\,, \end{aligned} \tag{C.75}$$

JHEP01(2023)130

$$0 = \hat{fl}''_{f;8;1} + \frac{3(5\rho-2)}{2\rho(1+\rho)}\,\hat{fl}'_{f;8;1} - \frac{4(11\rho+8)}{\rho^2(1+\rho)^2}\,\hat{fl}_{f;8;1} + \frac{(\rho+2)\alpha_1\rho^3 k'_1}{120(1+\rho)^9}\Big(154\rho^4+607\rho^3 + 991\rho^2+768\rho+384\Big) + \frac{13 s_{8;1}\rho^7\gamma_0}{2(1+\rho)^{10}} + \frac{\alpha_1(37\rho^2+24\rho+24)}{144(1+\rho)^9}\Big(33\rho^4+192\rho^3+448\rho^2 + 512\rho+256\Big)\,. \tag{C.76}$$

We show here that the most important constant, i.e., $s_{8;1}$ can be computed analytically:

- Substituting
$$\alpha_1 = s_{8;1}\cdot v\,, \qquad fl_{g;8;1} = s_{8;1}\cdot fl_{g;8;0}\cdot J_{g;8;1}\,, \tag{C.77}$$
and using (B.12), we find a general analytic solution for $J'_{g;8;1}$,
$$\begin{aligned} J'_{g;8;1} = {}& \frac{3\rho^3 v}{16(1+\rho)^{5/2}}\,\ln\frac{\sqrt{1+\rho}+1}{\sqrt{1+\rho}-1} + \frac{(1+\rho)^{11/2}\,C_1}{\rho^5(33\rho^4+192\rho^3+448\rho^2+512\rho+256)^2} \\ & - \frac{1}{840\rho^5(1+\rho)^2(33\rho^4+192\rho^3+448\rho^2+512\rho+256)^2}\Big((\rho+2)(343035\rho^{14} \\ & +3076920\rho^{13}+8036280\rho^{12}-17283840\rho^{11}-182325120\rho^{10}-613628928\rho^9 \\ & -1212027904\rho^8-1507459072\rho^7-1026850816\rho^6+74186752\rho^5+1002176512\rho^4 \\ & +1149239296\rho^3+700448768\rho^2+234881024\rho+33554432)v+8(1+\rho) \\ & \times(14175\rho^{12}+186200\rho^{11}+1114000\rho^{10}+3973568\rho^9+9149312\rho^8+11880448\rho^7 \\ & -2265088\rho^6-45760512\rho^5-98402304\rho^4-112459776\rho^3-74973184\rho^2 \\ & -27262976\rho-4194304)\Big)\,. \end{aligned} \tag{C.78}$$
Analyticity of $fl_{g;8;1}$, and thus $J'_{g;8;1}$, in the limit $\rho\to\infty$ requires
$$C_1 = 0\,, \tag{C.79}$$
while normalizability of $fl_{g;8;1}$ sets
$$v = \frac{1}{2}\,. \tag{C.80}$$

- We continue with (C.75), setting
$$\hat{fl}_{w;8;1} = s_{8;1}\cdot\frac{1}{\beta_0}fl_{w;8;0}\cdot H_{w;8;1}\,, \tag{C.81}$$
allows to solve analytically for $H'_{w;8;1}$,
$$\begin{aligned} H'_{w;8;1} = {}& -\frac{\rho}{7168(1+\rho)^{5/2}(11\rho^2+40\rho+40)^2}\Big(7623\rho^6+69696\rho^5+270400\rho^4 \\ & +573440\rho^3+716800\rho^2+516096\rho+172032\Big)\ln\frac{\sqrt{1+\rho}+1}{\sqrt{1+\rho}-1} \\ & + \frac{(1+\rho)^{11/2}}{(11\rho^2+40\rho+40)^2\rho^9}\,C_1 - \frac{1}{225792(1+\rho)^2(11\rho^2+40\rho+40)^2\rho^9}\Big(3584(1+\rho) \\ & \times(3969\rho^{12}+28616\rho^{11}+69184\rho^{10}+45824\rho^9+27456\rho^8-439296\rho^7 \end{aligned}$$

JHEP01(2023)130

$$-6150144\rho^6-24600576\rho^5-49201152\rho^4-56229888\rho^3-37486592\rho^2$$
$$-13631488\rho-2097152)\beta_0-3(\rho+2)(160083\rho^{14}+1036728\rho^{13}+727608\rho^{12}$$
$$-12423936\rho^{11}-51946368\rho^{10}-99511296\rho^9-109388800\rho^8-48627712\rho^7$$
$$+163610624\rho^6+624689152\rho^5+1112276992\rho^4+1149239296\rho^3+700448768\rho^2$$
$$+234881024\rho+33554432)\Big)\,. \tag{C.82}$$

Analyticity of $\hat{fl}_{w;8;1}$, and thus $H'_{w;8;1}$, in the limit $\rho\to\infty$ requires

$$C_1=0\,, \tag{C.83}$$

while normalizability of $\hat{fl}_{w;8;1}$ sets

$$\beta_0=-\frac{3}{112}\,. \tag{C.84}$$

- Substituting

$$\hat{fl}_{f;8;1}=s_{8;1}\cdot\frac{1}{\gamma_0}fl_{f;8;0}\cdot B_{f;8;1}\,, \tag{C.85}$$

allows to solve analytically for $B'_{f;8;1}$,

$$B'_{f;8;1}=\frac{539\rho^4+2428\rho^3+4220\rho^2+3584\rho+1792}{35840(1+\rho)^{5/2}\rho}\ln\frac{\sqrt{1+\rho}+1}{\sqrt{1+\rho}-1}+\frac{(1+\rho)^{11/2}}{\rho^{13}}C_1$$
$$-\frac{1}{62092800(1+\rho)^2\rho^{13}}\Big(268800(1+\rho)(273\rho^{12}-728\rho^{11}+2288\rho^{10}-9152\rho^9$$
$$+54912\rho^8-878592\rho^7-12300288\rho^6-49201152\rho^5-98402304\rho^4-112459776\rho^3$$
$$-74973184\rho^2-27262976\rho-4194304)\gamma_0+11(\rho+2)(169785\rho^{14}+312060\rho^{13}$$
$$+2529660\rho^{12}+17283840\rho^{11}+50552960\rho^{10}+78883328\rho^9+71192064\rho^8$$
$$+63537152\rho^7+279535616\rho^6+937033728\rho^5+1668415488\rho^4+1723858944\rho^3$$
$$+1050673152\rho^2+352321536\rho+50331648)\Big)\,. \tag{C.86}$$

Analyticity of $\hat{fl}_{f;8;1}$, and thus $B'_{f;8;1}$, in the limit $\rho\to\infty$ requires

$$C_1=0\,, \tag{C.87}$$

while normalizability of $\hat{fl}_{f;8;1}$ sets

$$\gamma_0=\frac{11}{11200}\,. \tag{C.88}$$

- Consider now (C.74): introducing

$$\hat{fl}_{K;8;2}=fl_{g;8;0}\cdot G_{K;8;2}\,, \tag{C.89}$$

we solve for $G'_{K;8;2}$,

$$G'_{K;8;2}=-\frac{3\rho^3}{9800(1+\rho)^{5/2}(33\rho^4+192\rho^3+448\rho^2+512\rho+256)^2}\Big(373527\rho^8$$
$$+4265712\rho^7+21950064\rho^6+66764544\rho^5+131942272\rho^4+174469120\rho^3$$

JHEP01(2023)130

$$
\begin{aligned}
&+151818240\rho^2+80281600\rho+20070400\Big)\ln\frac{\sqrt{1+\rho}+1}{\sqrt{1+\rho}-1}\\
&+\frac{(1+\rho)^{11/2}}{\rho^5(33\rho^4+192\rho^3+448\rho^2+512\rho+256)^2}\,C_1\\
&+\frac{1}{514500\rho^5(1+\rho)^2(33\rho^4+192\rho^3+448\rho^2+512\rho+256)^2}\Big((\rho+2)(\\
&117661005\rho^{14}+1029936600\rho^{13}+3458168280\rho^{12}+4151454720\rho^{11}\\
&-5844802560\rho^{10}-27053374464\rho^9-37550953472\rho^8-30962548736\rho^7\\
&-76202098688\rho^6-243316424704\rho^5-433231888384\rho^4-447628705792\rho^3\\
&-272824795136\rho^2-91486158848\rho-13069451264)-2450(1+\rho)(14175\rho^{12}\\
&+186200\rho^{11}+1114000\rho^{10}+3973568\rho^9+9149312\rho^8+11880448\rho^7-2265088\rho^6\\
&-45760512\rho^5-98402304\rho^4-112459776\rho^3-74973184\rho^2-27262976\rho\\
&-4194304)s_{8;1}^2\Big)\,.
\end{aligned}
\tag{C.90}
$$

Analyticity of $\hat{fl}_{K;8;2}$, and thus $G_{K;8;2}$, in the limit $\rho\to\infty$ requires

$$
C_1=0\,,
\tag{C.91}
$$

while normalizability of $\hat{fl}_{K;8;2}$ sets

$$
s_{8;1}^2=\frac{3116}{1225}\qquad\Longrightarrow\qquad s_{8;1}=\pm\frac{2\sqrt{779}}{35}\,.
\tag{C.92}
$$

C.1.5 Details of $s=8+\mathcal{O}(b)$ branch: $(\mathbf{C}_s)$

From (C.7), here

$$
s_{8;0}=8\,,\;\; fl_{w;8;0}=\boxed{1}\cdot\;\frac{\rho^6}{(1+\rho)^s}\;{}_2F_1\left(\frac{9}{2},6-s;9;-\rho\right)\Big|_{s=s_{8;0}}=\frac{\rho^6(11\rho^2+40\rho+40)}{40(1+\rho)^8}\,,
\tag{C.93}
$$

where we highlighted the (fixed) overall normalization of the linearized fluctuations; the latter implies that in the UV, i.e., $\rho\to 0$, expansion of $fl_{w;8;k\geq 1}$ the order $\mathcal{O}(\rho^6)$ terms are absent. Because the leading order fluctuation spectra (C.5), (C.6), (C.7) and (C.8) are degenerate at $s_{8;0}$, the equations for $fl_{g;8;k}$, $fl_{K;8;k}$ and $fl_{f;8;k}$ will necessarily contain zero modes; specifically, if $fl_{g;8;k\geq 1}$, $fl_{K;8;k\geq 1}$ and $fl_{f;8;k\geq 1}$ are solutions, so are $(fl_{g;8;k}+\frac{\alpha_k}{\alpha_0}\cdot fl_{g;8;0})$, $(fl_{K;8;k}+\frac{\beta_k}{\alpha_0}\cdot fl_{g;8;0})$ and $(fl_{f;8;k}+\frac{\gamma_k}{\gamma_0}\cdot fl_{f;8;0})$,

$$
\begin{aligned}
fl_{g;8;0}&=\alpha_0\cdot{}_2F_1\left(\frac{5}{2},4-s;5;-\rho\right)\Big|_{s=s_{8;0}}\\
&=\alpha_0\cdot\frac{\rho^4(33\rho^4+192\rho^3+448\rho^2+512\rho+256)}{256(1+\rho)^8}\,,\\
fl_{f;8;0}&=\gamma_0\cdot{}_2F_1\left(\frac{13}{2},8-s;13;-\rho\right)\Big|_{s=s_{8;0}}=\gamma_0\cdot\frac{\rho^8}{(1+\rho)^8}\,,
\end{aligned}
\tag{C.94}
$$

JHEP01(2023)130

for an arbitrary set of constants $\{\alpha_k, \beta_k, \gamma_k\}$. As in section B.1.1, the zero modes at order k will be completely fixed at order $k+1$. We find it convenient to set

$$\begin{aligned} fl_{g;8;k\geq 1} &\equiv \alpha_k \cdot \frac{1}{\alpha_0} fl_{g;8;0} + \hat{fl}_{g;8;k}\,, \qquad fl_{K;8;k\geq 1} \equiv \beta_k \cdot \frac{1}{\alpha_0} fl_{g;8;0} + \hat{fl}_{K;8;k}\,, \\ fl_{f;8;k\geq 1} &\equiv \gamma_k \cdot \frac{1}{\alpha_0} fl_{f;8;0} + \hat{fl}_{f;8;k}\,, \end{aligned} \tag{C.95}$$

with the understanding that in the UV expansion of $\hat{fl}_{g;8;k}$ and $\hat{fl}_{K;8;k}$ the order $\mathcal{O}(\rho^4)$ terms are absent, and in the UV expansion of $\hat{fl}_{f;8;k}$ and the order $\mathcal{O}(\rho^8)$ terms are absent.

The subleading set of equations involving constants α_0, β_1, γ_0, $s_{8;1}$, and functions $\{\hat{fl}_{g;8;1}, \hat{fl}_{K;8;1}, fl_{w;8;1}, \hat{fl}_{f;8;1}\}$ reads:

$$\begin{aligned} 0 =& \hat{fl}''_{g;8;1} + \frac{3(5\rho-2)}{2\rho(1+\rho)}\hat{fl}'_{g;8;1} - \frac{12}{\rho(1+\rho)^2}\hat{fl}_{g;8;1} + 2k_1'\hat{fl}'_{K;8;1} + \frac{8k_1'\hat{fl}_{K;8;1}}{1+\rho} \\ &+ \frac{\rho^3 k_1'(\rho+2)(33\rho^4+144\rho^3+272\rho^2+256\rho+128)\beta_1}{32(1+\rho)^9} - \frac{\rho^6\gamma_0(3\rho^2(k_1')^2(1+\rho)-28)}{4(1+\rho)^9} \\ &+ \frac{\rho^3\alpha_0 s_{8;1}(45\rho^4+320\rho^3+960\rho^2+1536\rho+1280)}{512(1+\rho)^{10}} + \frac{11\rho^2}{20(1+\rho)^{10}}\Bigg(\frac{5}{352}\alpha_0\rho(\rho+2) \\ &\times(1+\rho)(33\rho^4+144\rho^3+272\rho^2+256\rho+128)(f'_{2;1}+4f'_{3;1}-4g'_1)+\rho^4\Bigg(\rho^2 \\ &+ \frac{40}{11}(\rho+1)\Bigg)(1+\rho)^2(k_1')^2 - \frac{75\alpha_0\rho^2 h_1}{32}\left(\rho^4+\frac{64}{11}\rho^3+\frac{448}{33}\rho^2+\frac{512}{33}\rho+\frac{256}{33}\right) \\ &- \frac{15}{8}(1+\rho)\left(\alpha_0\left(\rho^4+\frac{64}{11}\rho^3+\frac{448}{33}\rho^2+\frac{512}{33}\rho+\frac{256}{33}\right)-\frac{32}{15}\rho^4-\frac{256}{33}\rho^3-\frac{256}{33}\rho^2\right)\Bigg), \end{aligned} \tag{C.96}$$

$$\begin{aligned} 0 =& \hat{fl}''_{K;8;1} + \frac{3(5\rho-2)}{2\rho(1+\rho)}\hat{fl}'_{K;8;1} - \frac{12}{\rho(1+\rho)^2}\hat{fl}_{K;8;1} - \frac{\rho^2\alpha_0}{64(1+\rho)^9}\Bigg(\rho k_1'(\rho+2)(33\rho^4 \\ &+144\rho^3+272\rho^2+256\rho+128)+384\rho^3+66\rho^4+896\rho^2+1024\rho+512\Bigg) \\ &- \frac{3\rho k_1'(\rho+2)-14)\gamma_0\rho^6}{(1+\rho)^9} + \frac{(\rho k_1'(\rho+2)(11\rho^2+30\rho+30)+22\rho^2+80\rho+80)\rho^4}{5(1+\rho)^9}\,, \end{aligned} \tag{C.97}$$

$$\begin{aligned} 0 =& fl''_{w;8;1} + \frac{3(5\rho-2)}{2\rho(1+\rho)}fl'_{w;8;1} - \frac{12(2\rho+1)}{\rho^2(1+\rho)^2}fl_{w;8;1} - \frac{2}{5}k_1'\hat{fl}'_{K;8;1} - \frac{8k_1'\hat{fl}_{K;8;1}}{5(1+\rho)} \\ &- \frac{\rho^3 k_1'(\rho+2)(33\rho^4+144\rho^3+272\rho^2+256\rho+128)\beta_1}{160(1+\rho)^9} + \frac{\rho^5(63\rho^2+280\rho+360)s_{8;1}}{80(1+\rho)^{10}} \\ &+ \frac{(33\rho^4+192\rho^3+448\rho^2+512\rho+256)(\rho^2(k_1')^2(1+\rho)+4)\rho^2\alpha_0}{1280(1+\rho)^9} - \frac{\gamma_0\rho^6}{20(1+\rho)^9}\Bigg(\\ &\rho^2(k_1')^2(1+\rho)-32\rho(\rho+2)(f'_{3;1}-f'_{2;1})+80(f_{2;1}-f_{3;1})+12\Bigg) - \frac{\rho^4}{800(1+\rho)^{10}}\Bigg(\\ &8\rho(\rho+2)(1+\rho)(11\rho^2+30\rho+30)(11f'_{2;1}-16f'_{3;1})+209\left(\rho^2+\frac{40}{11}(\rho+1)\right)\Bigg(-\frac{10}{19}\rho \\ &\times(\rho+2)(1+\rho)h_1'+\rho^2(1+\rho)^2(k_1')^2+\left(\frac{215}{19}\rho^2-\frac{80}{19}(\rho+1)\right)h_1+\frac{80(1+\rho)}{19}\Bigg(k_1 \\ &+\frac{19}{4}f_{2;1}-11f_{3;1}-\frac{3}{20}\Bigg)\Bigg)\Bigg)\,, \end{aligned} \tag{C.98}$$

JHEP01(2023)130

$$
\begin{aligned}
0 = {} & \hat{fl}''_{f;8;1} + \frac{3(5\rho-2)}{2\rho(1+\rho)}\hat{fl}'_{f;8;1} - \frac{4(11\rho+8)}{\rho^2(1+\rho)^2}\hat{fl}_{f;8;1} + \frac{2(31\rho^2-120\rho-120)k_1'\hat{fl}'_{K;8;1}}{45\rho^2} \\
& + \frac{16(k_1'\rho(28\rho^3-5\rho^2+30\rho+60)+185\rho^2+120\rho+120)\hat{fl}_{K;8;1}}{45(1+\rho)\rho^4} + \frac{\beta_1}{720(1+\rho)^9}\Big(6\rho^3 \\
& \times(\rho+2)(154\rho^4+607\rho^3+991\rho^2+768\rho+384)k_1' + 5(37\rho^2+24\rho+24)(33\rho^4+192\rho^3 \\
& + 448\rho^2+512\rho+256)\Big) + \frac{\alpha_0}{11520(1+\rho)^9}\Big(-\rho^2(1+\rho)(31\rho^2-120\rho-120)(33\rho^4 \\
& + 192\rho^3+448\rho^2+512\rho+256)(k_1')^2 + 240\rho^5(\rho+2)(11\rho^2+35\rho+35)g_1' + 4(149\rho^2 \\
& + 120(\rho+1))(33\rho^4+192\rho^3+448\rho^2+512\rho+256)\Big) - \frac{27\rho^4\gamma_0}{40(1+\rho)^{10}}\Big(-\frac{2}{243}\rho(\rho+2) \\
& \times(1+\rho)(157\rho^2-660\rho-660)(f'_{2;1}+4f'_{3;1}) - \frac{830}{243}\rho(\rho+2)(1+\rho)\left(\rho^2-\frac{276}{83}(\rho+1)\right) \\
& \times h_1' + \left(\rho^2-\frac{20}{9}(\rho+1)\right)\rho^2(1+\rho)^2(k_1')^2 + \Big(-\frac{11840}{81} + \frac{455}{27}\rho^4 - \frac{58900}{243}\rho^3 - \frac{94420}{243}\rho^2 \\
& - \frac{23680}{81}\rho\Big)h_1 - \frac{20}{243}(1+\rho)(1331\rho^2+732\rho+732)(f_{2;1}+4f_{3;1}) + \frac{59440}{243}\Big(\rho^2 \\
& + \frac{444}{743}(\rho+1)\Big)(1+\rho)k_1 + \frac{2000}{81} + \left(\frac{8116}{243} - \frac{260s_{8;1}}{27}\right)\rho^3 + \frac{14116}{243}\rho^2 + \frac{4000}{81}\rho\Big) \\
& + \frac{187\rho^2}{600(1+\rho)^{10}}\Big(-\frac{26}{17}\rho(\rho+2)\left(\rho^4+\frac{1900}{429}\rho^3+\frac{4300}{429}\rho^2+\frac{800}{143}(2\rho+1)\right)(1+\rho)f'_{2;1} \\
& + \frac{328}{51}\left(\rho^2+\frac{120}{41}(\rho+1)\right)\rho(\rho+2)(1+\rho)\left(\rho^2+\frac{30}{11}(\rho+1)\right)f'_{3;1} + \left(\rho^2+\frac{40}{11}(\rho+1)\right) \\
& \times\left(\frac{50}{51}\left(\rho^2+\frac{12}{5}(\rho+1)\right)\rho(\rho+2)(1+\rho)h_1' + \rho^2\left(\rho^2-\frac{60}{17}(\rho+1)\right)(1+\rho)^2(k_1')^2\right. \\
& + \frac{25}{17}\left(\rho^2+\frac{12}{5}(\rho+1)\right)(\rho+4)\left(\rho+\frac{4}{3}\right)h_1 - \frac{400}{51}(1+\rho)\Big(-\left(\frac{31}{4}\rho^2+\frac{39}{5}(\rho+1)\right)f_{2;1} \\
& \left.+\left(\frac{13}{2}\rho^2+\frac{24}{5}(\rho+1)\right)f_{3;1} + \left(\rho^2+\frac{12}{5}(\rho+1)\right)k_1 + \frac{287}{100}\rho^2+3(\rho+1)\Big)\Big)\Big)\Big)\,. \qquad \text{(C.99)}
\end{aligned}
$$

Eqs. (C.96)—(C.99) are solved subject to the asymptotic expansions,

- in the UV, i.e., as $\rho \to 0$,

$$
\hat{fl}_{g;8;1} = \Big(0 + (2\alpha_0 + 4\beta_1)\ln\rho\Big)\rho^4 + \mathcal{O}(\rho^5\ln\rho)\,, \qquad \text{(C.100)}
$$

$$
\hat{fl}_{K;8;1} = 0\,\rho^4 + 0\,\rho^5 + \left(\frac{2}{3} - \frac{1}{6}\alpha_0\right)\rho^6 + \mathcal{O}(\rho^7)\,, \qquad \text{(C.101)}
$$

$$
\begin{aligned}
fl_{w;8;1} = {} & \left(\frac{2}{15}\alpha_0 + \frac{4}{15}\beta_1\right)\rho^4 + \left(-\frac{4}{5}\alpha_0 - \frac{8}{5}\beta_1\right)\rho^5 + \left(0 + \left(\frac{3}{20}\alpha_0 - \frac{1}{10}\beta_1\right)\ln\rho\right)\rho^6 \\
& + \mathcal{O}(\rho^7\ln\rho)\,, \qquad \text{(C.102)}
\end{aligned}
$$

$$
\begin{aligned}
fl_{f;8;1} = {} & \left(\frac{16}{27}\alpha_0 + \frac{32}{27}\beta_1\right)\rho^2 + \cdots + \Big(0 - \Big(\frac{32}{9}\alpha_0 k_{4;0;1} - \frac{32}{15}\beta_1 k_{4;0;1} + \frac{397}{1200}\alpha_0 \\
& + \frac{9}{400}\beta_1 - 2\gamma_0\Big)\ln\rho - \left(\frac{1}{12}\alpha_0 + \frac{1}{20}\beta_1\right)\ln^2\rho\Big)\rho^8 + \mathcal{O}(\rho^9\ln^2\rho)\,, \qquad \text{(C.103)}
\end{aligned}
$$

JHEP01(2023)130

n	$s_{n;1}^{(A)\&(B)}$	$s_{n;1}^{(C)}$
4	$\pm\frac{\sqrt{130}}{5}$	–
5	$\pm\sqrt{2}$	–
6	$\pm\frac{\sqrt{1390}}{25}$	6.03(2)
7	$\pm\frac{\sqrt{1490}}{25}$	5.39(7)
8	$\pm\frac{2\sqrt{779}}{35}$	5.06(0)

Table 3. Leading corrections to the conformal spectra on branches (A_s), (B_s) and (C_s).

it is completely specified by $\{\alpha_0, \beta_1, \gamma_0, s_{8;1}\}$; we further highlighted arbitrary constants, fixed to zero by the overall normalization (C.93), and the extraction of the zero modes in $fl_{g;8;1}$, $fl_{K;8;1}$ and $fl_{f;8;1}$ (C.95);

- in the IR, i.e., as $y \equiv \frac{1}{\rho} \to 0$,

$$\hat{f}l_{g;8;1} = \hat{f}l^h_{g;8;1;0} + \mathcal{O}(y)\,, \qquad \hat{f}l_{K;8;1} = \hat{f}l^h_{K;8;1;0} + \mathcal{O}(y)\,, \qquad fl_{w;8;1} = fl^h_{w;8;1;0} + \mathcal{O}(y)\,,$$
$$\hat{f}l_{f;8;1} = fl^h_{f;8;1;0} + \mathcal{O}(y)\,, \tag{C.104}$$

it is completely specified by

$$\{\hat{f}l^h_{g;8;1;0}\,,\ \hat{f}l^h_{K;8;1;0}\,,\ fl^h_{w;8;1;0},\,,\ \hat{f}l^h_{f;8;1;0}\,,\ \alpha_0\,,\ \beta_1\,,\ \gamma_0\,,\ s_{8;1}\}\,. \tag{C.105}$$

In total, the UV and IR expansions are completely determined by the parameters (C.105), which is precisely what is needed to find a unique solution for four second order ODEs (C.96)–(C.99). Solving these equations we find

$$s_{8;1} = 5.0601(3)\,. \tag{C.106}$$

C.1.6 Select values of $s_{4\leq n\leq 8;1}$

Extending the computations of sections C.1.1 and C.1.3, we collect in the table 3 leading corrections to the conformal spectra on branches (A_s), (B_s) and (C_s) for $4 \leq n \leq 8$. These results are used to highlight the features of the spectra presented in figure 10.

D Critical point $H = H_{\text{crit}_3}$

The chiral symmetry breaking mode of fluctuations about TypeA$_s$ background becomes marginal at $H = H_{\text{crit}_3}$, see figure 7. It signals the origin of TypeA$_b$ background [17], which exists only for $H > H_{\text{crit}_3}$. In this section we first construct TypeA$_b$ background perturbatively in $A \propto \sqrt{H - H_{\text{crit}_3}}$, and then study the $H = H_{\text{crit}_3}$ marginal mode in this perturbative TypeA$_b$ background geometry. We find that this mode becomes unstable, i.e.,

$$\mathfrak{Im}[\mathfrak{w}_{\chi\text{SB}}]\Big|_{\text{TypeA}_b} = 0 + 36.0098(5)\cdot A^2 + \mathcal{O}(A^4)\,, \tag{D.1}$$

where the precise definition of A is given by (D.2).

JHEP01(2023)130

D.1 TypeA$_b$ background in the vicinity of $H = H_{\text{crit}_3}$

TypeA$_s$ background is a special case of TypeA$_b$ background, constraint by (B.1). From (A.16) and (A.17),

$$\begin{aligned} f_a - f_b = & \underbrace{\left(2f_{a,3,0}+\frac{1}{2}f_{a,1,0}\right)}_{\equiv 2A}\rho^3 - \frac{f_{a,1,0}}{2}\left(2f_{a,3,0}+\frac{1}{2}f_{a,1,0}\right)\rho^4 \\ & + \left(\frac{8f_{a,1,0}^2+4K_0-9}{32}\left(2f_{a,3,0}+\frac{1}{2}f_{a,1,0}\right)+\frac{1}{4}k_{2,3,0}+\frac{1}{8}\left(2f_{a,3,0}+\frac{1}{2}f_{a,1,0}\right)\ln\rho\right)\rho^5 \\ & + \mathcal{O}(\rho^6\ln\rho)\,, \end{aligned} \tag{D.2}$$

which provides a precise definition of A. A vanishes exactly at[22] $K_0 = K_{0,\text{crit}_3}$

$$K_0\Big|_{\text{crit}_3} = \ln\frac{H^2_{\text{crit}_3}}{\Lambda^2}\,. \tag{D.3}$$

Perturbatively in A, TypeA$_b$ background can be represented as

$$f_a = f_3(\rho) + \sum_{k=1}^{\infty} A^{2k-1}\cdot\delta f_{a;2k-1}(\rho) + \sum_{k=1}^{\infty} A^{2k}\cdot\delta f_{a;2k}(\rho)\,, \tag{D.4}$$

$$f_b = f_3(\rho) - \sum_{k=1}^{\infty} A^{2k-1}\cdot\delta f_{a;2k-1}(\rho) + \sum_{k=1}^{\infty} A^{2k}\cdot\delta f_{a;2k}(\rho)\,, \tag{D.5}$$

$$f_c = f_2(\rho) + \sum_{k=1}^{\infty} A^{2k}\cdot\delta f_{c;2k}(\rho)\,, \tag{D.6}$$

$$K_1 = K(\rho) + \sum_{k=1}^{\infty} A^{2k-1}\cdot\delta k_{1;2k-1}(\rho) + \sum_{k=1}^{\infty} A^{2k}\cdot\delta k_{1;2k}(\rho)\,, \tag{D.7}$$

$$K_3 = K(\rho) - \sum_{k=1}^{\infty} A^{2k-1}\cdot\delta k_{1;2k-1}(\rho) + \sum_{k=1}^{\infty} A^{2k}\cdot\delta k_{1;2k}(\rho)\,, \tag{D.8}$$

$$K_2 = 1 + \sum_{k=1}^{\infty} A^{2k-1}\cdot\delta k_{2;2k-1}(\rho)\,, \tag{D.9}$$

$$g\Big|_{\text{TypeA}_b} = g(\rho)\Big|_{\text{TypeA}_s} + \sum_{k=1}^{\infty} A^{2k}\cdot\delta g_{2k}(\rho)\,, \tag{D.10}$$

$$h\Big|_{\text{TypeA}_b} = h(\rho)\Big|_{\text{TypeA}_s} + \sum_{k=1}^{\infty} A^{2k}\cdot\delta h_{2k}(\rho)\,. \tag{D.11}$$

To compute (D.1) we need perturbative solution of TypeA$_b$ background to order $k = 3$ inclusive. As we now explain, orders $k = \{0,1\}$, and $k = \{2,3\}$ must be solved simultaneously.

D.1.1 $k = \{0,1\}$

At leading $k = 0$ order we have TypeA$_s$ background, labeled by K_0; namely, a coupled system of 4 second-order ODEs for $\{f_3, K, g, h\}$ and a single first-order ODE for f_2. At

[22] We use computation SchemeI with $b \equiv 1$, see [17].

JHEP01(2023)130

order $k=1$, the equations for $\{\delta f_{a;1}, \delta k_{1;1}, \delta k_{2;1}\}$ are just the equations for the marginal mode — they are equivalent to (B.3)–(B.5), see also (B.2), with the following identification,

$$\delta f_{a;1} \equiv f_3 \cdot F\,, \qquad \delta k_{1;1} \equiv \chi_1\,, \qquad \delta k_{2;1} \equiv \chi_2\,, \tag{D.12}$$

and with

$$s = 0\,. \tag{D.13}$$

They are solved subject to the asymptotics:

- In the UV, i.e., as $\rho \to 0$,

$$\delta f_{a;1} = \boxed{1} \cdot r^3 + \cdots + \left(\delta f_{a;1;7,0} + \left(\frac{275}{384} + \frac{3}{64}\delta k_{1;1;3,0}\left(K_0 - \frac{5}{4}\right) + \frac{7}{256}K_0 + 3f_{c,4,0}\right)\ln\rho + \left(-\frac{15}{128} - \frac{3}{64}\delta k_{1;1;3,0} + \frac{9}{64}K_0\right)\ln^2\rho - \frac{1}{8}\ln^3\rho\right)\rho^7 + \mathcal{O}(\rho^8\ln^3\rho)\,, \tag{D.14}$$

$$\delta k_{1;1} = \rho^3(\delta k_{1;1;3,0} + 2\ln\rho) + \rho^4\left(-\frac{1}{2}(3\delta k_{1;1;3,0}+2)f_{a,1,0} - 3f_{a,1,0}\ln\rho\right) + \mathcal{O}(\rho^5\ln^2\rho)\,, \tag{D.15}$$

$$\delta k_{2;1} = \rho^3\left(-1 + \frac{3}{2}\delta k_{1;1;3,0} + 3\ln\rho\right) - \rho^4\left(\frac{9}{4}f_{a,1,0}\delta k_{1;1;3,0} + \frac{9}{2}f_{a,1,0}\ln\rho\right) + \mathcal{O}(\rho^5\ln^2\rho)\,, \tag{D.16}$$

it is characterized by 2 parameters

$$\{\ \delta k_{1;1;3,0}\,,\ \delta f_{a;1;7,0}\ \}\,. \tag{D.17}$$

In (D.14) we highlighted the overall normalization, dictated by our definition of the amplitude A, see (D.2). Of course, the asymptotic expansions (D.14)–(D.16) depend on the parameters of the $k=0$ order background, i.e.,

$$\{\ K_0\,,\ f_{a,1,0}\,,\ g_{4,0}\,,\ f_{c,4}\,,\ f_{a,6,0}\,,\ f_{a,8,0}\ \}\,. \tag{D.18}$$

Comparing with (A.23), because of the constraint (B.1), we find that $\{f_{a,3,0},\ k_{2,3,0},\ f_{a,7,0}\}$ are not independent and instead are determined by (D.18):

$$\begin{aligned} f_{a,3,0} &= -\frac{1}{4}f_{a,1,0}\,, \qquad k_{2,3,0} = 0\,,\\ f_{a,7,0} &= \frac{431}{76800}f_{a,1,0}K_0^2 + \left(-\frac{981}{1024000} + \frac{1}{40}f_{c,4,0} - \frac{53}{1920}f_{a,1,0}^2\right)f_{a,1,0}K_0 + \left(-\frac{1362319}{61440000}\right.\\ &\quad \left. + \frac{1}{80}f_{a,1,0}^4 + \frac{77}{46080}f_{a,1,0}^2 - \frac{1}{320}f_{c,4,0} - 2f_{a,6,0} - \frac{1}{40}g_{4,0}\right)f_{a,1,0}\,. \end{aligned} \tag{D.19}$$

- In the IR, i.e., as $y \equiv \frac{1}{\rho} \to 0$,

$$\delta f_{a;1} = \frac{1}{y}\left(\delta f^h_{a;1;0} + \mathcal{O}(y)\right), \qquad \delta k_{1;1} = \delta k^h_{1;1;0} + \mathcal{O}(y)\,, \qquad \delta k_{2;1} = \delta k^h_{2;1;0} + \mathcal{O}(y)\,, \tag{D.20}$$

JHEP01(2023)130

it is characterized by 3 parameters

$$\left\{ \delta f^h_{a;1;0} \,,\, \delta k^h_{1;1;0} \,,\, \delta k^h_{2;1;0} \right\} . \tag{D.21}$$

As in UV, the asymptotic expansions (D.20) depend on the parameters of the $k=0$ order background, i.e.,

$$\left\{ f^h_{a,0} \,,\, f^h_{c,0} \,,\, K^h_{1,0} \,,\, g^h_0 \right\} . \tag{D.22}$$

Comparing with (A.26), because of the constraint (B.1), we find that $\{f^h_{b,0},\, K^h_{2,0},\, K^h_{3,0}\}$ are not independent and instead are determined by (D.22):

$$f^h_{b,0} = f^h_{a,0} \,, \qquad K^h_{3,0} = K^h_{1,0} \,, \qquad K^h_{2,0} = 1 \,. \tag{D.23}$$

In total we have 7 second-order ODEs (4 from $k=0$ order and 3 from $k=1$ order) and 1 additional first-order ODE from the $k=0$ order. Thus in total, we need $7\times 2+1=15$ adjustable parameters to find a solution. This is precisely what we have: $6+4=10$ parameters from order $k=0$, see (D.18) and (D.22), and $2+3=5$ parameters from order $k=1$, see (D.17) and (D.21). Note the coupling of orders $k=0$ and $k=1$ occurs because we traded the parameter s, we set it zero in (D.13), for a requirement to tune K_0 to insure that the $k=1$ order deformation $\{\delta f_{a;1}, \delta k_{1;1}\, \delta k_{2;1}\}$ is normalizable, i.e., the corresponding fluctuations (see (D.12)) are marginal.

Solving the order $k=0$ and $k=1$ equations numerically we recover

$$K_0 = K_0\Big|_{\text{crit}_3} = -0.1636(3) \,, \tag{D.24}$$

originally reported in [17].

D.1.2 $k=\{2,3\}$

We will not present the equations for order $k=\{2,3\}$ perturbative representation of the background TypeA$_b$: they can be straightforwardly derived from the general equations for this background (see appendix B of [17]) using the ansatz (D.4)–(D.11). Since the equation for f_c is of the first-order, so will be the equations for $\delta f_{c;2k}$. The equations for the other functions are always of the second-order. We will discuss the asymptotics and count the parameters.

At order $k=2$ we have a coupled system of 4 second-order ODEs for $\{\delta f_{a;2},\, \delta k_{1;2},\, \delta g_2,\, \delta h_2\}$ and the first-order ODE for $\delta f_{c;2}$. They are solved subject to the asymptotics:

- In the UV, i.e., as $\rho\to 0$,

$$\begin{aligned}\delta f_{a;2} = {}& \rho\ \delta f_{a;2;1,0} + \rho^2\left(\frac{1}{2}\delta f_{a;2;1,0} f_{a,1,0} - \frac{1}{4}\delta k_{1;2;0,0}\right) + \cdots + \rho^6\Big(\delta f_{a;2;6,0} + \cdots \\ & + \frac{3}{640}\delta k_{1;2;0,0}\ln^3\rho\Big) + \mathcal{O}(\rho^7\ln^4\rho) \,,\end{aligned} \tag{D.25}$$

$$\begin{aligned}\delta f_{c;2} = {}& \rho\ \delta f_{a;2;1,0} + \rho^2\left(\frac{1}{2}\delta f_{a;2;1,0} f_{a,1,0} - \frac{1}{4}\delta k_{1;2;0,0}\right) - \frac{1}{4}\rho^3\delta f_{a;2;1,0} + \rho^4\Big(\delta f_{c;2;4,0} \\ & + \frac{1}{16}\delta k_{1;2;0,0}\ln\rho\Big) + \mathcal{O}(\rho^5\ln^2\rho) \,,\end{aligned} \tag{D.26}$$

JHEP01(2023)130

$$\delta k_{1;2}=\delta k_{1;2;0,0}+\rho\delta f_{a;2;1,0}+\rho^2\Big(-\frac{1}{2}\delta f_{a;2;1,0}f_{a,1,0}+\frac{1}{8}\delta k_{1;2;0,0}\Big)+\mathcal{O}(\rho^3\ln\rho)\,, \tag{D.27}$$

$$\begin{aligned}\delta g_2=&\frac{1}{2}\rho^3\delta f_{a;2;1,0}+\rho^4\Big(\delta g_{2;4,0}+\Big(-\frac{3}{8}\delta f_{a;2;1,0}f_{a,1,0}-\frac{5}{64}\delta k_{1;2;0,0}+3\delta f_{c;2;4,0}\Big)\ln\rho\\&+\frac{3}{32}\delta k_{1;2;0,0}\ln^2\rho\Big)+\cdots+\rho^8\Big(\delta g_{2;8,0}+\cdots-\frac{3}{512}\delta k_{1;2;0,0}\ln^5\rho\Big)+\mathcal{O}(\rho^9\ln^6\rho)\,,\end{aligned} \tag{D.28}$$

$$\delta h_2=\frac{1}{4}\delta k_{1;2;0,0}+\rho\Big(-\frac{1}{2}\delta f_{a;2;1,0}K_0-\frac{1}{2}\delta k_{1;2;0,0}f_{a,1,0}+\delta f_{a;2;1,0}\ln\rho\Big)+\mathcal{O}(\rho^2\ln\rho)\,, \tag{D.29}$$

it is characterized by 6 parameters

$$\{\ \delta k_{1;2;0,0}\,,\ \delta f_{a;2;1,0}\,,\ \delta f_{c;2;4,0}\,,\ \delta g_{2;4,0}\,,\ \delta f_{a;2;6,0}\,,\ \delta g_{2;8,0}\ \}\ . \tag{D.30}$$

- In the IR, i.e., as $y\equiv\frac{1}{\rho}\to 0$,

$$\delta f_{a;2}=\frac{1}{y}\Big(\delta f^h_{a;2;0}+\mathcal{O}(y)\Big)\,,\qquad \delta f_{c;2}=\frac{1}{y}\Big(\delta f^h_{c;2;0}+\mathcal{O}(y)\Big)\,,\quad \delta k_{1;2}=\delta k^h_{1;2;0}+\mathcal{O}(y)\,, \tag{D.31}$$

$$\begin{aligned}\delta g_2=&\,\delta g^h_{2;0}+\mathcal{O}(y)\,,\qquad \delta h_2=y^3\cdot\Big(\frac{(K^h_{1,0})^2}{(f^h_{a,0})^4f^h_{c,0}}\Big(-\frac{2(\delta f^h_{a;1,0})^2}{(f^h_{a,0})^2}+\frac{4\delta f^h_{a;2,0}}{f^h_{a,0}}+\frac{\delta f^h_{c;2,0}}{f^h_{c,0}}\Big)\\&+\frac{2K^h_{1,0}}{(f^h_{a,0})^4f^h_{c,0}}(\delta k^h_{1;1;0}\delta k^h_{2;1;0}-\delta k^h_{1;2;0})+\Big(-\frac{9}{40(f^h_{a,0})^2f^h_{c,0}}+\frac{3}{5(f^h_{a,0})^3}-\frac{f^h_{c,0}}{10(f^h_{a,0})^4}\\&-\frac{9g^h_0}{10(f^h_{a,0})^4f^h_{c,0}}\Big)(\delta f^h_{a;1,0})^2+\Big(-\frac{3}{5(f^h_{a,0})^2}+\frac{f^h_{c,0}}{5(f^h_{a,0})^3}+\frac{3g^h_0}{5(f^h_{a,0})^3f^h_{c,0}}\Big)\delta f^h_{a;2,0}\\&-\frac{3g^h_0}{10(f^h_{a,0})^2f^h_{c,0}}(\delta k^h_{2;1;0})^2+\Big(-\frac{1}{10(f^h_{a,0})^2}+\frac{3g^h_0}{10(f^h_{a,0})^2(f^h_{c,0})^2}\Big)\delta f^h_{c;2,0}-\frac{3}{10(f^h_{a,0})^2f^h_{c,0}}\delta g^h_{2;0}\\&-\frac{6g^h_0\delta f^h_{a;1,0}\delta k^h_{2;1;0}}{5(f^h_{a,0})^3f^h_{c,0}}-\frac{27(\delta k^h_{1;1;0})^2}{40(f^h_{a,0})^2g^h_0f^h_{c,0}}\Big)+\mathcal{O}(y^4)\,,\end{aligned} \tag{D.32}$$

it is characterized by 4 parameters

$$\{\ \delta f^h_{a;2;0}\,,\ \delta f^h_{c;2;0}\,,\ \delta k^h_{1;2;0}\,,\ \delta g^h_{2;0}\ \}\,. \tag{D.33}$$

At order $k=3$ we have a coupled system of 3 second-order ODEs for $\{\delta f_{a;3},\,\delta k_{1;3},\,\delta k_{2;3}\}$. They are solved subject to the asymptotics:

- In the UV, i.e., as $\rho\to 0$,

$$\begin{aligned}\delta f_{a;3}=&\,\boxed{0}\cdot\rho^3-\frac{1}{2}\rho^4\delta f_{a;2;1,0}+\rho^5\Big(\frac{1}{2}\delta f_{a;2;1,0}f_{a,1,0}+\frac{1}{8}\delta k_{1;2;0,0}+\frac{3}{16}\delta k_{1;3;3,0}\Big)\\&+\rho^7\Big(\delta f_{a;3;7,0}+\cdots+\Big(\frac{9}{64}\delta k_{1;2;0,0}-\frac{3}{64}\delta k_{1;3;3,0}\Big)\ln^2\rho\Big)+\mathcal{O}(\rho^8\ln^3\rho)\,,\end{aligned} \tag{D.34}$$

$$\begin{aligned}\delta k_{1;3}=&\,\rho^3\delta k_{1;3;3,0}+\rho^4\Big(-\frac{3}{2}\delta f_{a;2;1,0}\delta k_{1;1;3,0}-\frac{3}{2}\delta k_{1;3;3,0}f_{a,1,0}-\delta f_{a;2;1,0}-3\delta f_{a;2;1,0}\ln\rho\Big)\\&+\mathcal{O}(\rho^5\ln\rho)\,,\end{aligned} \tag{D.35}$$

$$\delta k_{2;3}=\frac{3}{2}\rho^3\delta k_{1;3;3,0}-\frac{9}{4}\rho^4\Big(\delta f_{a;2;1,0}\delta k_{1;1;3,0}+\delta k_{1;3;3,0}f_{a,1,0}+2\delta f_{a;2;1,0}\ln\rho\Big)+\mathcal{O}(\rho^5\ln\rho)\,, \tag{D.36}$$

JHEP01(2023)130

it is characterized by 2 parameters

$$\{\ \delta f_{a;3;7,0}\,,\ \delta k_{1;3;3,0}\ \}\,. \tag{D.37}$$

In (D.34) we highlighted the parameter fixed to zero, as dictated by our definition of the amplitude A, see (D.2).

- In the IR, i.e., as $y \equiv \frac{1}{\rho} \to 0$,

$$\delta f_{a;3} = \frac{1}{y}\Big(\delta f^h_{a;3;0} + \mathcal{O}(y)\Big)\,, \qquad \delta k_{1;3} = \delta k^h_{1;3;0} + \mathcal{O}(y)\,, \qquad \delta k_{2;3} = \delta k^h_{2;3;0} + \mathcal{O}(y)\,, \tag{D.38}$$

it is characterized by 3 parameters

$$\Big\{\ \delta f^h_{a;3;0}\,,\ \delta k^h_{1;3;0}\,,\ \delta k^h_{2;3;0}\ \Big\}\,. \tag{D.39}$$

In total we have 7 second-order ODEs (4 from $k=2$ order and 3 from $k=3$ order) and 1 additional first-order ODE from the $k=2$ order. Thus in total, we need $7\times 2+1=15$ adjustable parameters to find a solution. This is precisely what we have: $6+4=10$ parameters from order $k=2$, see (D.30) and (D.33), and $2+3=5$ parameters from order $k=3$, see (D.37) and (D.39). Here the coupling of orders $k=2$ and $k=3$ occurs because we have an *additional* parameter at order $k=2$, and we are *lacking* one parameter at order $k=3$. Specifically, $\delta k_{1;2;0,0}$, see (D.30), is needed to parameterize background solutions TypeA$_b$, away from $K_0 = K_{0,\text{crit}_3}$:

$$K_0 - K_{0,\text{crit}_3} = \ln\frac{H^2}{H^2_{\text{crit}_3}} = \delta k_{1;2;0,0}\cdot A^2 + \mathcal{O}(A^4)\,. \tag{D.40}$$

On the other had, at order $k=3$ we have 3 second-order ODEs for $\{\delta f_{a;3},\ \delta k_{1;3},\ \delta k_{2;3}\}$, however we have only $2+3=5$ adjustable parameter (see (D.37) and (D.39)) — the *missing* parameter is the highlighted one in (D.34), that we are forced to set to zero as part of the definition of the amplitude A (D.2).

Solving the order $k=2$ and $k=3$ equations numerically we find

$$\delta k_{1;2;0,0} = 6.4889(0)\,. \tag{D.41}$$

D.1.3 $K_0(A)$ and its perturbative approximation

To identify TypeA$_b$ DFP instability it is most convenient to construct numerically the corresponding TypeA$_b$ background by parameterizing it with A, as defined in (D.2), rather than using K_0, as it is done in [17]. This allows us to use the near-critical analysis of the marginal mode of section D.2 as an approximation for the spectral analysis of this mode at finite A, see figure 12. In figure 13 we compare $K_0(A)$ with its perturbative in A approximation given by (D.40). We find from numerical interpolation an excellent agreement,

$$\left[\frac{1}{2\delta k_{1;2;0,0}}\frac{d^2K_0(A)}{dA^2} - 1\right]\Big|_{A=0} = 1.33\cdot 10^{-15}\,. \tag{D.42}$$

JHEP01(2023)130

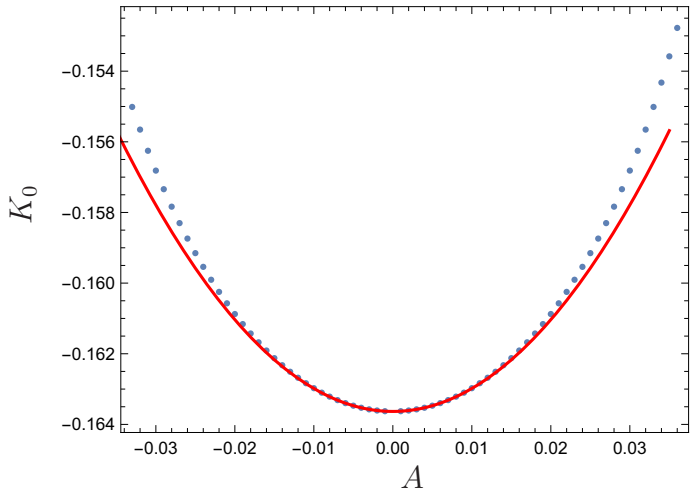

Figure 13. We construct TypeA$_b$ background geometry parameterizing it with A, defining the deviation from the critical point H_{crit_3}, see (D.2). The same geometry was parameterized with K_0 in [17]. Dots represent $K_0(A)$ for select values of A. The solid red curve is the perturbative approximation (D.40).

D.2 TypeA$_b$ background instability in the vicinity of $H = H_{\text{crit}_3}$

Perturbatively in A, the chiral symmetry breaking, marginal at $H = H_{\text{crit}_3}$, mode can be represented as, see (B.2),

$$fl_a = f_3(\rho)\cdot F(\rho) + \sum_{k=1}^{\infty} A^{2k-1}\cdot fl_{a;2k-1}(\rho) + \sum_{k=1}^{\infty} A^{2k}\cdot fl_{a;2k}(\rho)\,, \tag{D.43}$$

$$fl_b = -f_3(\rho)\cdot F(\rho) + \sum_{k=1}^{\infty} A^{2k-1}\cdot fl_{a;2k-1}(\rho) - \sum_{k=1}^{\infty} A^{2k}\cdot fl_{a;2k}(\rho)\,, \tag{D.44}$$

$$fl_c = \sum_{k=1}^{\infty} A^{2k-1}\cdot fl_{c;2k-1}(\rho)\,, \tag{D.45}$$

$$fl_{K_1} = \chi_1(\rho) + \sum_{k=1}^{\infty} A^{2k-1}\cdot fl_{K_1;2k-1}(\rho) + \sum_{k=1}^{\infty} A^{2k}\cdot fl_{K_1;2k}(\rho)\,, \tag{D.46}$$

$$fl_{K_2} = \chi_2(\rho) + \sum_{k=1}^{\infty} A^{2k}\cdot fl_{K_2;2k}(\rho)\,, \tag{D.47}$$

$$fl_{K_3} = -\chi_1(\rho) + \sum_{k=1}^{\infty} A^{2k-1}\cdot fl_{K_1;2k-1}(\rho) - \sum_{k=1}^{\infty} A^{2k}\cdot fl_{K_1;2k}(\rho)\,, \tag{D.48}$$

$$fl_g = \sum_{k=1}^{\infty} A^{2k-1}\cdot fl_{g;2k-1}(\rho)\,, \tag{D.49}$$

$$fl_h = \sum_{k=1}^{\infty} A^{2k-1}\cdot fl_{h;2k-1}(\rho)\,, \tag{D.50}$$

with

$$-\,\mathfrak{Im}[\mathfrak{w}_{\chi\text{SB}}]\Big|_{\text{TypeA}_b} \equiv s = 0 + \sum_{k=1}^{\infty} A^{2k}\cdot s_{2k}\,. \tag{D.51}$$

JHEP01(2023)130

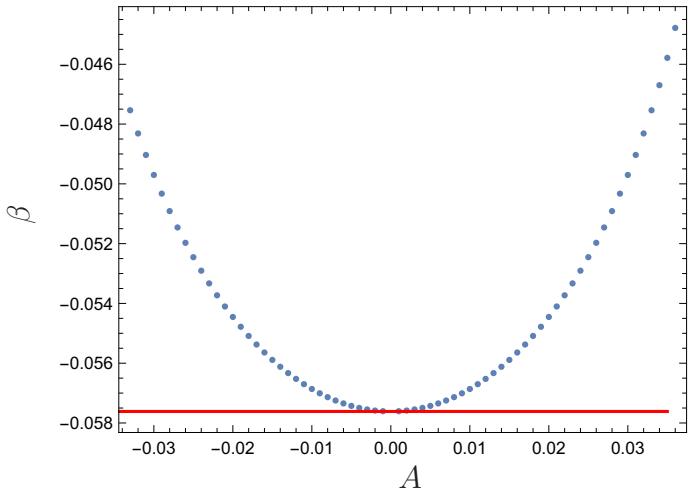

Figure 14. Dots represent the amplitude of the zero mode $\beta(A)$ as given by (D.54). The solid red line is the perturbative approximation (D.53).

The equations of motion for the terms of the perturbative expansion of the fluctuations can be derived from the general equations of appendix A, using the perturbative TypeA$_b$ background ansatz (D.4)–(D.11), and (D.43)–(D.51). Since fl_h can always be algebraically determined from the remaining modes, see (A.13), we find that the same is true for its perturbative terms $fl_{h,2k-1}$.

We summarize below the salient features of the numerical analysis.

- Order $k = 0$. Here, the fluctuations are represented by the marginal chiral symmetry breaking mode, see (B.2), (B.3)–(B.5) with $s = 0$.

- At any even order in k there is a zero mode: if $\{fl_{a;2k}, fl_{K_1;2k}, fl_{K_2;2k}\}$ is a solution of the equations of motion, so is

$$\{\ fl_{a;2k} + f_3 F\ ,\ fl_{K_1;2k} + \chi_1\ ,\ fl_{K_2;2k} + \chi_2\ \}\ , \tag{D.52}$$

  with an arbitrary amplitude $f_{3,0} \equiv \beta_{2k}$, see (B.10). These arbitrary at order $2k$ parameters are fixed at order $2k + 1$. For example, we find in this manner

$$\beta_0 = -0.05761(4)\ . \tag{D.53}$$

- Order $k = 1$. At this order the fluctuations are $\{fl_{a;1},\ fl_{c;1},\ fl_{K_1;1},\ fl_{g_1}\}$. Since there is no contribution to s at this order, i.e., $s_1 = 0$ in (D.51), the zero mode amplitude at the previous order, β_0, is needed to find a unique solution.

- Order $k = 2$. At this order the fluctuations are $\{fl_{a;2},\ fl_{K_1;2},\ fl_{K_2;2}\}$; additionally, the equations explicitly depend on s_2 parameter in (D.51). The equations for the fluctuations also require the input of the background TypeA$_b$ up to order $k = 2$ inclusive.

JHEP01(2023)130

- In figure 14 we compare the zero mode amplitude $\beta(A)$, extracted in computing numerically $s(A)$ in TypeA$_b$ DFP at finite A,

$$\beta(A) = \lim_{\rho\to 0} \frac{fl_a(\rho) - fl_b(\rho)}{2\rho^3} \equiv \sum_{k=0}^{\infty} A^{2k} \cdot \beta_{2k}\,, \tag{D.54}$$

  with its perturbative approximation at $A = 0$, see (D.53). Numerically interpolating the finite A results we find a good agreement,

$$\left[\frac{\beta(A)}{\beta_0} - 1\right]\Big|_{A=0} = -2.0(7)\cdot 10^{-5}\,. \tag{D.55}$$

- Numerical analysis at order $k = 2$ provide the value of s_2,

$$s_2 = -36.0098(5)\,, \tag{D.56}$$

  which implies that marginal at $H = H_{\text{crit}_3}$ fluctuations become unstable in TypeA$_b$ for $H > H_{\text{crit}_3}$. The frequency of this mode at finite A is presented in figure 12. Numerically interpolating the finite A results for $s(A)$ we find a good agreement with the leading nontrivial order perturbative approximation, (D.51),

$$\left[\frac{1}{2s_2}\frac{d^2 s(A)}{dA^2} - 1\right]\Big|_{A=0} = 1.1(7)\cdot 10^{-3}\,. \tag{D.57}$$

References

[1] A. Buchel, *A bestiary of black holes on the conifold with fluxes*, *JHEP* **06** (2021) 102 [arXiv:2103.15188] [INSPIRE].

[2] I.R. Klebanov and M.J. Strassler, *Supergravity and a confining gauge theory: Duality cascades and chi SB resolution of naked singularities*, *JHEP* **08** (2000) 052 [hep-th/0007191] [INSPIRE].

[3] O. Aharony, A. Buchel and A. Yarom, *Holographic renormalization of cascading gauge theories*, *Phys. Rev. D* **72** (2005) 066003 [hep-th/0506002] [INSPIRE].

[4] N. Seiberg, *Electric-magnetic duality in supersymmetric nonAbelian gauge theories*, *Nucl. Phys. B* **435** (1995) 129 [hep-th/9411149] [INSPIRE].

[5] A. Buchel, *Finite temperature resolution of the Klebanov-Tseytlin singularity*, *Nucl. Phys. B* **600** (2001) 219 [hep-th/0011146] [INSPIRE].

[6] N. Chai, A. Dymarsky, M. Goykhman, R. Sinha and M. Smolkin, *A model of persistent breaking of continuous symmetry*, *SciPost Phys.* **12** (2022) 181 [arXiv:2111.02474] [INSPIRE].

[7] J.M. Maldacena, *The Large N limit of superconformal field theories and supergravity*, *Adv. Theor. Math. Phys.* **2** (1998) 231 [hep-th/9711200] [INSPIRE].

JHEP01(2023)130

[8] O. Aharony, S.S. Gubser, J.M. Maldacena, H. Ooguri and Y. Oz, *Large N field theories, string theory and gravity*, *Phys. Rept.* **323** (2000) 183 [hep-th/9905111] [INSPIRE].

[9] A. Buchel, *Chiral symmetry breaking in cascading gauge theory plasma*, *Nucl. Phys. B* **847** (2011) 297 [arXiv:1012.2404] [INSPIRE].

[10] O. Aharony, A. Buchel and P. Kerner, *The Black hole in the throat: Thermodynamics of strongly coupled cascading gauge theories*, *Phys. Rev. D* **76** (2007) 086005 [arXiv:0706.1768] [INSPIRE].

[11] A. Buchel, *Klebanov-Strassler black hole*, *JHEP* **01** (2019) 207 [arXiv:1809.08484] [INSPIRE].

[12] A. Buchel, *Transport properties of cascading gauge theories*, *Phys. Rev. D* **72** (2005) 106002 [hep-th/0509083] [INSPIRE].

[13] A. Buchel, *Hydrodynamics of the cascading plasma*, *Nucl. Phys. B* **820** (2009) 385 [arXiv:0903.3605] [INSPIRE].

[14] A. Buchel and A.A. Tseytlin, *Curved space resolution of singularity of fractional D3-branes on conifold*, *Phys. Rev. D* **65** (2002) 085019 [hep-th/0111017] [INSPIRE].

[15] A. Buchel, *Quantum phase transitions in cascading gauge theory*, *Nucl. Phys. B* **856** (2012) 278 [arXiv:1108.6070] [INSPIRE].

[16] A. Buchel and D.A. Galante, *Cascading gauge theory on dS_4 and String Theory landscape*, *Nucl. Phys. B* **883** (2014) 107 [arXiv:1310.1372] [INSPIRE].

[17] A. Buchel, *χSB of cascading gauge theory in de Sitter*, *JHEP* **05** (2020) 035 [arXiv:1912.03566] [INSPIRE].

[18] N.D. Birrell and P.C.W. Davies, *Quantum Fields in Curved Space*, Cambridge Monographs on Mathematical Physics, Cambridge University Press, Cambridge, U.K. (1984) [DOI] [INSPIRE].

[19] A. Buchel, *Dynamical fixed points in holography*, *JHEP* **02** (2022) 128 [arXiv:2111.04122] [INSPIRE].

[20] T. Dauxois, *Fermi, pasta, ulam, and a mysterious lady*, *Physics Today* **61** (2008) 55.

[21] V. Balasubramanian, A. Buchel, S.R. Green, L. Lehner and S.L. Liebling, *Holographic Thermalization, Stability of Anti-de Sitter Space, and the Fermi-Pasta-Ulam Paradox*, *Phys. Rev. Lett.* **113** (2014) 071601 [arXiv:1403.6471] [INSPIRE].

[22] U.H. Danielsson, E. Keski-Vakkuri and M. Kruczenski, *Black hole formation in AdS and thermalization on the boundary*, *JHEP* **02** (2000) 039 [hep-th/9912209] [INSPIRE].

[23] A. Buchel and A. Karapetyan, *de Sitter Vacua of Strongly Interacting QFT*, *JHEP* **03** (2017) 114 [arXiv:1702.01320] [INSPIRE].

[24] A. Buchel, L. Lehner and R.C. Myers, *Thermal quenches in $N = 2^*$ plasmas*, *JHEP* **08** (2012) 049 [arXiv:1206.6785] [INSPIRE].

[25] A. Buchel, L. Lehner, R.C. Myers and A. van Niekerk, *Quantum quenches of holographic plasmas*, *JHEP* **05** (2013) 067 [arXiv:1302.2924] [INSPIRE].

[26] A. Buchel, R.C. Myers and A. van Niekerk, *Universality of Abrupt Holographic Quenches*, *Phys. Rev. Lett.* **111** (2013) 201602 [arXiv:1307.4740] [INSPIRE].

[27] A. Buchel, *Ringing in de Sitter spacetime*, *Nucl. Phys. B* **928** (2018) 307 [arXiv:1707.01030] [INSPIRE].

JHEP01(2023)130

[28] J. Casalderrey-Solana, C. Ecker, D. Mateos and W. Van Der Schee, *Strong-coupling dynamics and entanglement in de Sitter space*, *JHEP* **03** (2021) 181 [arXiv:2011.08194] [INSPIRE].

[29] A. Buchel, *Master equations for de Sitter DFPs*, *JHEP* **09** (2022) 227 [arXiv:2207.09887] [INSPIRE].

[30] A. Buchel, *Verlinde Gravity and AdS/CFT*, arXiv:1702.08590 [INSPIRE].

[31] *Collection of the equations*, available as Maple worksheet, https://github.com/abuchel-hepth/cascading-gauge-theory-DFP-stability/blob/main/attachement_formulars.mw.

[32] A. Buchel, *Entanglement entropy of $\mathcal{N}=2^*$ de Sitter vacuum*, *Nucl. Phys. B* **948** (2019) 114769 [arXiv:1904.09968] [INSPIRE].

[33] R. Minasian and D. Tsimpis, *On the geometry of nontrivially embedded branes*, *Nucl. Phys. B* **572** (2000) 499 [hep-th/9911042] [INSPIRE].

[34] A. Buchel, *On branches of the KS black hole*, *Nucl. Phys. B* **957** (2020) 115094 [arXiv:2005.00854] [INSPIRE].

JHEP01(2023)130